Dynamic Downscaling to Study Climate Change Impacts on Water Resources in India

IIT Delhi, IIT Madras, Anna University, Banaras Hindu University

June 2022

This is a Draft Report and yet to be accepted by Competent Authority

The data obtained from the study is available on NIH Roorkee website. To obtain access to the data, please contact the Member Secretary, INCCC.

The contact details of Member Secretary. INCCC are as follows:

Shri R.P. Pandey,
Member Secretary (INCCC)
National Institute of Hydrology
Roorkee - 247667 (Uttarakhand), India.
Phone : 01332-249216 , 276220, 278478
Fax : +91-1332-272123
Email : inccc.nih@gmail.com, rppandey@gmail.com

Introduction

In order to achieve the objectives of providing downscaled (~50 km resolution) climate model output, the following methods have been adopted in the project:

- Time-slice technique
- Nested Regional Models (RCMs)

The multiple approaches (in addition to the statistical downscaling being carried out with IIT Bombay's coordination) will provide us with a true representation of the uncertainties in regional climate change. These approaches to dynamical downscaling along with the particulars of models and scenarios chosen are described in greater detail below. Table 1 summarizes the different models, scenarios, resolutions and domains chosen for downscaling by the various groups. The progress of the individual groups are presented in separate sections that follow.

S. No.	Institution	Downscaling Model	Downscaled Resolution	CGCM to be downscaled	Scenario Runs planned	Years	Domain
1	IIT Delhi	CAM5	~50km	CCCMA-CanESM2, CNRM-CM5, MIROC5, MPI-ESM-LR, NorESM1-M.	Historical, RCP4.5, and RCP8.5	Historical: 1950-2005 RCP scenarios: 2006-2100	Entire Globe
2	IIT Madras	WRF	25km	CanESM2 and NorESM1	Historical, RCP4.5, and RCP8.5	Historical: 1950-2005. RCP scenarios: 2006-2100	Entire Country
3	Anna University	PRECIS	25 km	HADGEM2-ES	Historical, RCP4.5, and RCP8.5	Historical: 1970-2005 RCP scenarios: 2006-2100	Entire Country
4	BHU	RegCM4.6	25 km	MPI-ESM-LR and NorESM1-M	Historical, RCP4.5, and RCP8.5	Historical: 1950-2005 RCP scenarios: 2019-2100	Entire Country

Table 1: Summary of downscaling models to be used by each of the groups and the models chosen for downscaling.

Final Report

(2018-2022)

Dynamic Downscaling to Study Climate Change Impacts on Water Resources in India

Submitted by

Prof. Krishna AchutaRao

Prof. Dilip Ganguly

Centre for Atmospheric Sciences

Indian Institute of Technology Delhi

June 2022

Introduction:

The IIT Delhi group is performing simulations for "present day" and "future" with an Atmospheric General Circulation Model (AGCM) running at a higher resolution (~50km). For this purpose we have chosen the National Center for Atmospheric Research (NCAR) Community Atmospheric Model version 5.2 (CAM5). Version 5.2 of the Community Atmosphere Model (CAM) is the sixth generation of the NCAR atmospheric GCM and has again been developed through a collaborative process of users and developers in the Atmosphere Model Working Group (AMWG) with significant input from the Chemistry Climate Working Group (Chem-Clim WG) and the Whole Atmosphere Working Group (WAMWG). The Atmosphere Model Working Group1 (AMWG) of the Community Earth System Model (CESM) project guides the current development of CAM. CAM is used as both a standalone model and as the atmospheric component of the CESM.

The Community Atmosphere Model Version 5 (CAM5):

The salient features of the CAM5 are as follows:

- ~3 mb model top pressure
- Choice of 0.5^{o}, 1^{o}, 2^{o} horizontal resolution
- Choice of 30 or 60 vertical layers
- 30-minute time step
- Finite volume (Fv) dynamical core
- Community Land Model (CLM4.5)
- UW moist turbulence
- UW shallow convection
- UW macrophysics
- Zhang-McFarlane deep convection
- *Morrison-Gettelman* 2-moment stratiform microphysics
- RRTMG radiation scheme
- Choice of 3-mode Modal Aerosol Model (MAM3), 7-mode (MAM-7)

Downscaling simulations:

As per the Terms of Reference, the downscaling simulations will be performed for at least five CMIP5 AOGCMs and 2 future scenarios - RCP4.5 and RCP8.5. For this purpose five AOGCMs were chosen in consultation with the Statistical Downscaling project (PI: Prof. Subimal Ghosh, IIT Bombay) funded by the Ministry of Water Resources. The selected models to be downscaled are CCCMA-CanESM2, CNRM-CM5, MIROC5, MPI-ESM-LR, NorESM1-M.

For the use of Ministry of Water Resources projects, the model resolution chosen is 0.47°x0.63° (~ 0.5°). The model data will be provided at a nominal 50km resolution. Details of file formats etc. will be worked out with the end user community. The variables stored will include the basic hydrological model inputs daily rainfall, maximum temperature, minimum temperature, relative humidity, net radiation, and wind speed. The model runs will be performed for the post 1950 period using historical simulations up to 2005. Beyond that there will be RCP8.5 and RCP4.5 scenarios from 5 models each that will be generated. The first test simulations were carried out using the observed SST and sea-ice boundary conditions. These simulations were verified against observations and found to be within reasonable bounds of error. The annual average of the surface (2m) air temperature is shown in Figure 1. Temperature and precipitation in the individual months of the 1951-1953 monsoon seasons were also validated (see Figure 2). A detailed report of the biases and their correction will be prepared when the model output is in the bias correction stage.

Steps followed to prepare the Boundary Conditions:

• Model outputs of sea surface temperature (SST) and sea-ice concentration (SIC) are re-gridded to the observed (Obtained from NCAR) grids 0.47°x0.63° (~ 0.5°).

• Model outputs are adjusted to preserve the sea-ice consistency relationship (Fiorino 2004) in line with the empirical relation in Hurrell et al. (2008).

• Observed BCs (SST and SIC) climatology for the reference/present day time period (1976-2005) is added to historical/RCPs time period model simulated anomaly (relative to same reference period).

• Prepared BCs are again adjusted to preserve the sea-ice consistency relationship.

• Used the bcgen utility to write the boundary condition in model readable format and again cross-check the sea-ice consistency.

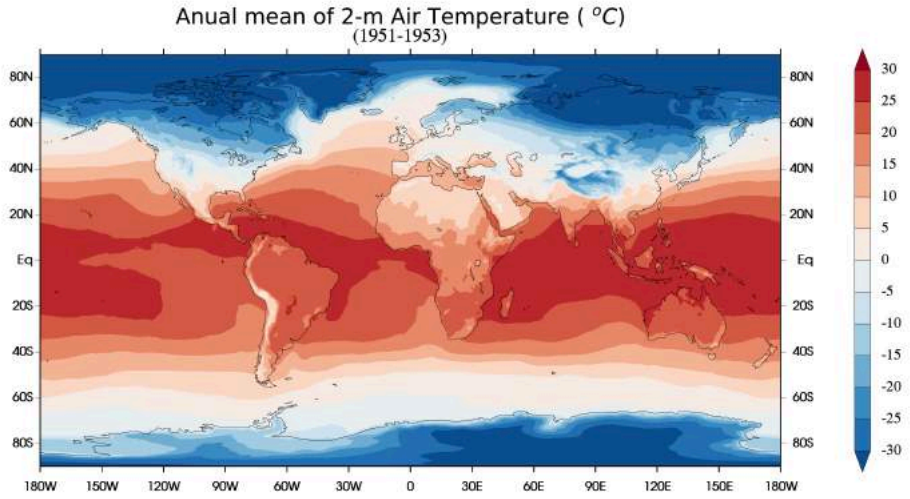

Figure 1: Annual mean of the surface (2m) air temperature (°C) field from the first three years (1951-1953) of the CAM5 simulation using observed SST and sea ice boundary conditions.

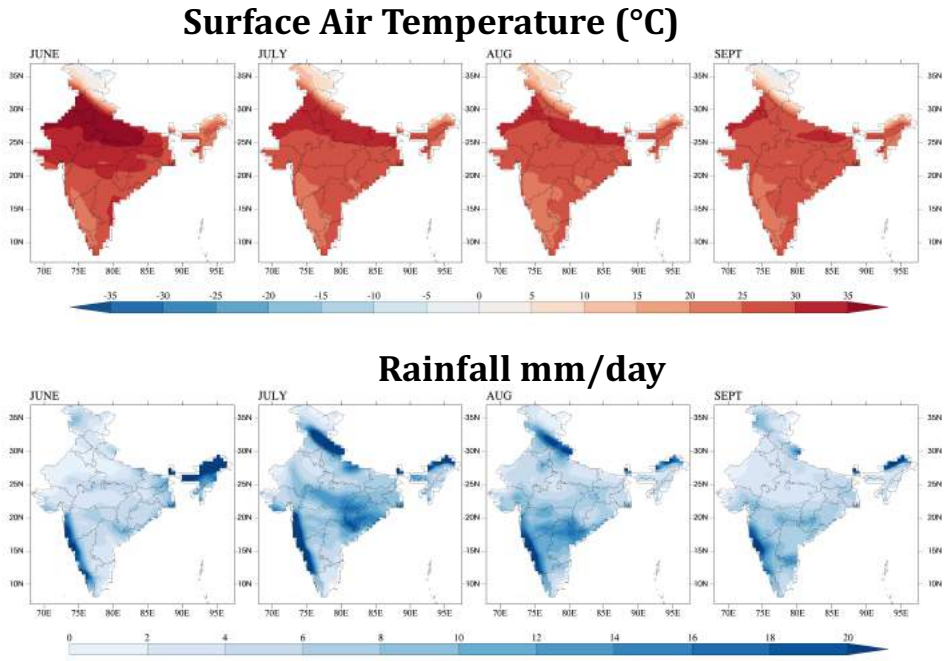

Figure 2: The individual monthly averages (during monsoon season) of surface (2m) air temperature (°C) is shown in the top row. The bottom row shows rainfall (mm/day) during the corresponding months.

Status of Simulations:

Test simulations were carried out at ~1 degree resolution to iron out issues with the boundary conditions. The CAM simulations using observed historical SST and sea-ice (post 1950) have been performed at the IIT Delhi supercomputing facility PADUM. The boundary conditions for the model's present day and future simulations have been created and simulations were ready to be performed in June 2019. However, the delays in procurement of Storage Server (to store and process the output) meant that the runs had to be put on hold. The Storage Server was finally delivered and installed on 19-06-2019. In the meantime, the IIT Delhi HPC PADUM was upgraded (hardware and software) in July 2019. The model was reinstalled on the HPC after the upgrade process.

The Historical period simulations were ready to resume at the end of July/beginning of August 2019. However, computing time allocation for Rs. 25 Lakhs on IITD Supercomputer PADUM was exhausted (amount from first year's budget allocation). Therefore, additional resources were requested in June 2019 to complete the simulations. Despite numerous reminders, no decision was forthcoming on either releasing the second year's funds or permitting the use of available funds from other budget heads but staying within the sanctioned amounts for different budget heads. A request was made at the progress review meeting convened on 24-03-2020. Following another report presentation on 17-06-2020, further clarifications on the budget requests were sought by INCCC on 06-07-2020. The approval to use available funds from other budget heads and the extension of the project up to 30-09-2021 were only received in March 2021 (Ref No. 28/8/2016-R&D/ dated 19-03-2021). This 6-month extension was not sufficient to restart the computations especially since the manpower needed to complete the simulations was no longer available.

The project had been jump-started with two research scholars working on this project who have experience in running the CESM CAM. However, both left on completing the PhD requirement at IIT Delhi by June 2019. New staff was to have been recruited and trained to complete the project. Training new staff to run the model requires at least 6 months with an additional 6 months' time required to perform the computations.

The lack of clarity on funds use, delays in approving extensions to the project deadline and the pandemic have all meant that the simulations could not be carried out.

References:

Fiorino, M., 2004: *A multi-decadal daily sea surface temperature and sea ice concentration data set for the ERA-40 reanalysis.* ECMWF, Shinfield Park, Reading, https://www.ecmwf.int/node/9396.

Hurrell, J., J. Hack, D. Shea, J. Caron, and J. Rosinski, 2008: A New Sea Surface Temperature and Sea Ice Boundary Dataset for the Community Atmosphere Model. *J. Clim.*, **21**, 5145–5153, doi:10.1175/2008jcli2292.1.

Final Report

Dynamic Downscaling to Study Climate Change Impacts on Water Resources in India using Weather Research and Forecasting Model

IIT, Madras

1. Introduction

Climate projections are required for effective Vulnerable, Impact, and Assessment (VIA) studies in agricultural and hydrological domain. Numerous Global Climate Models (GCMs) provide future projections for the Representative Concentration Pathway (RCP) scenarios until 2100 with a spatial resolution ranging from 250 to 600 km. However, the present resolution of the GCMs are coarser when compared to the exposure units of the impact assessments. Also, the predictability of inter-seasonal oscillations in Indian sub-tropics had been limited by the GCMs and there is systematic dry bias under climate change scenarios.

Average Temperature of India had seen a 0.7°C increase during 1901–2018. This rise in temperature is largely attributed to the Green House Gases (GHG)-induced warming forced by man-made changes in LULC and anthropogenic aerosols. It is expected by model models that by 2100 the average temperature rise in India would be roughly 4.4°C from the baseline period (1976-2005) in the high concentration pathway – RCP 8.5 scenario. Frequency and duration of heat waves and cold nights are expected to increase rapidly from earlier studies which have analyzed various GCM outputs across India (Krishnan R. et al., 2020). The total precipitation during the Indian summer monsoon (ISM) is expected to reduce in the future, while the rainfall extremes are projected to be more localized in nature and their intensity & frequency is anticipated to increase by most of the GCMs. The increased variability in ISM with widespread reduction in rainy days and increased moisture demand in warmer (increased temperature) atmosphere, the climate model projections strongly indicate a likelihood in the increased frequency, intensity and spatial extent of drought conditions in India by 2100 under RCP8.5 scenario (Krishnan R. et al., 2020). Thus, the alarming figures in terms of extremes in the climate variables increase the need to closely address the implications of climate change, but only after handling the uncertainty in the present GCM outputs.

Dynamical downscaling with Regional Climate Models (RCMs) help in introducing the small scale exchanges via representation of the land-sea contrasts, realistic coastlines and complex topographical details (Giorgi and Mearns, 1999). Thus, enhancing the spatio-temporal variability of the microclimatic variables derived from the climate projections at finer scales (Ratnam and Kumar, 2005; Dash et al., 2006; Raju et al., 2015). The convective processes were better resolved by the RCMs improving the regional patterns of Indian summer monsoon (ISM) circulation (Varikoden et al., 2018). However, significant experiments to select appropriate model parameterizations are needed to overcome bias and uncertainty (Mishra et al., 2014).

The objective of the project is twofold, one is to conduct dynamical downscaling of climate over India using Weather Research and Forecasting Model to derive daily micrometeorological variables at a spatial resolution of 25 km. Prior to using the model for projecting the future climate, it is important to assess the sensitivity of the model and thereby, the predictability in capturing the inter-annual variability of Indian climate. Once the dynamic downscaling exercise is completed, it is highly required to understand the model biases and the biases inherent in the input GCMs and its proliferation in the regionally downscaled variables. The second objective, bias correction aims at reducing above-mentioned systematic biases and to correct those bias in the future projections.

The report is organized in a way that the project overview is discussed in section 2, the detailed methodology used in the modelling exercise is elaborated in the methodology section in section 3. The detailed results and discussion (section 4) are organized to compile the learnings from sensitivity analysis of the Weather Research and Forecasting (WRF) regional climate model with respect to long-term climate simulations, in section 4.1. The final model setup and the performance of the raw weather variables like Precipitation and Temperature are discussed in detail in section 4.2. The bias corrected variables, the future projections and implication are elaborated in section 4.3. The section 5 enlists the major conclusions and the scope of the downscaling exercise.

2. Project Overview

a) Weather Research and Forecasting (WRF) regional climate model – to generate daily microclimatic variables (Surface Temperature, Precipitation, Wind speed, Relative humidity, Solar radiation) at 25 km spatial resolution for years 1951-2100 across India.

b) Global climate models selected - NORESM1 & CANESM2

c) Climate scenarios

- HISTORICAL - 1951-1980, 1981-2005
- RCP 4.5 - 2011-2040 (early), 2041-2070 (mid), 2071-2100 (late)
- RCP 8.5 - 2011-2040 (early), 2041-2070 (mid), 2071-2100 (late)

3. Methodology

3.1 Regional Climate Model

The regional climate model selected in the present study is Weather Research and Forecasting (WRF) model. WRF is a non-hydrostatic, fully compressible, terrain-following sigma coordinate mesoscale model developed by National Center for Atmospheric Research (NCAR) (Skamarock et al., 2008). The model is being used most widely for both research needs and numerical weather predictions. It provides wide range of physics options from simple to advanced, allows parallel computing and data assimilation. Studies have explored the performance of WRF model for climate downscaling and prediction of future extremes. The results are promising and superior amongst the available RCMs (Ratnam et al., 2005; Srinivas et al., 2013).

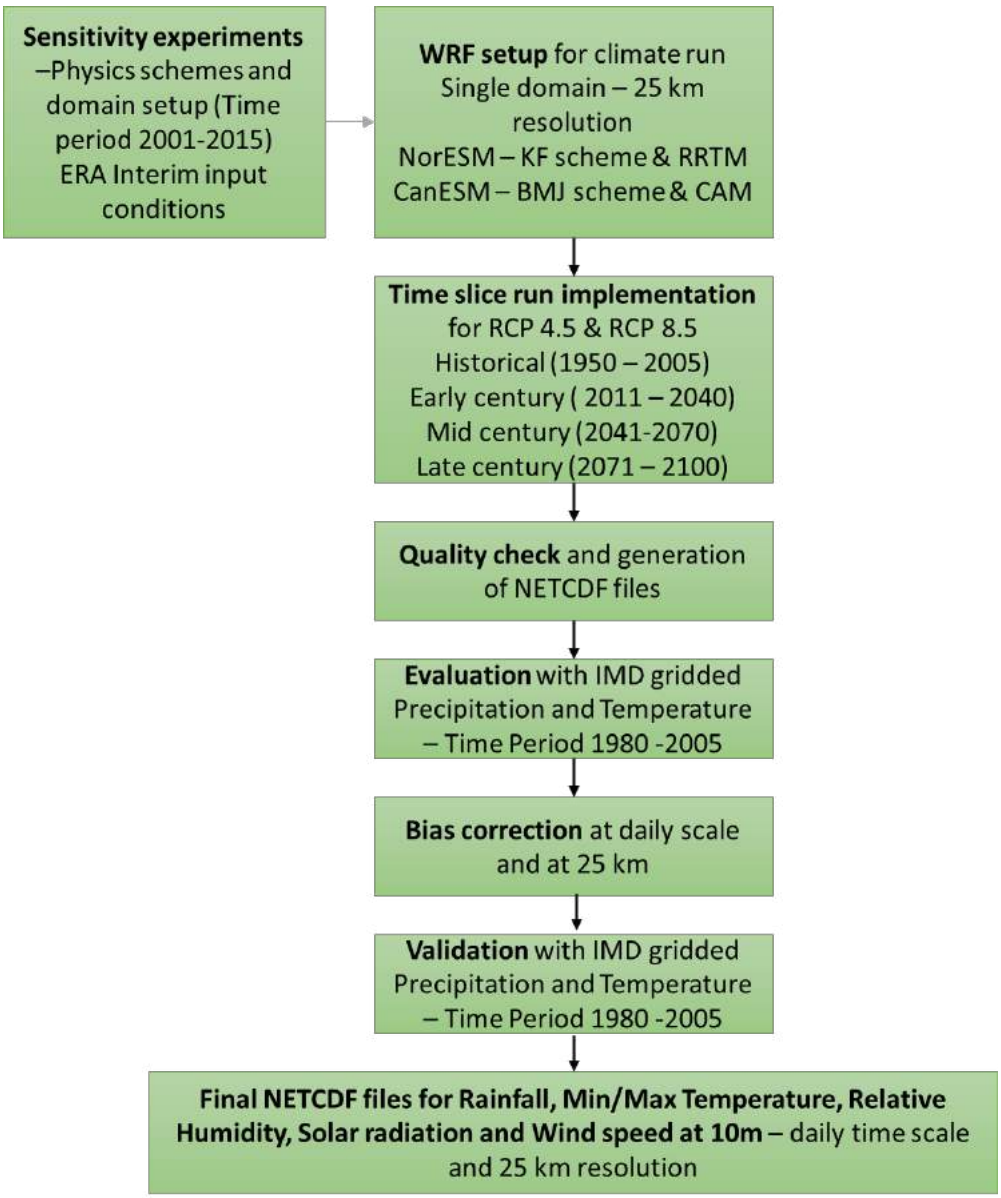

Fig. 1 Methodology adapted

3.2 Sensitivity experiments

3.2.1 Initial and Boundary conditions

In order to use the model for future predictions, it is important to evaluate its performance against the observed data both spatially and temporally. Reanalysis data are output of GCMs corrected to match global climatology by assimilation of data from surface and upper air observatories across the earth. Thus, they are considered to be the best available boundary conditions to force the RCMs. In the present study, the European Centre for Medium-Range Weather Forecasts Re-Analysis (ERA-Interim) and National Centers for Environmental Prediction (NCEP/NCAR) datasets were used. The resolution of NCEP/NCAR and ERA-Interim datasets were at 2.5 degree latitude/longitude (28 vertical levels) and 1 degree

latitude/longitude (60 vertical levels) respectively. The lateral boundary conditions were updated at 6 hourly time intervals.

3.2.2 Observational data

To validate the model output against observational data, India Meteorological Department (IMD) observed gridded datasets of precipitation and temperature is acquired. The IMD gridded rainfall dataset is available at resolution of 0.25◦ and temperature at 1◦ resolution.

3.2.3 Experimental Setup

The simulation domain for the current study is shown in the Fig. 2. The model was configured with two domains, a 125-km resolution outer domain (D1) (75 x 59 grid points) and a 25-km resolution inner domain (D2) (161 x 166 grid points) implemented as two-way nesting. Based on results from previous studies, various critical physics options are selected as listed in Table 1. The C01 is considered as the control run and the sensitivity analysis is performed for the normal monsoon year 2005. Later, the model with best physics combination is run for a time period of 15 year (2001-2015), to assess the model's ability in capturing the inter-annual variability and seasonal dynamics.

Table 1 Different Physics options selected for sensitivity analysis

Cases	Microphysics	Long-Wave Radiation	Short-wave Radiation	Planetary Boundary Layer	Cumulus Physics	Difference in physics
C01	WSM6	CAM	CAM	YSU	Tiedtke	Control Run
C02	WSM6	Dudhia	RRTM	YSU	Tiedtke	ra
C03	WSM6	CAM	CAM	YSU	Kain-Fritsch (KF)	cu
C04	WSM6	Dudhia	RRTM	YSU	Kain-Fritsch	ra, cu
C05	WSM3	Dudhia	RRTM	YSU	Kain-Fritsch	mp, ra, cu
C08	WSM6	Dudhia	RRTM	YSU	Betts-Miller-Janjic (BMJ)	ra, cu
C10	WSM6	CAM	CAM	YSU	Betts-Miller-Janjic	cu
C11	WSM6	CAM	CAM	YSU	Grell-Freitas	cu
C12	WSM6	CAM	CAM	YSU	New Tiedtke	cu
C13	WSM6	RRTMG	RRTMG	YSU	New Tiedtke	ra, cu

Note: The last column represents the changes made in the control run. ra – radiation physics; cu – cumulus scheme; mp – microphysics scheme.

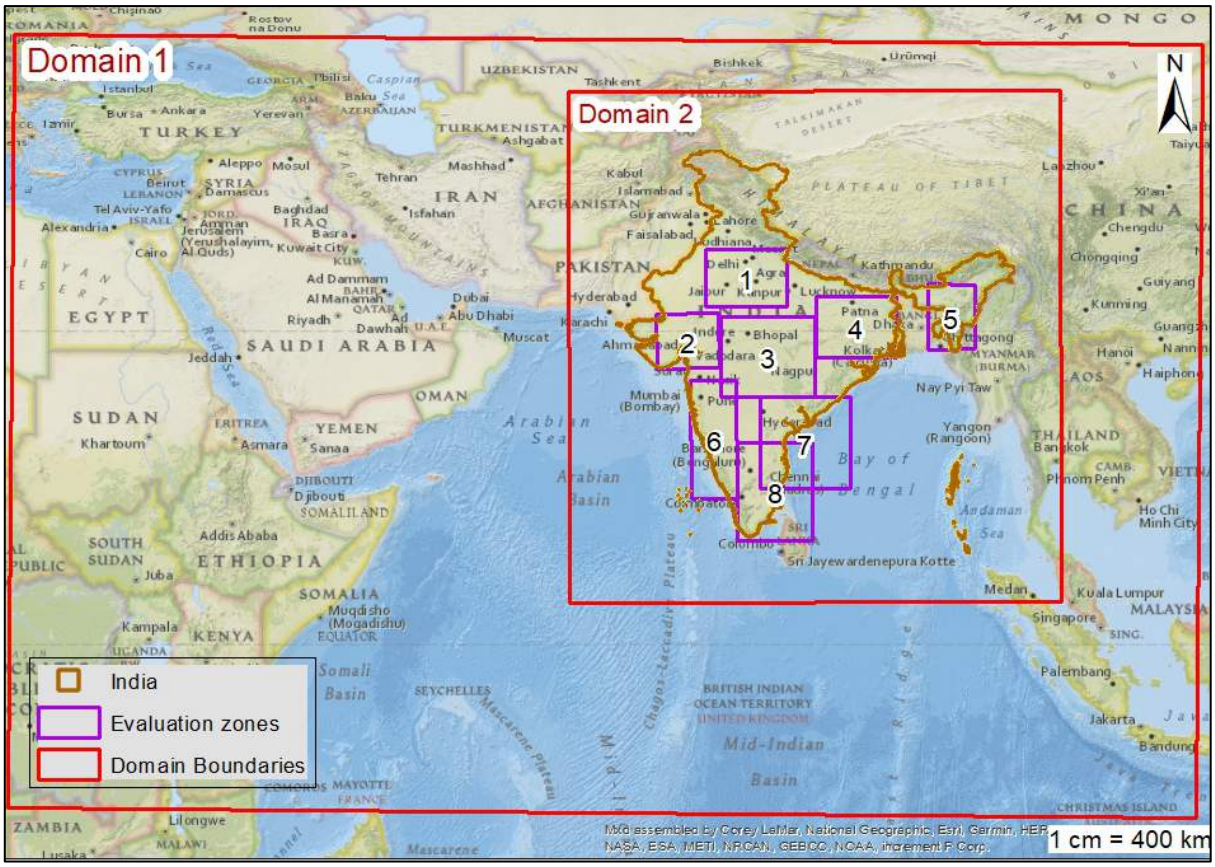

Fig. 2 Simulation domain and rainfall zones considered in the study.

3.2.4 Performance Evaluation

3.2.4.1 Grid-based Statistical analysis

Grid-based statistics like Root-Mean Squared Error (RMSE) and Percent Bias (PBIAS) are used to evaluate the performance of the model in the evaluation domain D2. The evaluation is done for annual time period as well as for different seasonal time slices Pre-Monsoon (Mar-Apr) (PM), South-west Monsoon (June-September) (SWM) and North-east Monsoon (October-December) (NEM).

3.2.4.2 Zonal based Statistical analysis

Seven major zones (Z1-Z7) are selected based on study by Dasari et al., 2011; Srinivas et al., 2013. An additional zone Z8 is added to evaluate the performance of the model in simulating rainfall patterns across Tamilnadu (Table 2). Zonal RMSE and BIAS, Average zonal rainfall where rain is 2.5 mm or more (threshold set as per IMD definition of rainy day), No of grids where rain is 2.5 mm or more and Coincidental grids percentage where rain is 2.5 mm or more (with differing thresholds10 mm, 20 mm and 50 mm) are used as evaluation metrics. No of rainy days within the zones are calculated and compared with the IMD data.

Table 2 Different evaluation zones

Zones	Region	No. of Grids
Zone 1 (Z1)	Northern	380
Zone 2 (Z2)	Northwest	267
Zone 3 (Z3)	Central	644
Zone 4 (Z4)	Eastern	390
Zone 5 (Z5)	Northeast	205
Zone 6 (Z6)	Southwest	213
Zone 7 (Z7)	Southeast	256
Zone 8 (Z8)	South	360

3.3 Downscaling Procedure

The final WRF model was setup with single domain (59 E – 105.9 E; 1.35 N – 48.1 N) at 25 km containing 191 x 191 grid points. The physics configuration will be discussed in Section 4.2. The model was run for five time slices historical 1 (1951-1980), historical 2 (1981-2005), early century (2011-2040; RCP4.5 and 8.5), mid-century (2041-2070; RCP4.5 and 8.5) and late century (2071-2100; RCP4.5 and 8.5) and for two GCMs – NORESM1 & CANESM2. Total 16 runs (5 time slices x 2 scenarios x 2 GCMs) were made with each run comprising 30 years simulation and dynamic time integration method was adapted in the WRF model. Each run implemented with 120 cores took about 30 days and the whole 150 year simulation downscaling two GCMs roughly took 300 days (~ 10 months) to complete. Server resources to preprocess, run and post-process the data, were utilized from Pan India institutes viz. IIT Bhuvaneshwar, IIT Madras AQUA server, IITM Pune Aditya server and internally purchased Linux server (56 processors - Intel(R) Xeon(R) Gold 5120 CPU @ 2.20GHz – 6 TB hard disk). The outputs of WRF was post-processed to calculate daily variables of Precipitation, Minimum Temperature, Maximum Temperature, Relative Humidity, Windspeed at 10 m and Solar radiation. 96 NetCDF files (8 time slices x 2 GCMs input x 6 climate variables) were generated with a size of ~ 800 MB each (total size of the final output– 80 GB). Initial data quality check was done to find spatially and temporally inconsistent values.

3.3.1 Initial and Boundary conditions

NorESM2 (the second version of the Norwegian Earth System Model) is modified version of CESM2 (the second version of the Community Earth System Model) with addition of models to represent the ocean and ocean biogeochemistry. Several upgrades in Atmospheric module like improved parameterization to represent radiation-cloud-aerosol interactions, deep convection schemes and albedo estimation. However, the study by Øyvind Seland et al., 2020 concluded NorESM2 to be a cold model like its predecessor CESM2 with reduced atmospheric long-wave cooling and consequently leading to positive SST biases predominantly in the

tropics. El Nino–Southern Oscillation (ENSO) and El-Nino teleconnections were better captured in the tropics, while the Madden–Julian Oscillation (MJO) had less agreeable representation in the model.

The second generation of Earth System Model CanESM2 is developed by the Canadian Centre for Climate Modelling and Analysis (CCCma) of Environment and Climate Change Canada (Yang and Saenko, 2012) at resolution 2.81° × 2.79°. The new model includes interactive effects between atmosphere-ocean general circulation model, a land-vegetation model, sea-ice model and terrestrial and oceanic interactive carbon cycle. CanESM2 has been reported to poorly capture the tropical cyclones (Shen et al., 2021) but reasonably represent the Asian Summer monsoon precipitation and temperature (Li et al., 2019).

The emissions, concentrations, and land-cover change projections are described by the Representative Concentration Pathways scenarios such as RCP2.6, RCP4.5 and RCP8.5. RCP4.5 represents a stabilization (without overshoot) in radiative forcing at 4.5 W/m2 post 2100. RCP8.5 represents a rise in radiative forcing to 8.5 W/m2 in 2100 (Krishnan R. et al., 2020). Here due to computational concerns, we had chosen RCP4.5 (conservative pathway) and RCP8.5 (high concentration pathway).

3.3 Procedure for deriving surface climate variables

The cumulative total cumulus/convective precipitation and the cumulative total non-convective precipitation outputs from WRF were summed up at 6-hourly basis to get the 6-hourly total precipitation. The daily precipitation (mm/day) was derived by accumulating the 6-hourly precipitation from WRF.

The minimum and maximum temperatures (°C) were calculated from the 6-hourly temperature at 2 m output from WRF. The daily relative humidity (%) was calculated from daily averaged temperature, mixing ratio, and pressure (Murray, 1967).

The wind speed (m/s) was calculated from daily zonal wind component (u) and meridional wind component (v) using sqrt (u^2+v^2). The solar radiation (W/m2) was derived from air temperature differences using Hargreaves method as described in Food and Agriculture Organization (FAO) Irrigation and Drainage Paper 56 entitled: Crop evapotranspiration - Guidelines for computing crop water requirement. (https://www.fao.org/3/x0490e/x0490e07.htm#solar%20radiation). The extraterrestrial radiation for daily periods used with the method along with diurnal temperature differences, are an approximation based on the Julian day and latitude of the place. To compare and validate the radiation fluxes more realistically with Indian Monsoon Data Assimilation and Analysis reanalysis (IMDAA) output variable Surface Downward Short Wave Radiation Flux, the daily averaged Downward Short Wave Flux at Ground Surface (SWDOWN) (W/m2) output from WRF was also used.

3.4 MTCLIM – deriving surface weather variables from statistically downscaled temperatures and precipitation grids

A parallel work was done by the IIT, Madras team to help IIT, Bombay derive the surface variables like Day Length in s, Vapour Pressure Deficit in Pa and solar radiation in W m-2 using the MTCLIM procedure. The implementation of MTCLIM involved quality check on the downscaled variables from IITB and grid-based implementation of MTCLIM procedure. A total of 30 runs (2 statistical downscaling methods x 5 global models x 2 scenarios & historical) (http://www.regclimindia.in/) were performed, with each run approximately taking 5 days. The learnings on the size and format of the publically presented output data for each variable were derived from this exercise.

3.5 Bias correction

A methodology based on daily correction factors for bias in rainfall was adapted based on Smitha et al., 2018. We applied Quantile mapping (QM) bias correction on a sliding window basis in which the distribution of RCM rainfall matches with the observed rainfall distribution. We use IMD observed daily rainfall and diurnal temperature data at 0.25 degree and 1 degree resolution respectively. The bias correction through the QM method was achieved by using a transfer function and we used gamma distribution to fit the rainfall data in this study. For the bias correction of each RCM grid, the nearest IMD grid was obtained. The daily rainfall values were corrected based on the data pooled for a 31-day sliding window for each day from the climatological period. The shape and scale parameters of gamma distributions were obtained for all the 365 days for observed and RCM rainfall data. The cumulative distribution function (CDF) values were acquired for each day RCMs value and we obtained the corrected rainfall for this CDF value using the inverse of the gamma function derived from the corresponding day's observed data. The correction for rainfall and temperature was multiplicative and additive respectively. In case of dry pixel in the 31-day window, the effect of neighborhood was also considered to apply the procedure.

4. Results and Discussion

4.1 Highlights from sensitivity analysis

Fig. 3 represent the monthly accumulated rainfall values for the year 2005 averaged across different zones. Highest variability was noticed in the months of June-July-August-September (JJAS) i.e. during the South-west monsoon (SWM) season. Under prediction of summer monsoon rains were observed in all zones. Zones 2, 3 and 6 have high over-prediction of SWM rainfall. Highest under-prediction of rainfall in June month across all zones which demonstrated the delay in onset of SWM during the year 2005 by all the WRF simulations. Highest over-prediction was observed by C11 (GF cumulus + CAM) across all zones and months. The results indicate that the radiation physics schemes produce not only biases in radiation fluxes but more importantly, result in large bias in precipitation for year-long simulations.

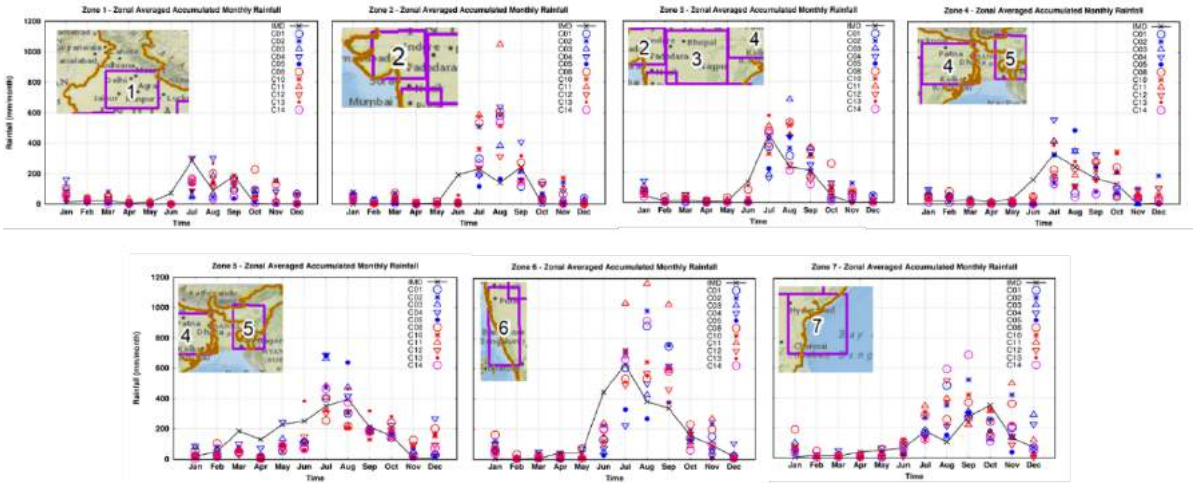

Fig. 3 Zonal-averaged monthly accumulated rainfall (mm/month) for the simulation year 2005

Table 3 lists the zonal RMSE of various evaluation metrics calculated for different cases in simulating Precipitation and Temperature. The cases C03 and C12 are highlighted as the performance was best in capturing the inter-annual and spatial variability amongst the other cases.

Table 3 RMSE of various metrics for Rainfall and Temperature

Cases	RMSE - Zone 1						RMSE - Zone 2						RMSE - Zone 3						RMSE - Zone 4					
	Rain	Max Rain	Rain > 2.5	Pix > 2.5	Tmax	Tmin	Rain	Max Rain	Rain > 2.5	Pix > 2.5	Tmax	Tmin	Rain	Max Rain	Rain > 2.5	Pix > 2.5	Tmax	Tmin	Rain	Max Rain	Rain > 2.5	Pix > 2.5	Tmax	Tmin
C01	5.46	55.65	10.33	88.37	3.65	1.65	11.12	97.21	12.44	72.01	3.15	2.27	7.55	81.43	9.94	153.66	2.13	1.60	6.24	67.07	9.30	111.95	3.73	2.50
C02	7.25	59.40	11.32	100.20	3.77	2.69	11.66	104.31	13.39	79.20	3.25	3.14	8.21	92.28	10.48	167.91	2.80	2.30	7.26	71.87	10.80	120.78	4.89	2.94
C03	6.09	51.87	9.71	103.29	3.57	1.47	9.41	57.34	11.22	68.57	3.36	2.24	9.77	102.58	12.98	163.10	2.12	1.97	7.49	63.67	9.63	91.38	3.82	2.85
C04	7.86	60.70	10.92	107.10	3.70	2.34	13.12	79.85	14.73	81.72	3.61	3.19	9.10	83.34	12.03	191.01	2.46	2.63	9.14	71.85	11.36	101.33	4.03	3.49
C05	5.00	50.03	9.28	84.68	4.23	2.67	6.92	51.48	9.68	55.83	3.96	2.49	7.91	76.64	10.94	165.81	2.38	2.01	9.33	61.02	10.36	101.49	3.75	3.09
C08	6.92	61.16	10.45	111.06	3.86	2.44	10.75	66.49	11.66	89.55	3.30	2.86	8.68	100.38	9.81	188.54	3.09	2.12	5.72	61.51	8.36	101.75	4.90	2.93
C10	5.16	52.68	9.42	95.34	3.49	1.68	9.27	71.75	10.54	86.22	2.71	2.33	7.17	73.05	8.38	154.53	2.68	1.65	6.85	60.47	9.45	91.78	4.63	2.48
C11	5.31	52.65	9.69	79.06	3.23	1.64	19.03	138.66	20.42	76.26	2.81	2.05	10.33	110.39	13.37	138.21	2.48	1.46	7.49	68.07	9.67	88.75	3.97	2.19
C12	4.65	48.64	8.81	96.48	3.56	1.59	7.61	66.35	8.97	77.70	3.31	2.37	6.41	50.71	8.07	157.75	2.54	1.53	7.07	65.26	9.88	118.25	3.63	2.73
C13	6.84	79.25	10.19	104.24	2.87	2.53	10.82	71.88	11.20	93.39	2.40	2.74	8.99	104.31	10.39	164.16	1.78	2.48	6.81	78.93	8.76	104.55	3.12	3.17

Cases	RMSE - Zone 5						RMSE - Zone 6						RMSE - Zone 7					
	Rain	Max Rain	Rain > 2.5	Pix > 2.5	Tmax	Tmin	Rain	Max Rain	Rain > 2.5	Pix > 2.5	Tmax	Tmin	Rain	Max Rain	Rain > 2.5	Pix > 2.5	Tmax	Tmin
C01	6.87	57.56	9.21	76.17	3.43	2.23	12.61	104.35	18.12	53.17	2.62	1.96	11.12	85.14	15.70	68.15	2.16	2.00
C02	8.38	60.87	10.13	77.42	4.20	3.64	14.68	92.02	19.63	61.95	3.29	2.13	11.78	89.83	15.96	70.44	3.05	2.18
C03	9.39	79.18	10.33	72.82	3.45	2.51	10.98	68.54	18.45	47.08	2.35	2.12	10.18	78.59	15.41	64.58	2.00	2.15
C04	10.69	61.61	11.82	74.95	3.56	3.53	13.34	75.73	19.82	60.70	2.76	2.35	9.32	67.48	14.79	70.74	2.64	2.31
C05	7.99	52.91	9.02	70.36	3.80	2.84	10.16	61.67	17.67	51.47	2.25	1.90	6.74	54.77	11.44	58.38	2.14	1.94
C08	9.09	60.15	10.82	83.60	3.78	3.47	10.80	74.24	18.21	61.79	3.62	2.01	9.60	74.49	12.99	73.52	3.43	2.03
C10	7.90	60.24	10.75	75.64	3.34	2.41	10.04	74.48	16.94	51.98	3.11	1.86	8.98	69.73	12.53	63.05	2.71	1.87
C11	7.57	53.30	8.93	72.73	2.91	2.01	17.78	140.33	30.65	49.78	3.19	2.16	14.16	94.31	19.29	63.49	2.48	2.25
C12	8.14	58.49	10.08	79.08	3.26	2.19	9.62	66.50	16.77	53.66	2.75	1.82	11.37	74.07	17.10	67.50	2.22	1.96
C13	8.60	62.17	10.22	73.94	2.68	3.21	8.76	53.95	16.28	57.79	1.95	1.98	8.61	65.45	12.30	79.02	1.63	1.90

Finally, the best performing case C03 with WSM6 microphysics scheme, CAM radiation physics, Kain-Fritsch cumulus physics and NOAH LSM as land surface physics scheme was selected for the long-term run (2001-2007). Fig. 4 display the annual accumulated rainfall of C03 versus the IMD gridded precipitation. A wet bias in central India and south of Western Ghats was observed while the North-eastern parts display dry bias in the simulated annual precipitation. The SW monsoon is well simulated in all zones with onset is delayed in zone 6 and wide-spread underestimation in zone 6 and zone 2 (western coasts). For NEM, temporal shift (early simulation of peaks) in zone 7 and wide underestimation is noticed in the zone. The patterns widely match for the other zones. The PM in zone 5 is highly under-estimated.

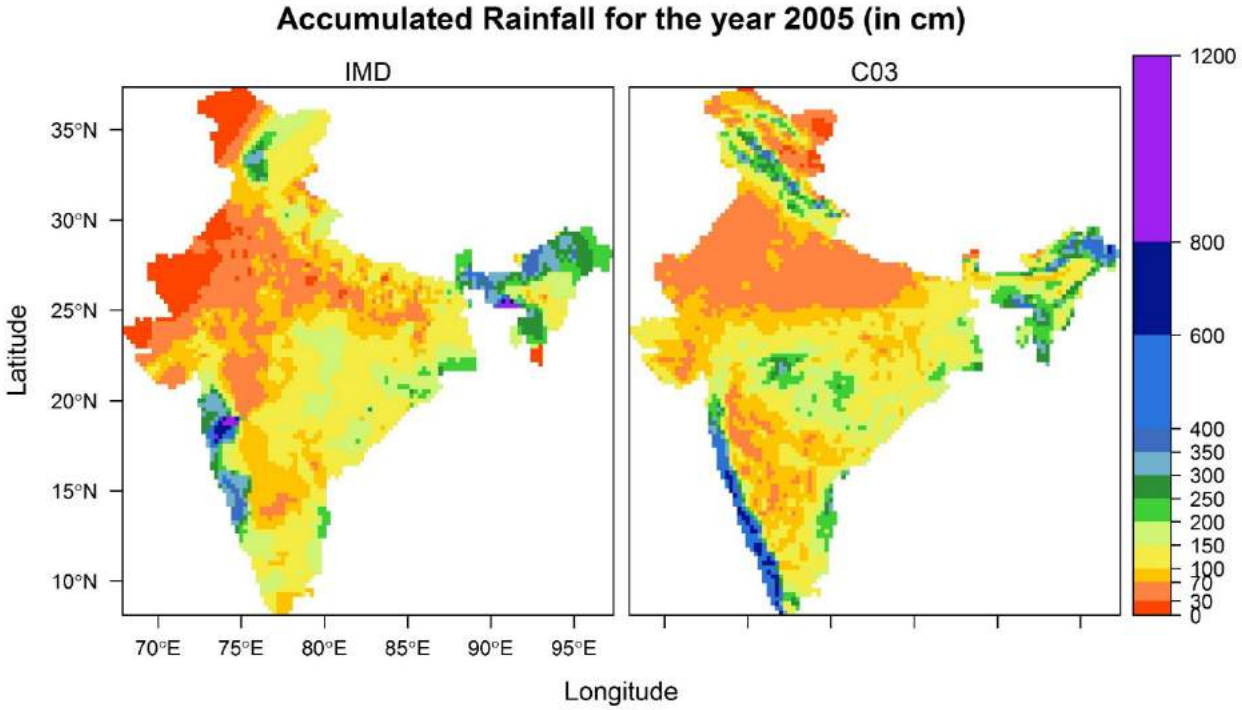

Fig. 4 Accumulated rainfall (mm/month) for the simulation year 2005

4.1.1 Long-term Analysis

4.1.1.1 Wet year – 2007

Spatial map of annual accumulated rainfall (Fig. 5a) shows general under-prediction of rainfall with slight over-prediction in the southern Western Ghats. High under-prediction was observed in the northern parts of Western Ghats, north-Himalayan region (Z1), central India, western India and North-East. The summer monsoon in the NE was highly under-predicted. The spatial pattern during NEM was widely captured by WRF simulation. The zonal statistics display that the performance across the zones was better during SWM and NEM time-period except for the Z2 (North-Western) and Z1 (Northern) (Fig. 6). Highest under-prediction in the number of rainy days for extreme rainfall events (>20 mm/day) was noticed in the zones Z2 (North-Western) and Z6 (South-Western). The performance for other rainfall categories is much better indicating higher skill of WRF in capturing low-moderately high rainfall events.

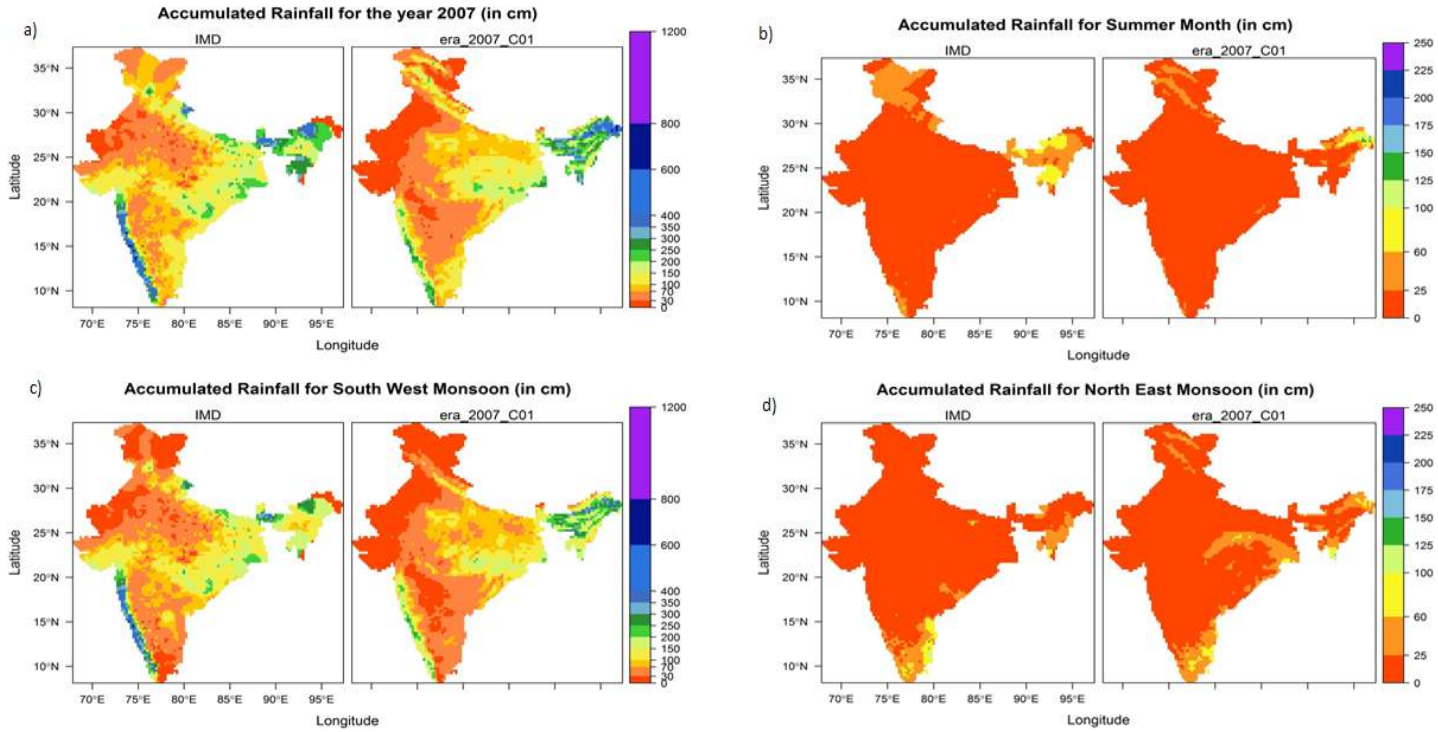

Fig. 5 Spatial maps of accumulated rainfall for the wet year 2007. a) Annual rainfall b) PM period c) SWM period and d) NEM period.

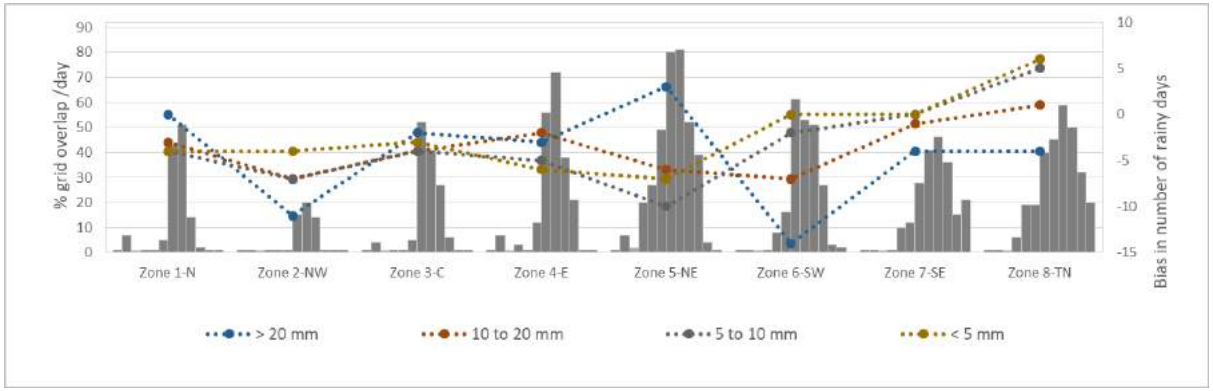

Fig. 6 Zonal statistics – Monthly averaged percent grid overlap/day in primary axis from Jan-Dec and annual-averaged bias in number of rainy days in secondary axis for the year 2007.

4.1.1.2 Dry year – 2004

Spatial map of annual accumulated rainfall (Fig. 7a) shows general under-prediction of rainfall with slight over-prediction in the southern Western Ghats. High under-prediction in the northern parts of Western Ghats, north-Himalayan region (Z1) and North-East. The summer monsoon in the NE is highly under-predicted. The spatial pattern during NEM is widely captured by WRF simulation. The zonal statistics display that the performance across the zones is better during SWM and NEM time-period except for the Z2 (North-Western) and Z1 (Northern). Fig. 8 highlights good performance in NE region except during pre-monsoon months. The bias in rainy days shows high under-prediction in zone 6 especially for extreme rainfall days (>20 mm).

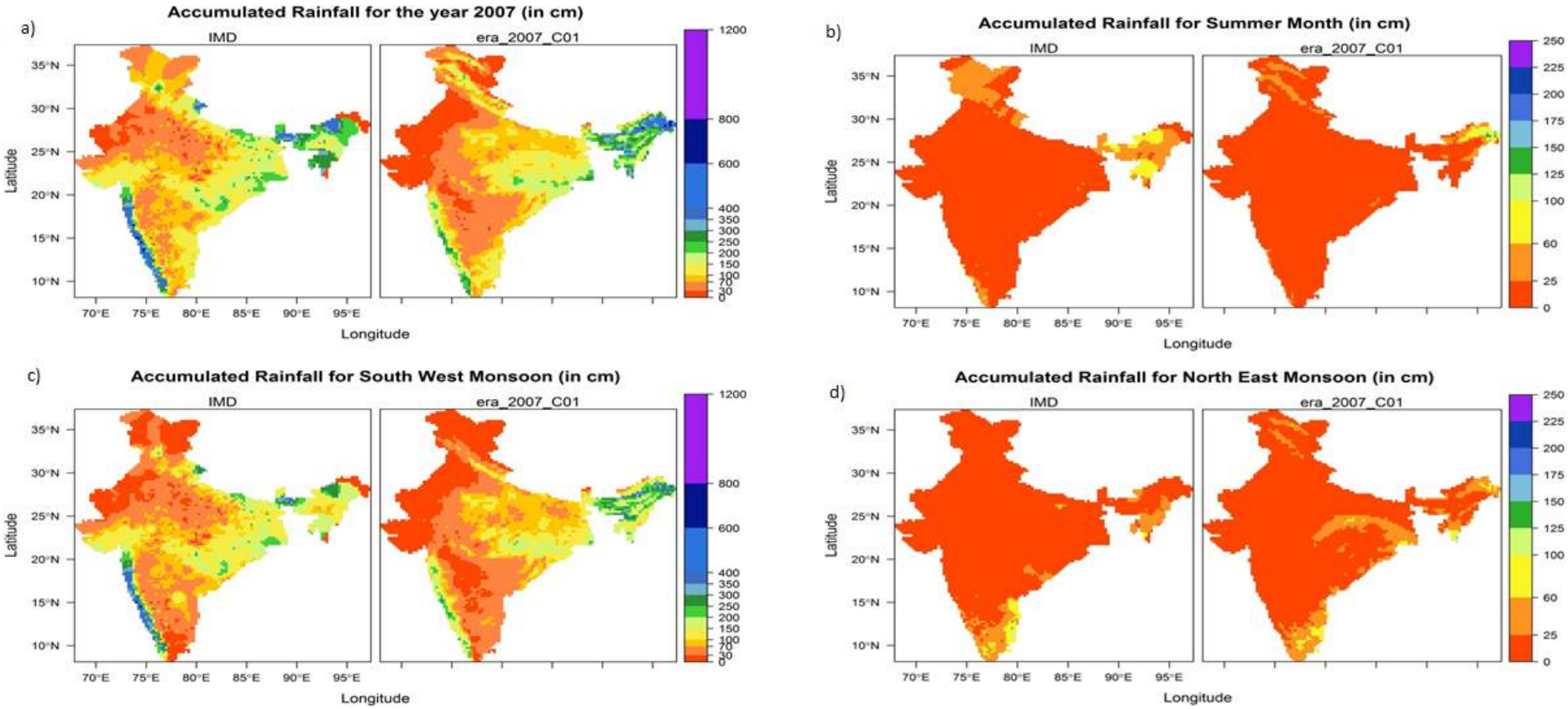

Fig.7 Spatial maps of accumulated rainfall for the wet year 2004. a) Annual rainfall b) PM period c) SWM period and d) NEM period.

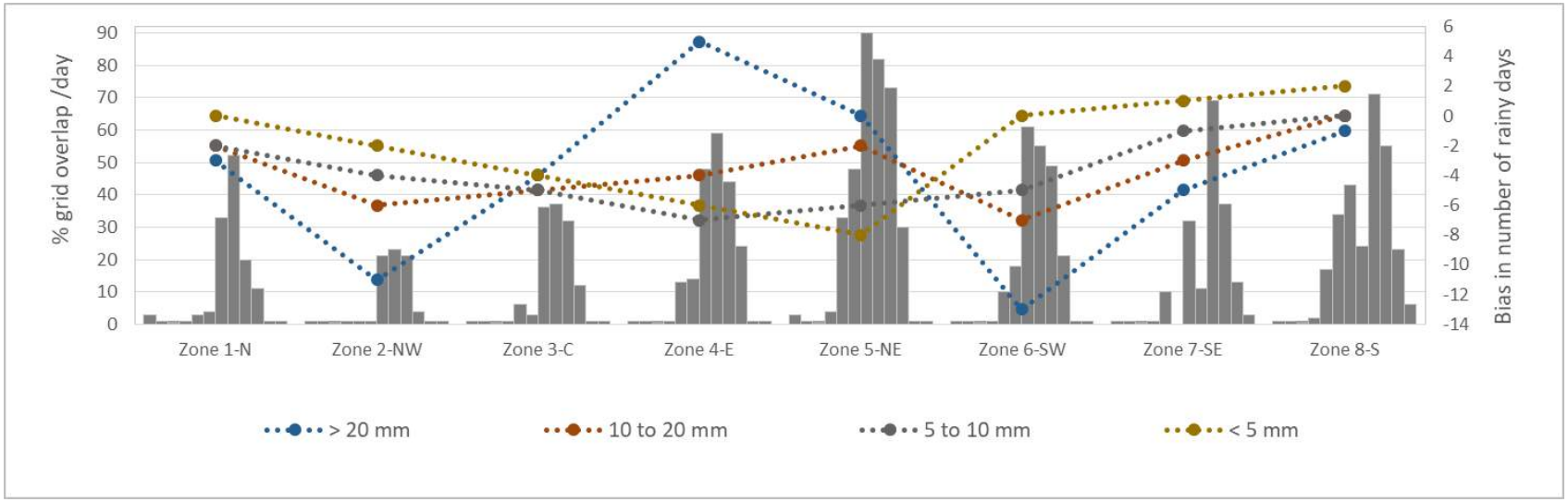

Fig. 8 Zonal statistics – Monthly averaged percent grid overlap/day in primary axis from Jan-Dec and annual-averaged bias in number of rainy days in secondary axis for the year 2004.

4.1.2 Overall Performance

The overall performance during PM (Fig. 9), SWM (Fig. 10) and NEM (Fig. 11) indicates similar that under-estimation North-eastern zone (Z5) during PM, dry-bias in Z6 during SWM and dry-bias in Z6 (east-coast) during NEM. The results are similar to the ones obtained from wet and dry year analysis. There is no much variability in the behavior of the model between years. However, the biases are amplified during the extreme years.

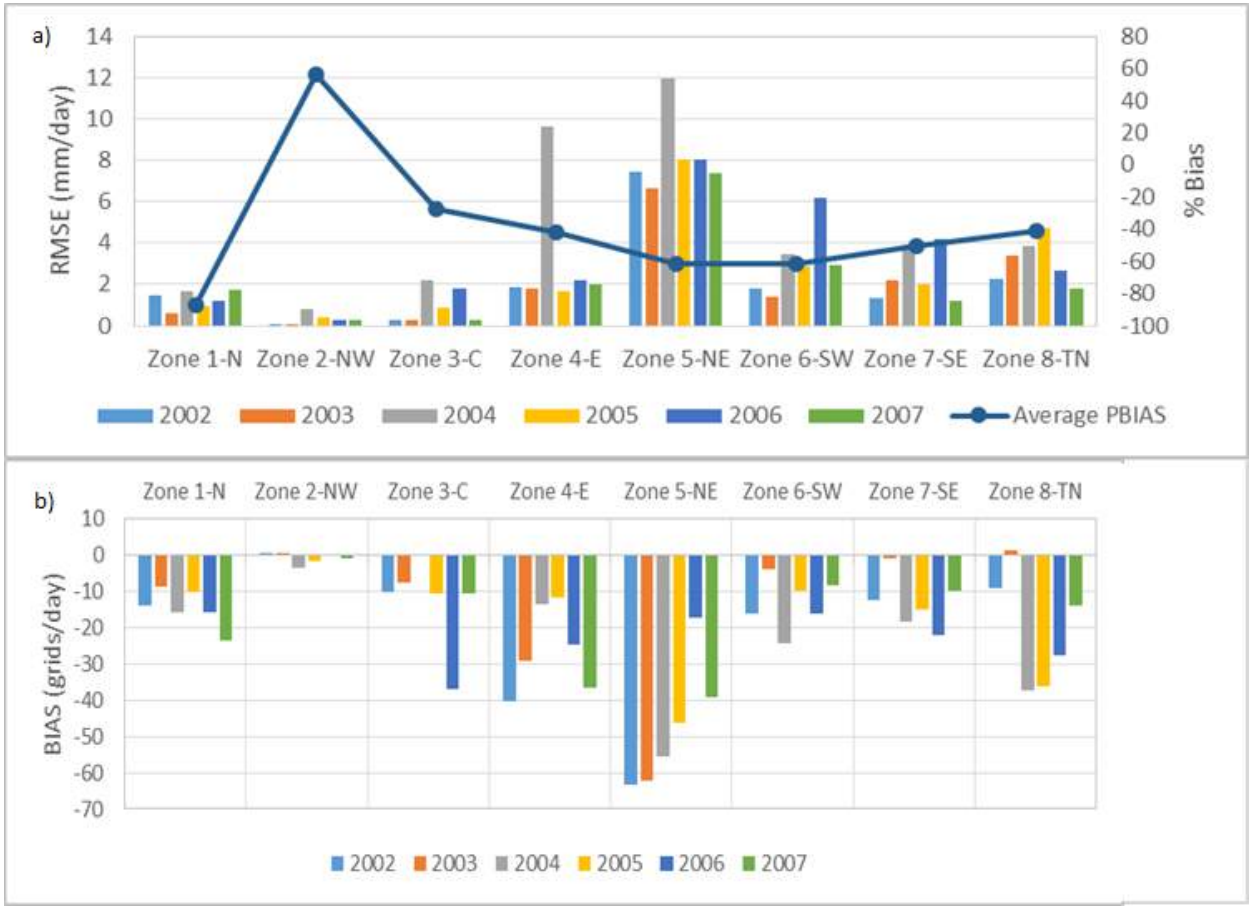

Fig. 9 Overall statistics across 2001-2007 for PM period. A) RMSE in mm/day for each zone along with percent bias in secondary axis and b) Bias in grids/day for all zones.

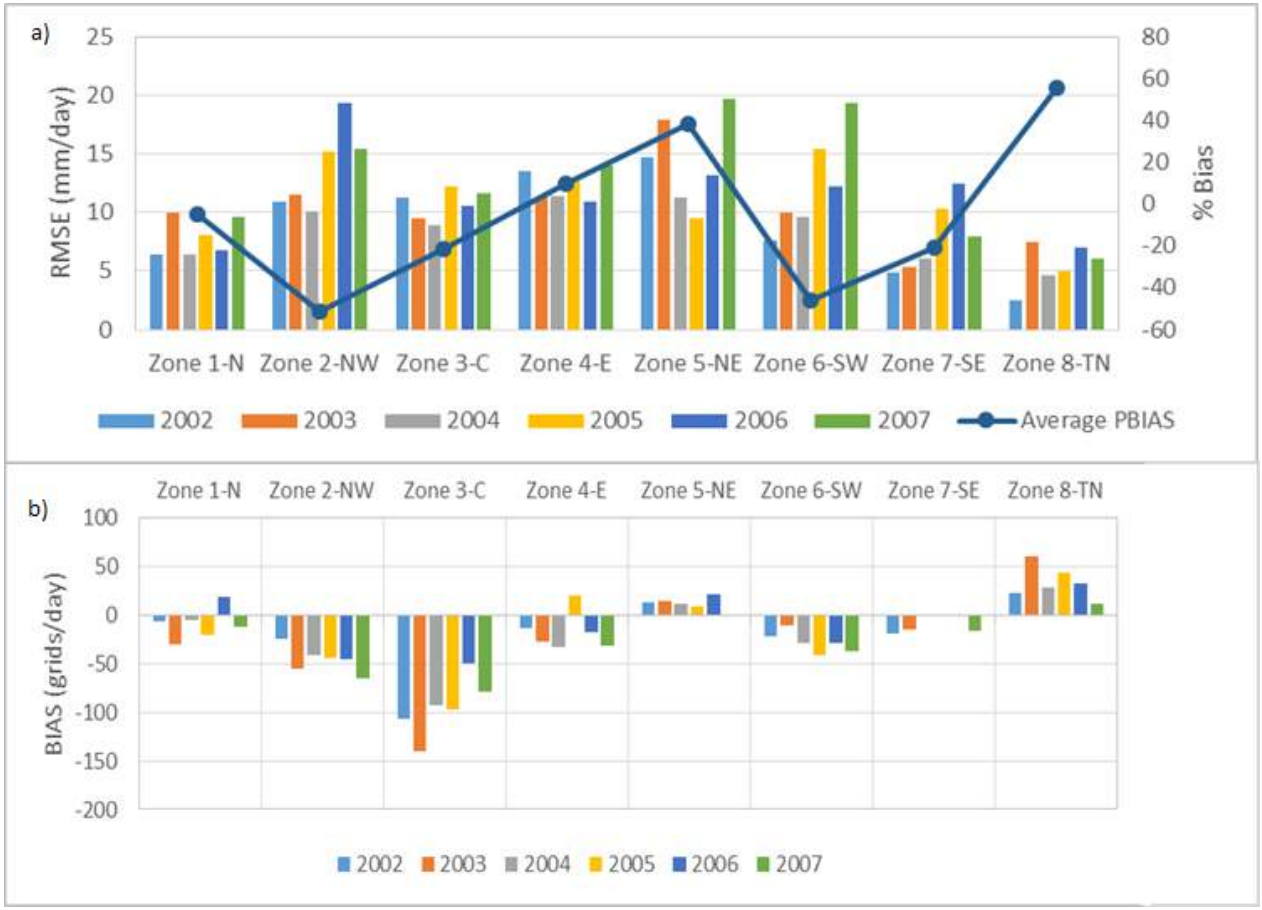

Fig. 10 Overall statistics across 2001-2007 for SWM period. A) RMSE in mm/day for each zone along with percent bias in secondary axis and b) Bias in grids/day for all zones.

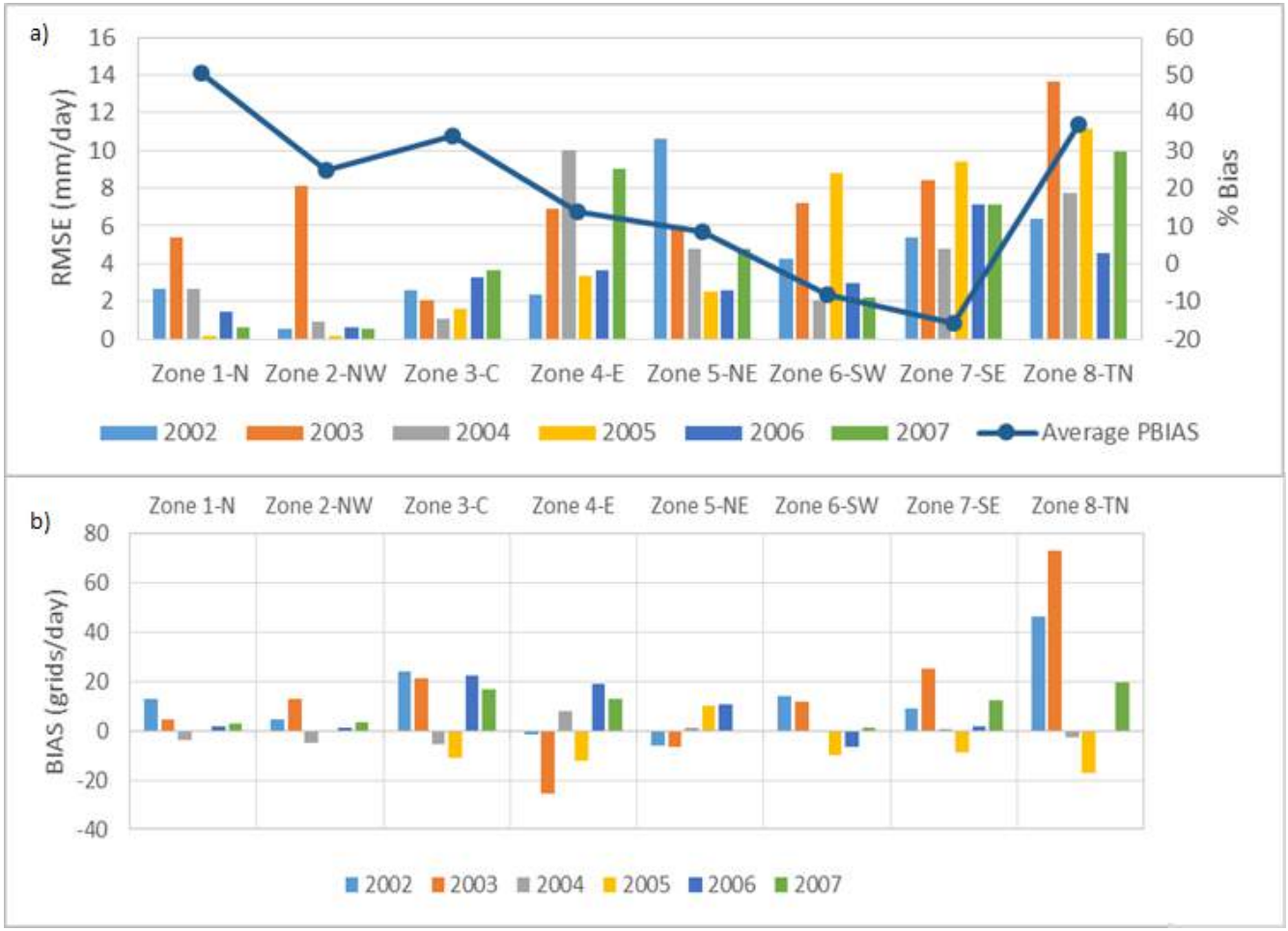

Fig. 11 Overall statistics across 2001-2007 for NEM period. A) RMSE in mm/day for each zone along with percent bias in secondary axis and b) Bias in grids/day for all zones.

4.1.3 Important conclusions from Sensitivity Experiments

- **Rainfall patterns** were widely captured – but mostly **under-predicted** – issues with predicting **extreme events**
- WRF model behavior was **similar across wet, dry and normal years** – yet, the biases were **larger during the dry year (2004)**
- **Good performance in north-eastern region** except during pre-monsoon months
- The **bias in rainy days highly under-predicted in zone 6 and zone 2 (western coasts) - especially for extreme rainfall (>20 mm)** – during South-West monsoon months - Onset of the South-west monsoon was poorly represented
- Spatial and Temporal shift in the simulated rainfall and number of rainy days was observed
- North-East monsoon widely captured – **but high temporal shifts was noticed in the east-coasts.**
- **Coastal zones – performed below par** when compared to zones in-land – for precipitation forecasts
- **KF cumulus scheme** performed well across seasons – but underestimated rainfall in general – **BMJ scheme performed well for South-West monsoon** but gave poor performance for North-East monsoon
- Two-domain setup – restricted rainfall development in inner domain – due to KF uncertainty – yet, earlier single domain studies –showed wet bias – due to large downscaling ratio and insufficient spatial spin-up

4.2 Final model configuration

The final WRF model was setup with single domain (59 E – 105.9 E; 1.35 N – 48.1 N) at 25 km containing 191 x 191 grid points. The physics options are listed in Table 4. Interestingly, the performance of the same set of selected physics options (KF-RRTM), largely under-predicted annual rainfall in the Central and North TN (Fig. 12). The number of rainy days (Fig. 13) was widely underpredicted in the CanESM with KF and RRTM schemes. Using BMJ and CAM schemes, improved in capturing the spatial pattern of rainfall and temperature in the Central and South India. However, North India is having a huge dry bias in the simulation with CanESM.

Table 4 Final model setup – Physics Configuration

Physics Scheme	**Selected Physics**	
	NorESM	CanESM
Cumulus schemes	Kain-Fritsch (KF)	Betts-Miller-Janjic (BMJ)
Radiation physics	RRTM	CAM

Microphysics	WSM6	WSM6
Planetary Boundary Layer	YSU	YSU
Land Surface Physics	Noah LSM	Noah LSM

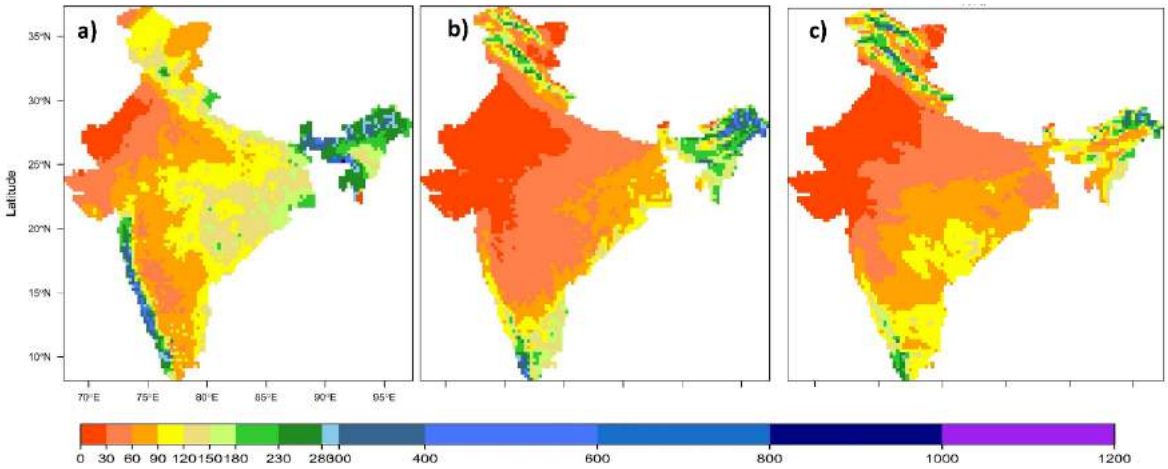

Fig. 14 Annual Rainfall (mm) calculated averaged across 2001-2015 from a) IMD b) CanESM with KF cumulus scheme and RRTM radiation scheme and c) CanESM with BMJ cumulus scheme and CAM radiation scheme

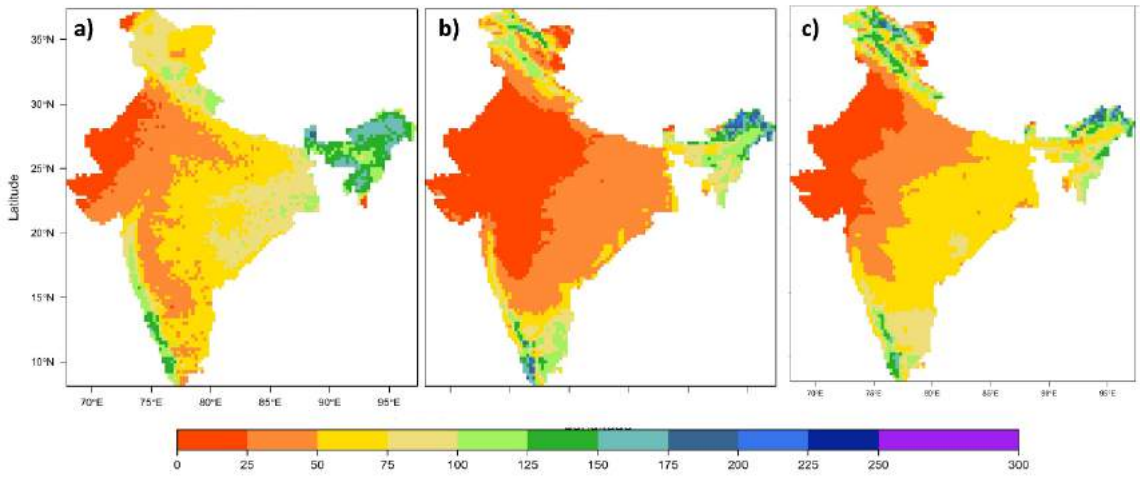

Fig. 15 Same as Fig. 14 but for Annual Rainy days

4.3 Bias in Downscaled Historical Climatology

This section contains detailed discussion on the characteristics of spatio-temporal bias existent with the downscaled variables viz. Precipitation and Temperature.

4.3.1 Spatial and Temporal Distribution of Precipitation bias

The spatial maps of WRF simulated annual rainfall averaged across 30 years (1951-2005) are shown in Fig. 16 (NorESM) and Fig. 17 (CanESM). The overall over-prediction of rainfall by NorESM and under-prediction of rainfall by CanESM is prominent from the figures which is also reflected in the annual rainy day plots (Fig. 18 and Fig. 19).

The cold bias of NorESM was most significant in the north, north-western and south-eastern parts of India (Zones 1, 2, 7 and 8). The heavy precipitation in the Western coast (Zone 6) was well captured by the NorESM simulations. Similar patterns were observed in the annual rainy days plot (Fig. 18). The zones 1-2 were simulated with increased duration of rainy days in magnitude of 30-40 days than IMD 30 year-mean by NorESM based simulations. NorESM seem to have captured the temporal distribution (peak during JJAS-SWM) of daily precipitation intensities during SWM from Zone 1-6 (Fig. 20). However, when we examine the 30-year mean plots of daily rainfall (Fig. 20), the consistent over-predictions by the NorESM simulations in the zone 1 was due to over-prediction in the month of August (Bias – 4.5 mm/day against 7 mm/day IMD 30-year mean) and September (Bias - 3.7 mm/day against 4.1 mm/day IMD 30-year mean). The zone 2 had similar over-prediction during August and September months. The intensity and duration of the rains in the months of August and September were on the higher scale for the zones 1 and 2 with NorESM simulations (Fig. 20). Zones 7 and 8 which does not have much rains during the South-west monsoon (Table 6), the NorESM based simulations highly over-predicted rain intensity (Fig. 16, Fig. 20) and the number of rainy days (Fig. 18). The NorESM based simulations showed huge deviation of 50-100 days in zones 7 and 8 from the IMD mean values. The bias for SWM period in zone 7 was 5.13 mm/day (against 4.42 mm/day IMD 30-year mean) and zone 8 was 5.27 mm/day (against 3.37 mm/day IMD 30-year mean) (Table 6). The huge cold bias in the zones 7 and 8 which belong to the leeward/rain-shadow regions during the activity of Asian summer monsoon (SWM) could be largely attributed to the inherent errors in the raw NorESM2 dataset (Øyvind Seland et al., 2020). Similarly the NEM pattern in the zones 7 and 8 (observed peak NEM activity) are also not well represented by the NorESM simulations. The duration and the intensity of rainfall extremes during the months of Oct-Nov was observed (Fig.20 and Table 6).

The CanESM simulations captured the overall spatial rainfall distribution better, yet very high under-prediction was observed in the Western Coast including Maharashtra and Karnataka coasts (Zone 6) (Fig. 20). The intensity and duration of the extremes during July, August and September was highly under-predicted by the CanESM simulations. Significant under-prediction was observed in the zones 1 and 2 mainly in the months of July-September (Fig. 20 and Table 6). Interestingly, the months of October-November and December were well represented by the CanESM simulations, particularly in the zones 7-8 (observed peak NEM activity).

The high rains in the North-eastern India (zone 5) was underrepresented in the simulations from both NorESM and CanESM models. The error could be resultant from the model uncertainty of being setup at convection-parameterizing scales (25 km), unable to represent the localized interactions. The RCM-WRF setup at 4 km for similar topographically complex regions of Western Ghats largely captured the spatio-temporal variability in the pre-monsoon convective type precipitation (Kirthiga et al., 2021). Both the model's simulation

show higher precipitation amounts in the Jammu and Kashmir region when compared to IMD which could be attributed to the error in the observed gridded IMD data owing to the sparse nature of the ground observatories.

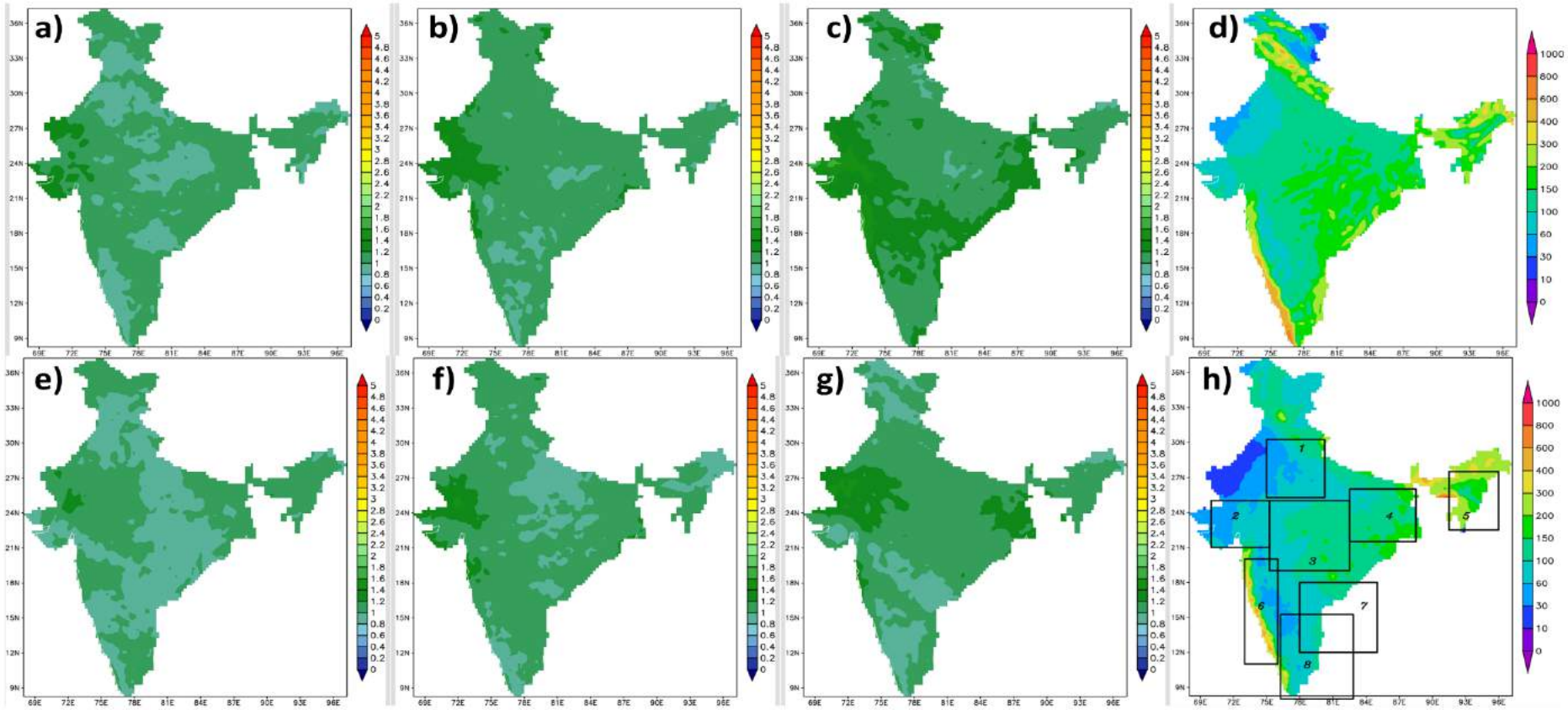

Fig. 16 Simulated Rainfall Comparison maps downscaled from NorESM model. d) Annual rainfall (cm) for baseline period (1981-2005) h) IMD Annual rainfall (cm) averaged across 1981-2005, also showing the evaluation zones in black boxes. The images a-c contains early, mid and late century Rainfall ratio against baseline scenario (simulated/baseline) for RCP 8.5. The images e-g contains early, mid and late century Rainfall ratio against baseline scenario for RCP 4.5.

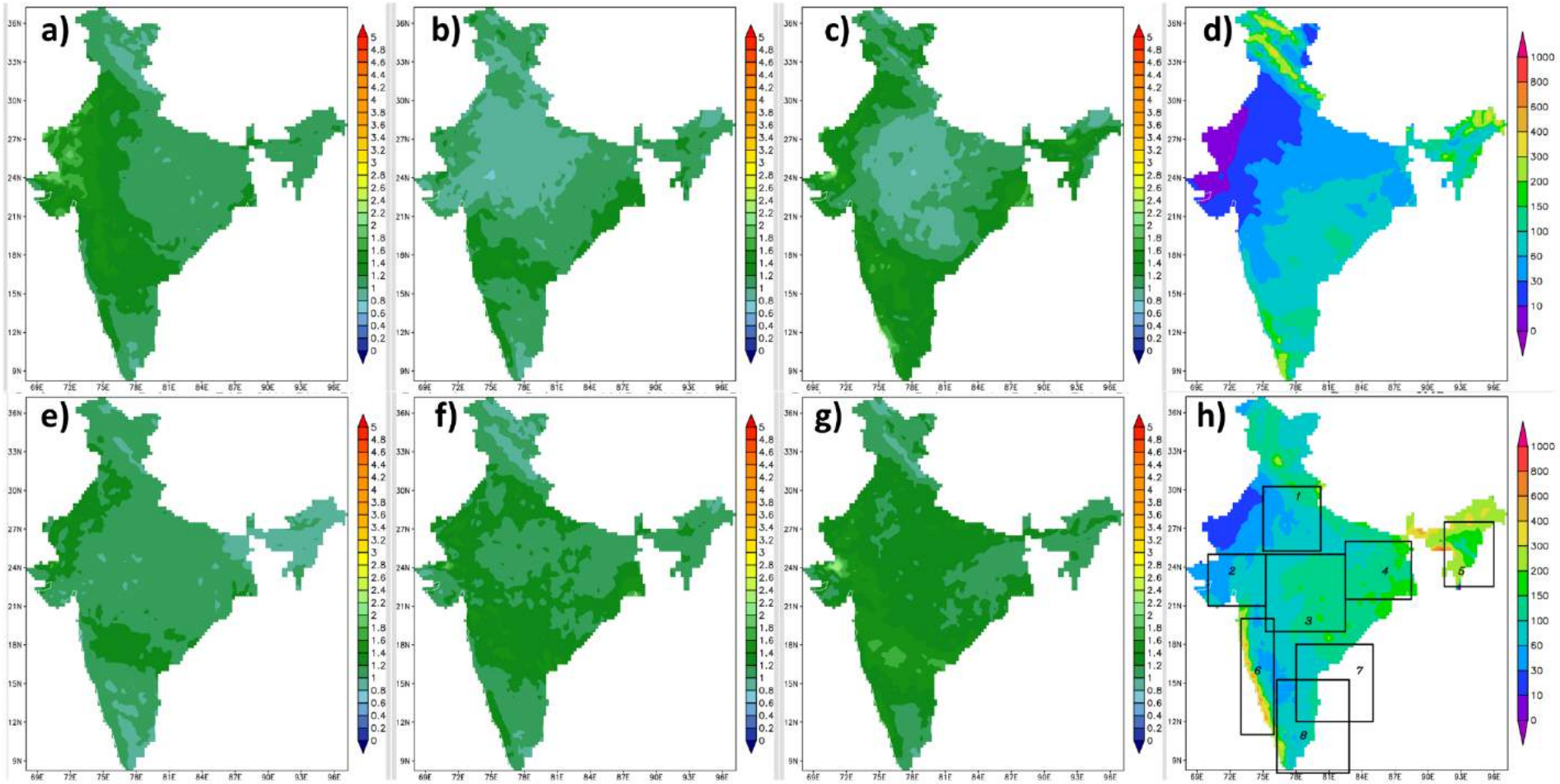

Fig. 17 Same as Fig. 16 but for CanESM model.

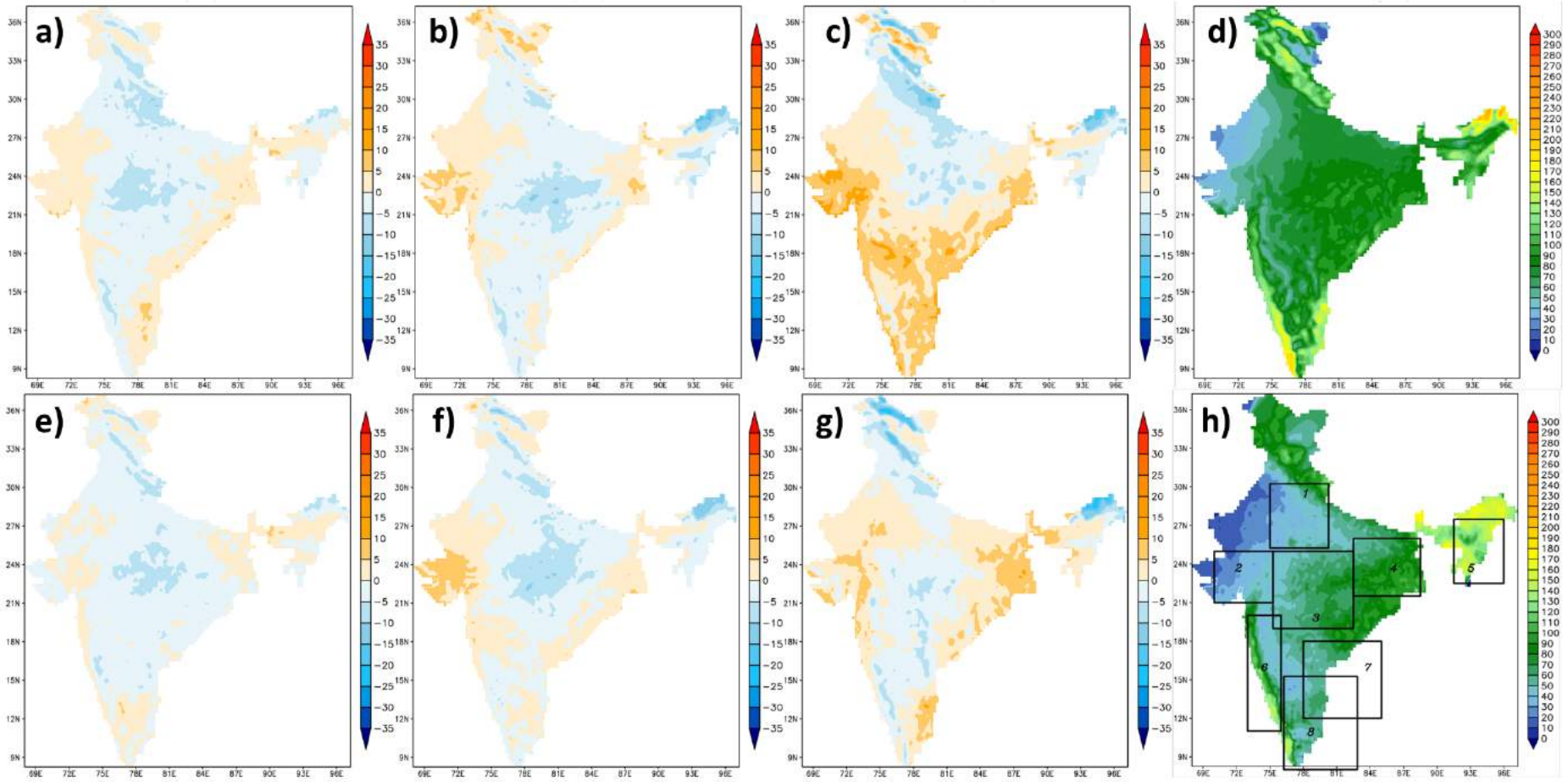

Fig. 18 Simulated Annual rainy day maps downscaled from NorESM model. d) Annual rainy days for baseline period (1981-2005) h) IMD annual rainy days averaged across 1981-2005, also showing the evaluation zones in black boxes. The images a-c contains early, mid and late

century rainy day difference against baseline scenario (simulated-baseline) for RCP 8.5. The images e-g contains early, mid and late century rainy day difference against baseline scenario for RCP 4.5.

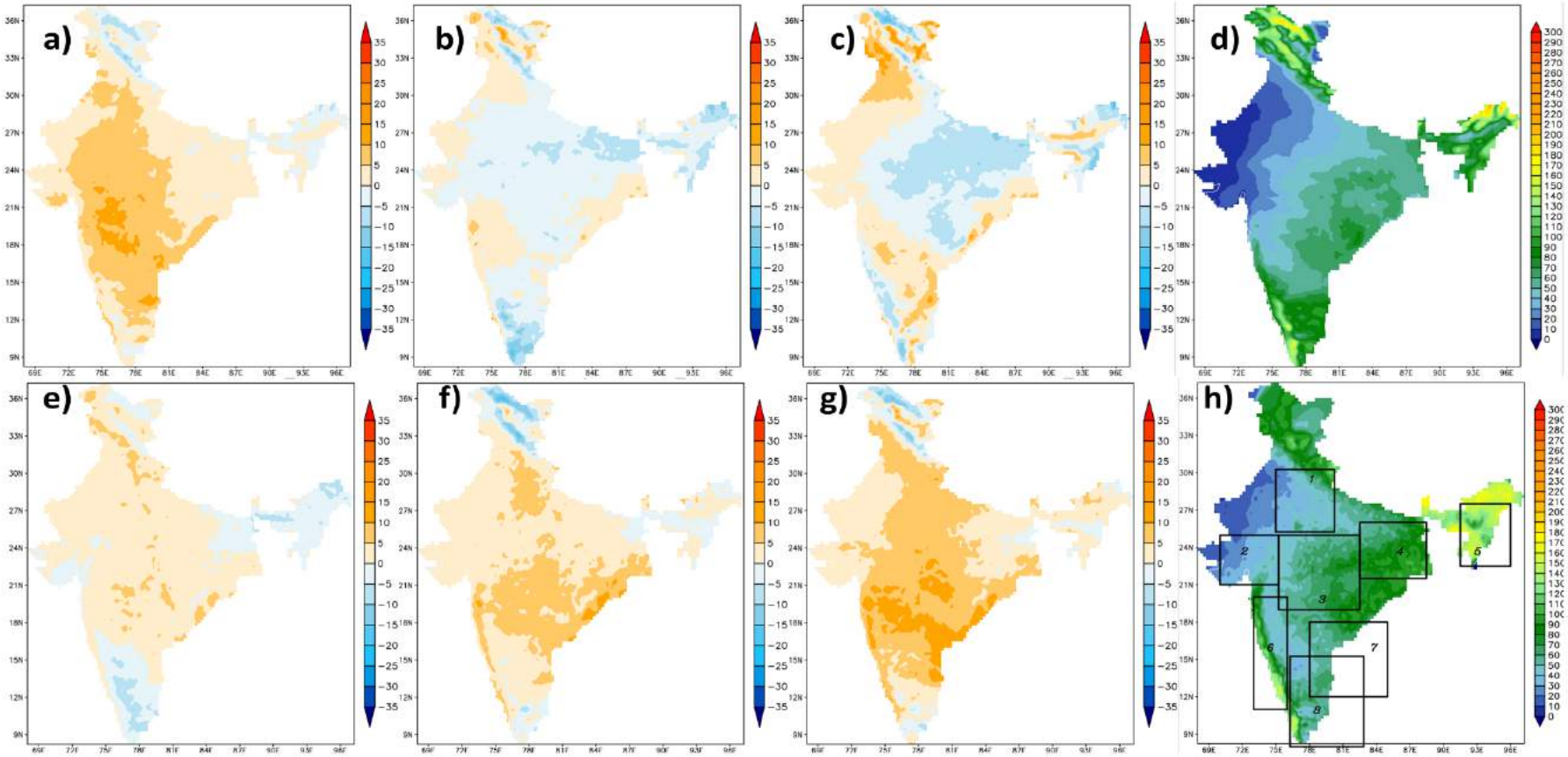

Fig. 19 Same as Fig. 18 but for CanESM model.

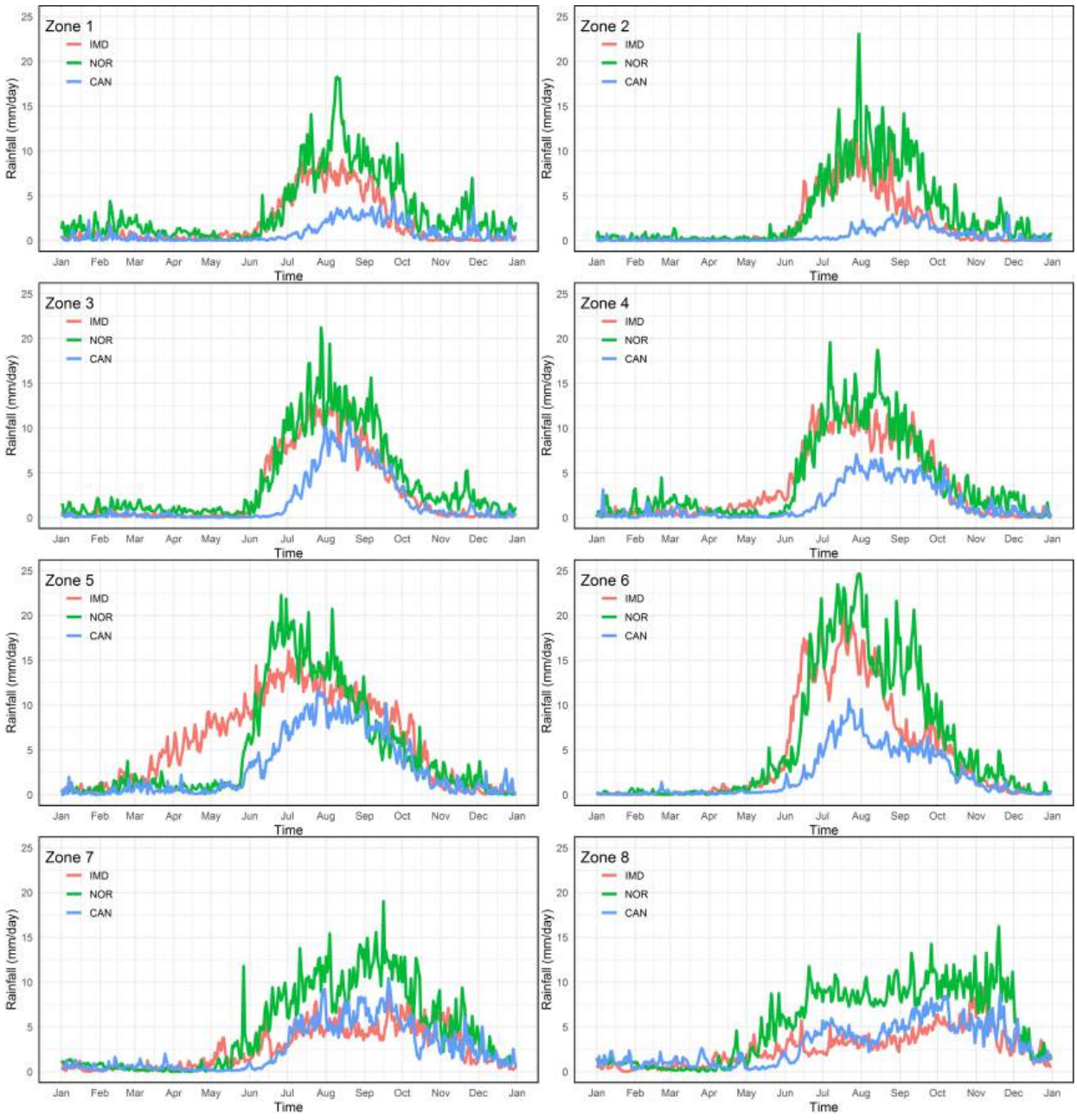

Fig. 20 Zone-wise plots of 30-year mean daily rainfall (mm/day)

Table 5 Monthly error statistics (mm/day) for Baseline2 30-year time period (1981-2005)

Month	NorESM (mm/day)	CanESM (mm/day)	IMD 30-year mean (mm/day)
Jan	0.39	0.05	0.35
Feb	0.38	-0.07	0.49

Mar	0.04	-0.17	0.64
Apr	-0.65	-1.01	1.26
May	-0.67	-1.82	2.14
Jun	0.47	-4.53	6.06
Jul	2.98	-4.48	9.06
Aug	3.58	-2.87	8.20
Sep	3.52	-0.78	5.78
Oct	1.53	-0.63	3.21
Nov	2.01	0.07	1.42
Dec	0.66	0.19	0.59

Table 6 Zone-wise seasonal error statistics (mm/day) for Baseline2 30-year time period (1981-2005)

Zones	Sources	Winter	Pre-Monsoon	SWM	NEM
Zone 1	NorESM	1.04	0.31	2.14	2.38
	CanESM	-0.18	-0.33	-3.46	-0.08
	IMD_30 year mean	0.55	0.44	5.15	0.35
Zone 2	NorESM	0.30	0.20	2.35	2.18
	CanESM	0.07	-0.04	-4.15	-0.11
	IMD_30 year mean	0.04	0.08	5.31	0.34
Zone 3	NorESM	0.61	0.55	1.67	1.87
	CanESM	-0.13	-0.13	-3.29	-0.06
	IMD_30 year mean	0.50	0.25	7.92	0.72
Zone 4	NorESM	0.59	-0.39	0.86	0.62
	CanESM	-0.12	-0.91	-5.16	-0.87

	IMD_30 year mean	0.94	1.17	8.82	1.12
Zone 5	NorESM	-0.25	-4.59	0.78	-0.77
	CanESM	-0.59	-5.13	-4.20	-1.13
	IMD_30 year mean	0.94	5.85	11.45	2.03
Zone 6	NorESM	0.14	0.11	2.89	2.31
	CanESM	0.11	-0.55	-6.64	-0.78
	IMD_30 year mean	0.06	0.80	11.75	1.80
Zone 7	NorESM	0.33	-0.09	5.13	2.99
	CanESM	0.17	-0.50	0.48	0.08
	IMD_30 year mean	0.38	0.87	4.42	3.38
Zone 8	NorESM	0.32	0.50	5.27	3.85
	CanESM	0.57	-0.44	1.08	0.64
	IMD_30 year mean	0.48	1.31	3.37	4.20

4.3.2 Diurnal variability of Temperature – Spatial and seasonal variability of temperature extremes

4.3.2.1 Maximum Temperature – Spatio-Temporal Bias

NorESM simulations clearly validated being driven by cold model (NORESM2 as referred in the global studies), and showed a huge under-prediction in the simulated Maximum Temperatures across India, except for North-eastern regions for which the spatial pattern is relatively better represented (Fig. 21). The huge under-prediction was prominent in the months of January, February, November and December across all zones (Fig. 23). The Winter season recorded a negative bias of 7 ^{o}C across India, while the lowest negative bias was observed in the South-west monsoon (SWM) of magnitude 1.8 ^{o}C across most SWM active zones (zone 1, 2, 3, 4) (Table 7).

CanESM based simulations better represented the spatial distribution of Maximum temperature (Fig. 22). Similar to the patterns observed in precipitation simulations, the zones 1, 2, 3 and 4 showed higher deviations in all the months (Fig. 23). Interestingly, the CanESM simulations over-predicted the rainfall in the JJAS as reflected by the under-prediction of precipitation extremes in the above-mentioned zones. The other months of Winter, Pre-monsoon and NEM are slightly under-predicted (Table 7).

Overall, the maximum temperature in the months of January, February, November and December was reflected in both the model based simulations, with a lower magnitude of under-prediction by CanESM simulations. The inherent cold bias in WRF model while simulating maximum temperatures could be attributed to the systematic bias.

Table 7 Maximum Temperature - Zone-wise seasonal error statistics (°C) for Baseline2 30-year time period (1981-2005)

Zones	Sources	Winter	Pre-Monsoon	SWM	NEM
Zone 1	NorESM	-8.39	-5.89	-0.39	-6.82
	CanESM	-2.88	-1.81	4.32	-1.80
	IMD_30 year mean	23.46	35.96	34.62	28.32
Zone 2	NorESM	-7.80	-4.09	-0.89	-6.68
	CanESM	-3.95	-2.74	1.91	-2.33
	IMD_30 year mean	28.75	37.25	32.66	31.68
Zone 3	NorESM	-8.41	-5.73	-1.33	-6.22
	CanESM	-4.56	-2.84	2.04	-2.85
	IMD_30 year mean	26.28	38.23	32.19	29.68
Zone 4	NorESM	-6.18	-4.15	-0.83	-4.27
	CanESM	-2.28	-0.35	2.33	-1.17
	IMD_30 year mean	23.63	36.54	32.87	28.50
Zone 5	NorESM	-4.34	-0.67	-2.07	-3.91
	CanESM	-2.15	1.30	-1.04	-2.37
	IMD_30 year mean	23.63	29.42	30.65	26.50
Zone 6	NorESM	-7.12	-3.45	-2.63	-5.34
	CanESM	-3.77	-1.85	-0.81	-3.42
	IMD_30 year mean	30.81	34.51	28.63	30.13
Zone 7	NorESM	-7.51	-4.86	-2.75	-4.63
	CanESM	-4.21	-2.02	-1.09	-2.88

	IMD_30 year mean	30.60	36.54	33.29	29.93
Zone 8	NorESM	-7.34	-4.67	-3.43	-4.49
	CanESM	-3.91	-1.82	-1.64	-2.86
	IMD_30 year mean	30.04	34.26	31.67	29.13

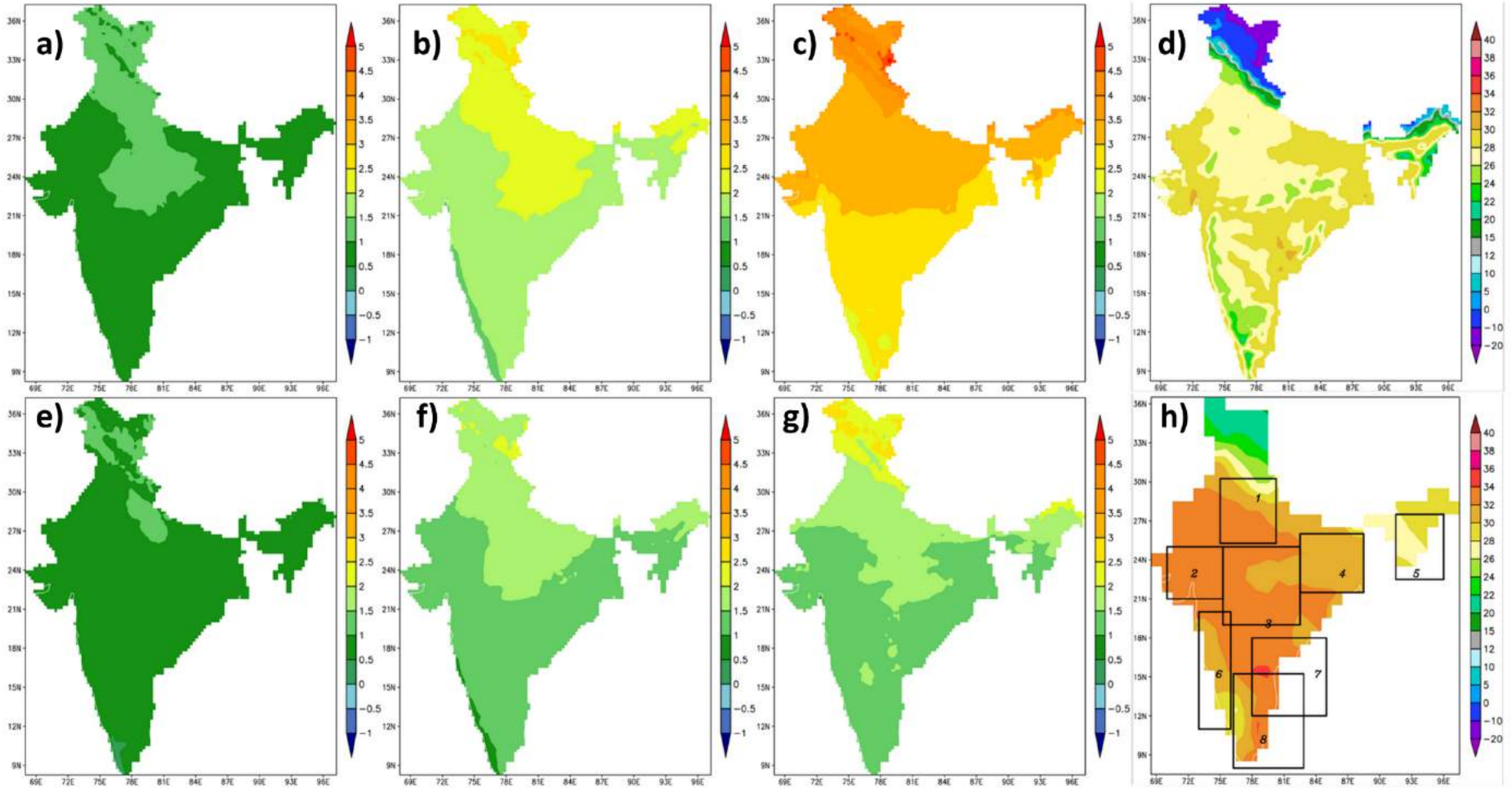

Fig. 21 Simulated Maximum Temperature maps downscaled from NorESM model. **d)** Maximum Temperature (°C) for baseline period (1981-2005) **h)** IMD Maximum Temperature (°C) averaged across 1981-2005, also showing the evaluation zones in black boxes. The images **a-c** contains early, mid and late century Maximum Temperature difference against baseline scenario (simulated-baseline) for RCP 8.5. The images e-g contains early, mid and late century Maximum Temperature difference against baseline scenario for RCP 4.5.

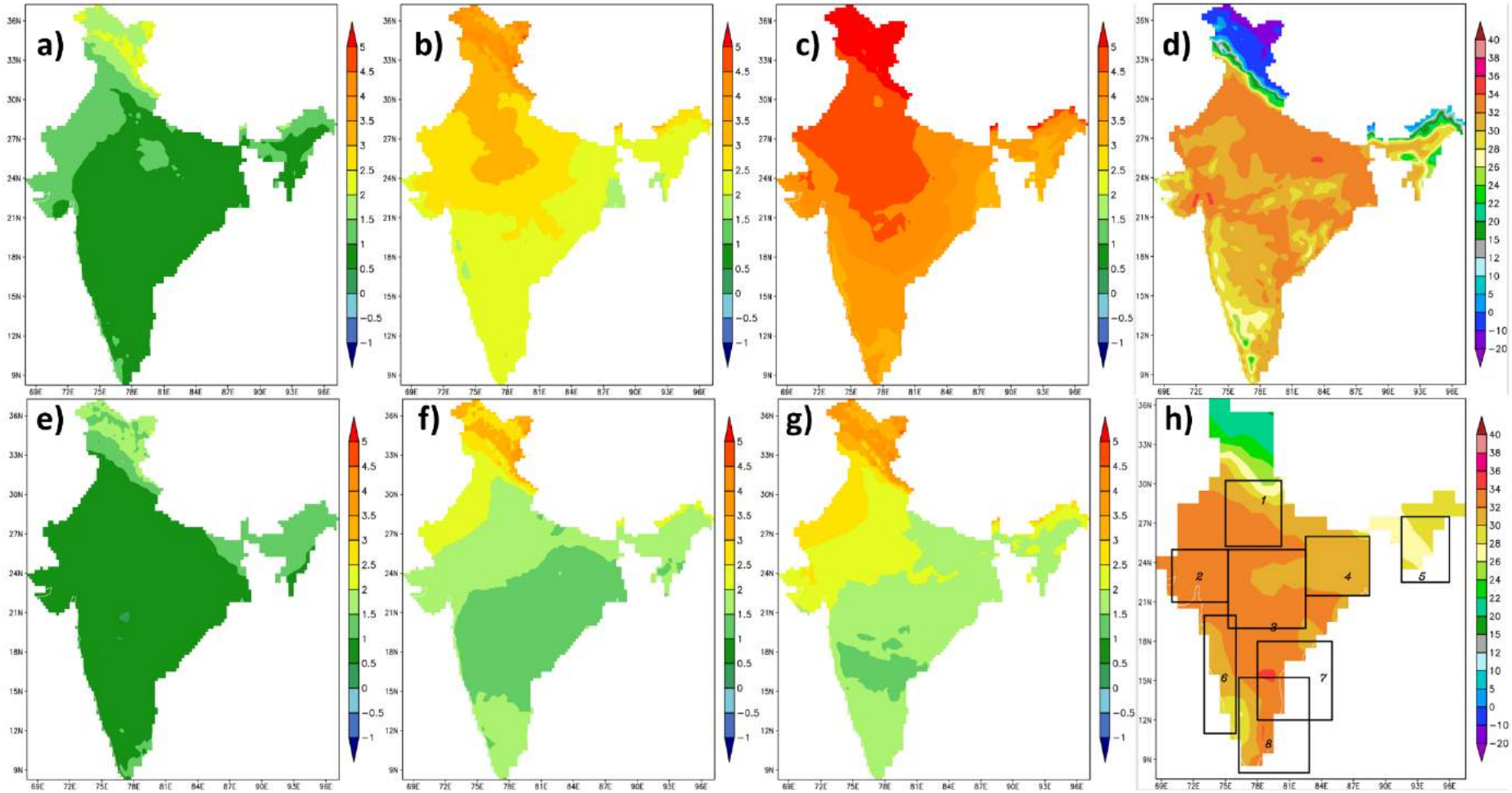

Fig. 22 Same as Fig. 21 but for CanESM model.

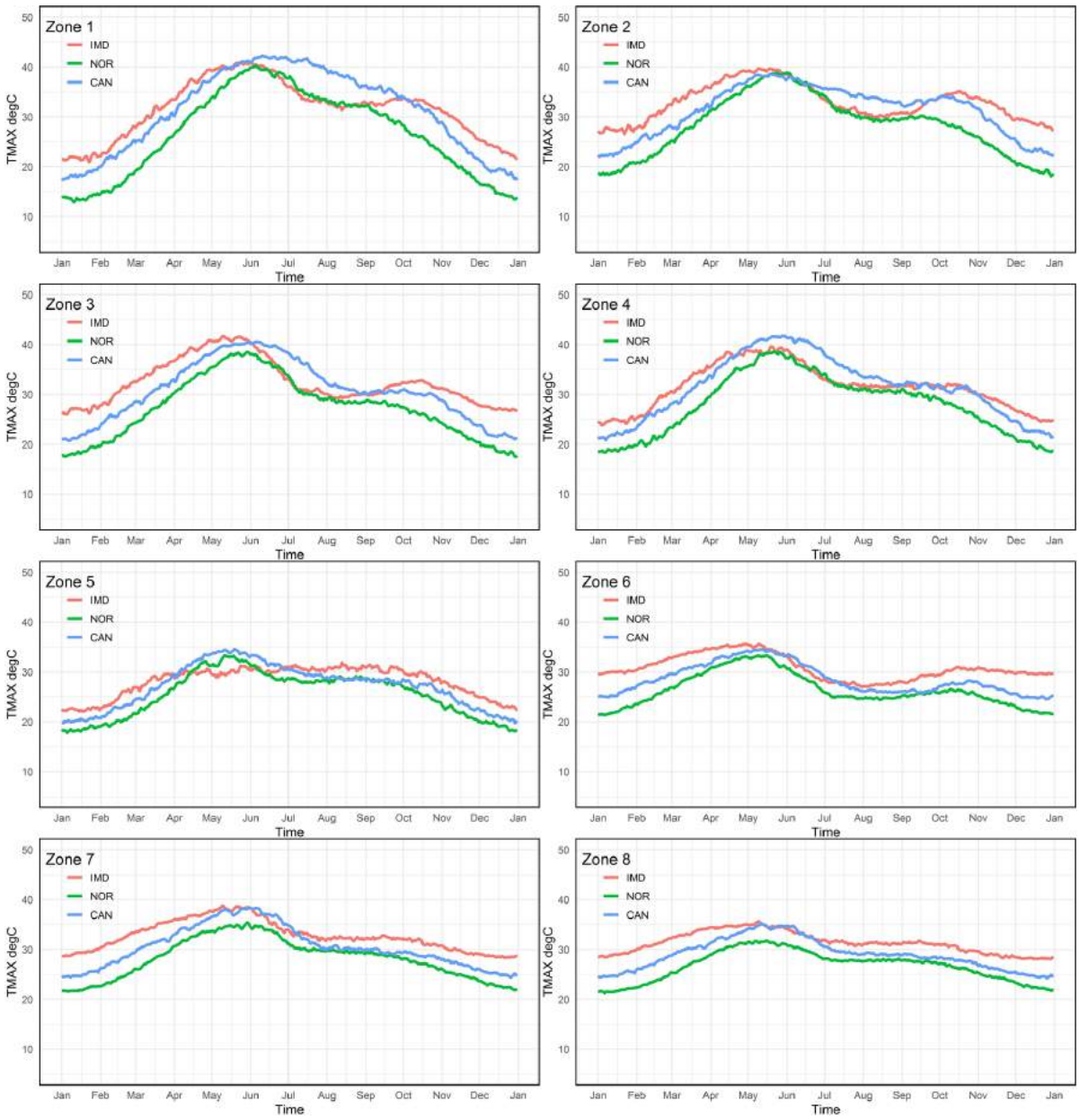

Fig. 23 Zone-wise plots of 30-year mean maximum temperature (ºC)

4.3.2.2 Minimum Temperature – Spatio-Temporal Bias

NorESM and CanESM simulations well represented the spatial (Fig. 24, 25) and temporal pattern (Fig. 26) of minimum temperature. A slight underestimation of minimum temperature is observed in zone 1 and 2 for CanESM and zones 1, 2 and 3 for NorESM. Slight under-prediction in the winter and summer (pre-monsoon) minimum temperatures were observed in both the model simulations. As discussed above, systematic bias could be resultant of model's uncertainty (cold bias) in representation of cold temperatures.

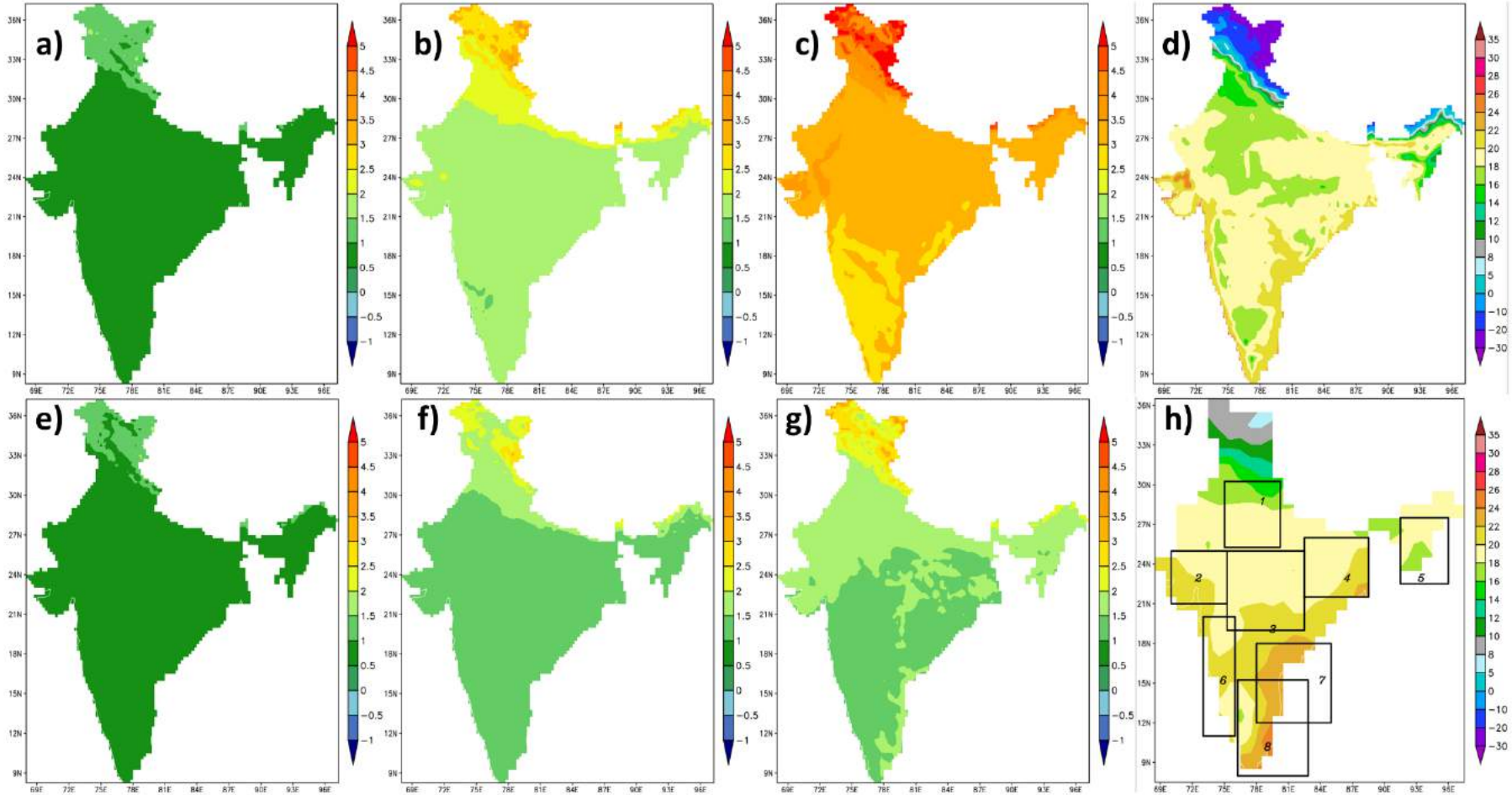

Fig. 24 Simulated Minimum Temperature maps downscaled from NorESM model. **d)** Minimum Temperature (ºC) for baseline period (1981-2005) **h)** IMD Minimum Temperature (ºC) averaged across 1981-2005, also showing the evaluation zones in black boxes. The images **a-c** contains early, mid and late century Minimum Temperature difference against baseline scenario (simulated-baseline) for RCP 8.5. The images e-g contains early, mid and late century Minimum Temperature difference against baseline scenario for RCP 4.5.

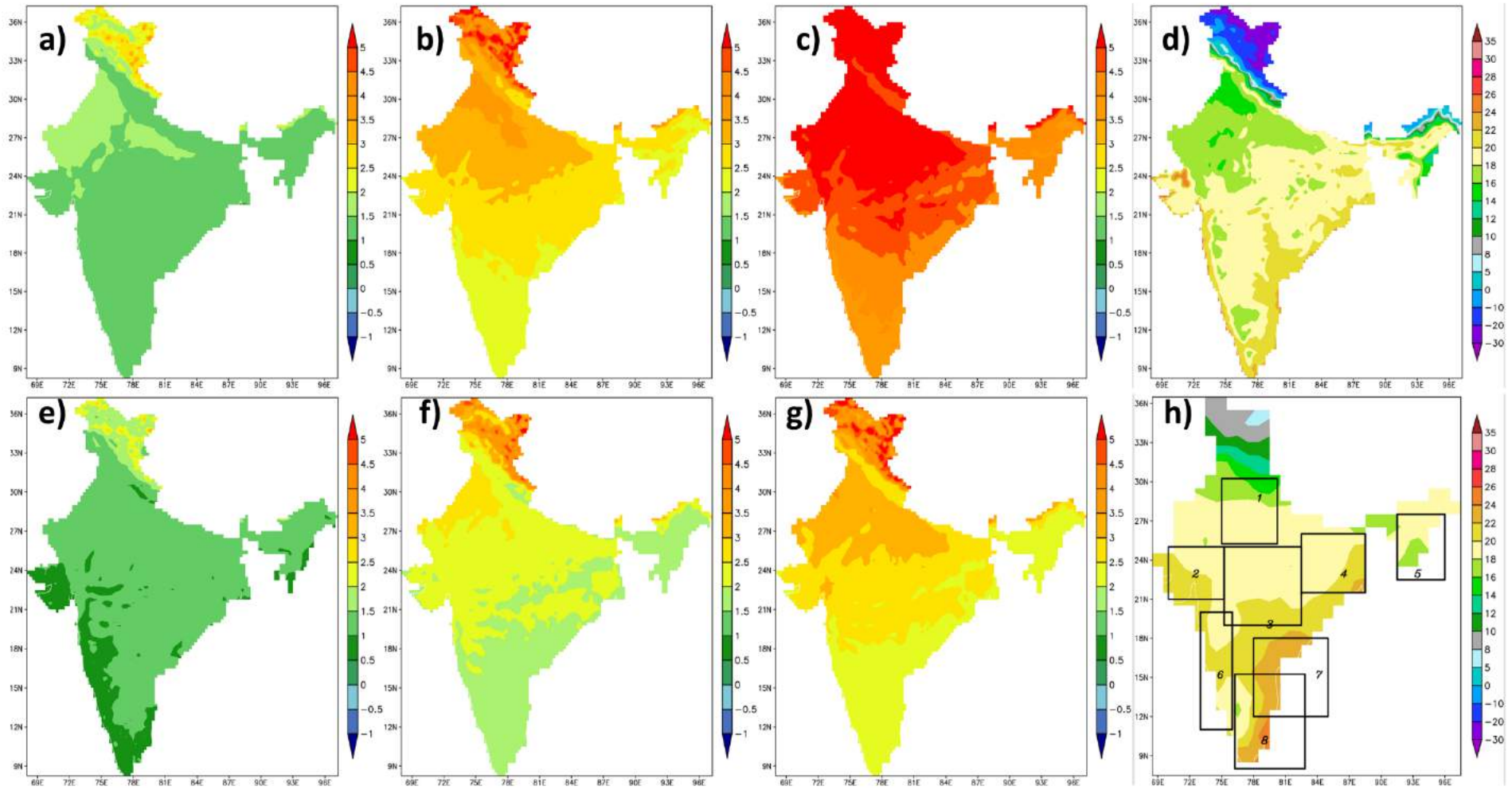

Fig. 25 Same as Fig. 24 but for CanESM model

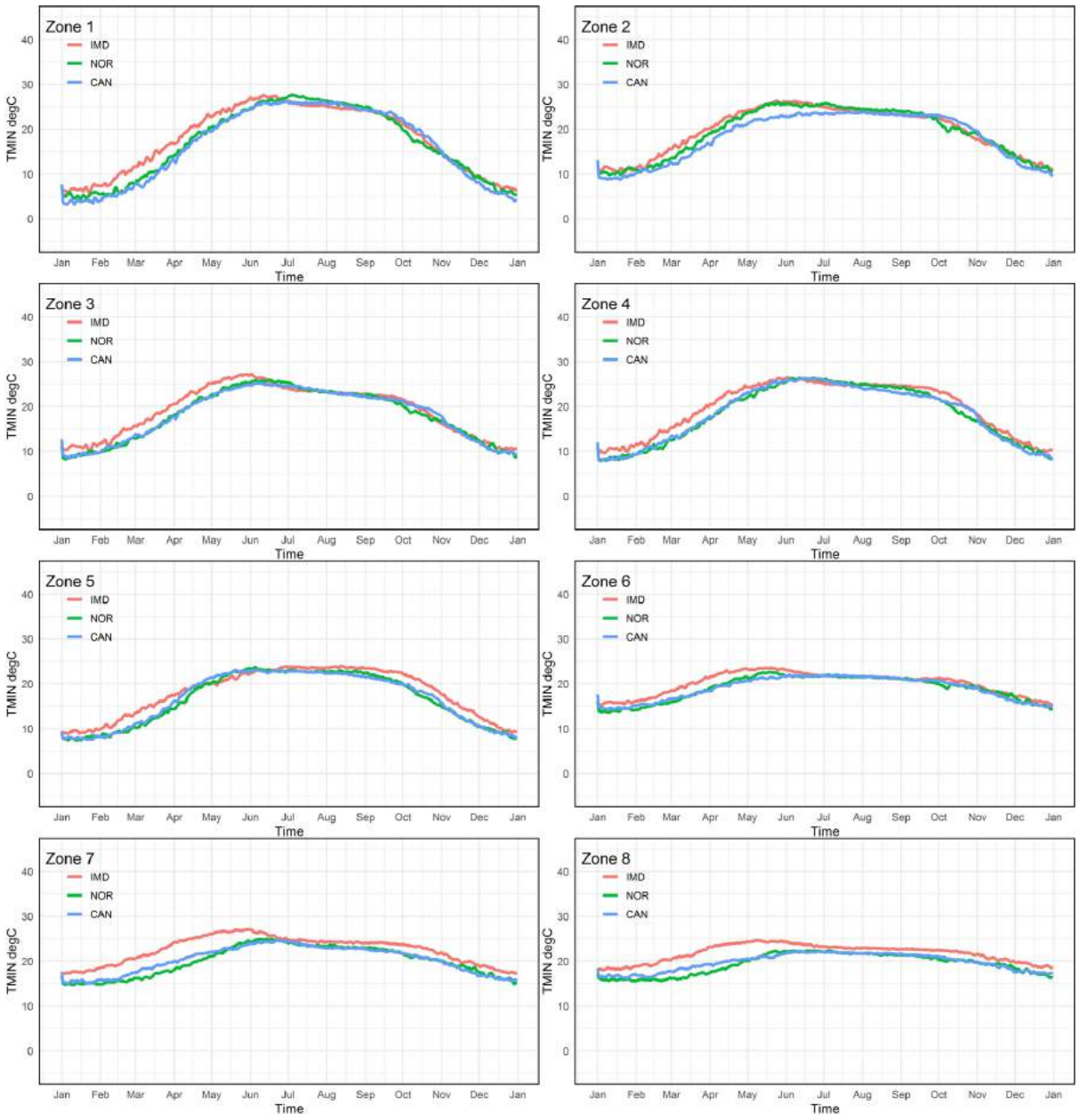

Fig. 26 Zone-wise plots of 30-year mean minimum temperature (°C)

4.4 Future Projections

The future projections for maximum temperature clearly showed increasing trends (Fig. 27) as observed by many recent studies (Krishnan R. et al., 2020). The inter-annual variability seem to have increased for mid and late century. The NorESM cold bias was reflected in the future projections of uncorrected data. The trend increase was also observed to be region-specific with higher increase in zonal-averaged maximum temperature in zones 1, 2, 3, 4 and 7 when compared to the other zones (Fig. 27). The difference between the scenarios in terms of simulated maximum temperatures were also well represented. The spatial extent of extreme maximum temperatures were more prominent in the central and north India during the end century in both model simulations (Fig. 21, 22).

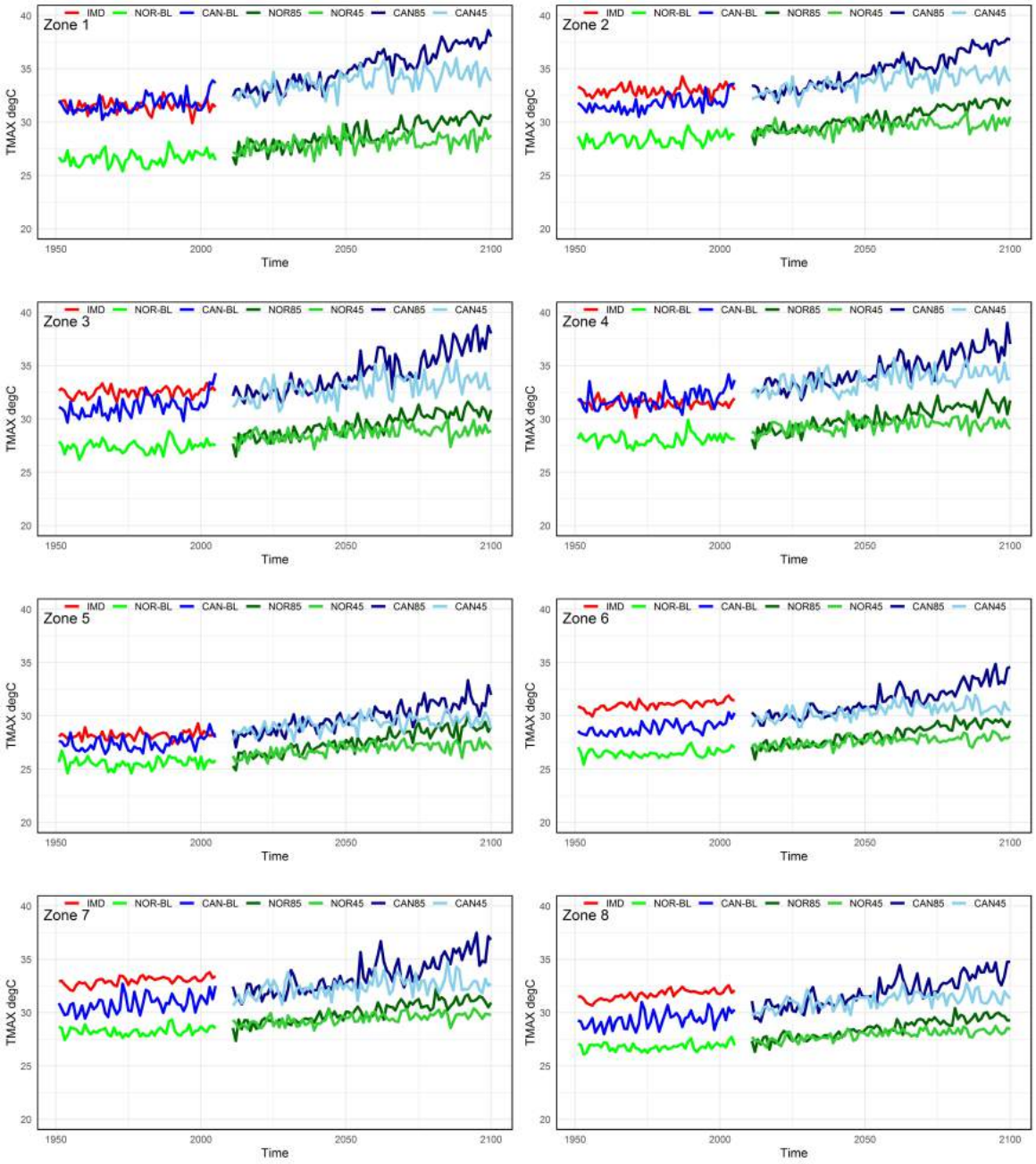

Fig. 27 Zone-wise yearly maximum temperatures (°C) across 1950-2100. The gap in the 2006-2010 in the graphs was due to the design of 30-year time slices as described in section 2.c.

The future projections for minimum temperature also clearly showed increasing trends (Fig. 28) as observed by many recent studies (Krishnan R. et al., 2020). Unlike the maximum temperatures good agreement between the CanESM and NorESM, due to the lower bias in capturing minimum temperature (section 4.3.2.2)

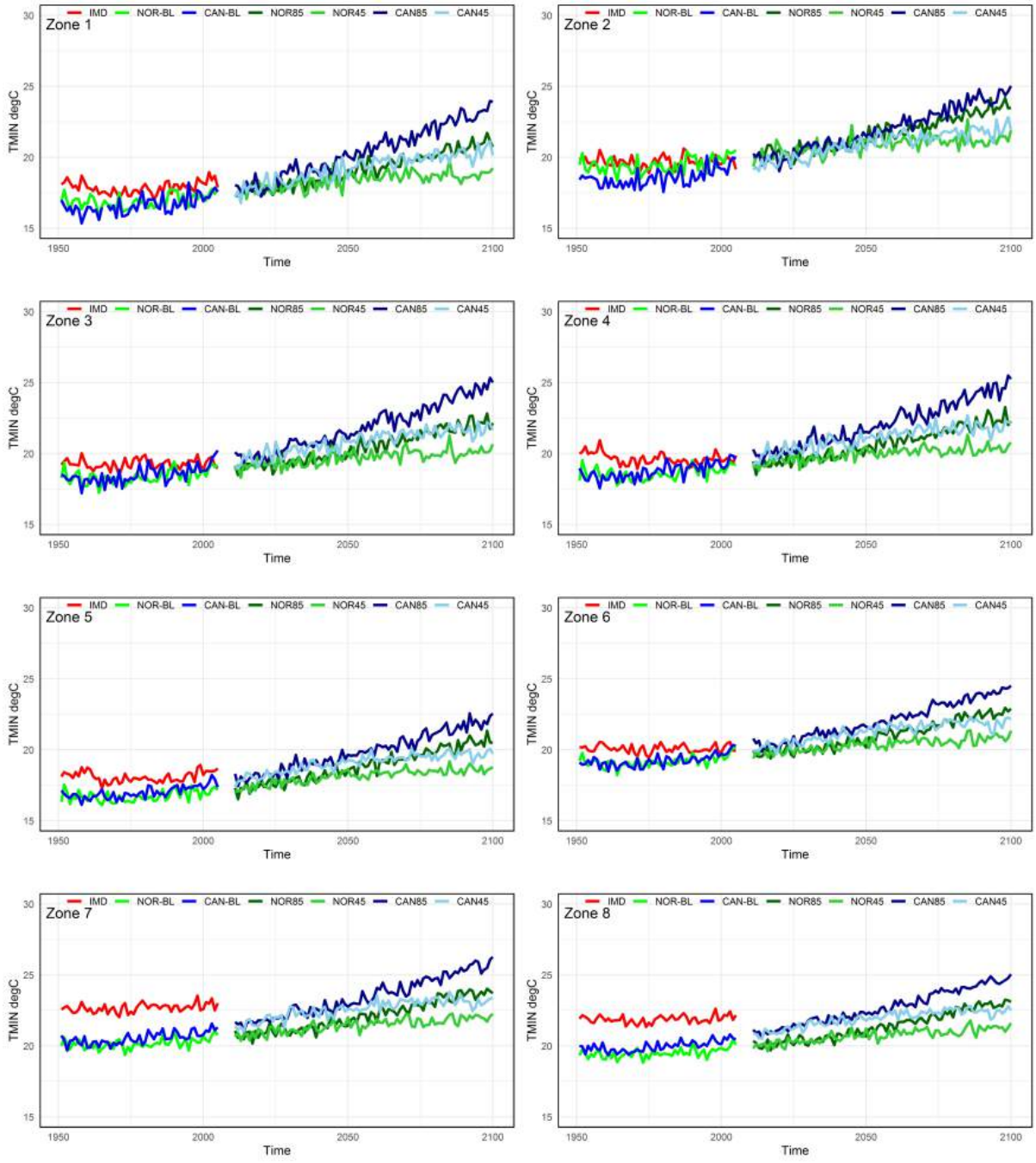

Fig. 28 Zone-wise yearly minimum temperatures (°C) across 1950-2100. The gap in the 2006-2010 in the graphs was due to the design of 30-year time slices as described in section 2.c.

The future projections for precipitation showed huge inter-annual variability (Krishnan R. et al., 2020). Huge inter-annual variability in the mid-end century was observed in both the

CanESM and NorESM models particularly in zone 6 – active SWM zone. The zones 7 and 8 (NEM active zone) also displayed huge variability, shifting the mid and end century mean from climatological mean (Fig. 29). The spatial plots (Fig. 16, 17) showed large deviations from baseline in the mid-late century was clustered in small zones. Interestingly, in both the model simulations, the RCP 4.5 scenario recorded a wide-spread decrease in number of rainy days (Fig. 18, 19).

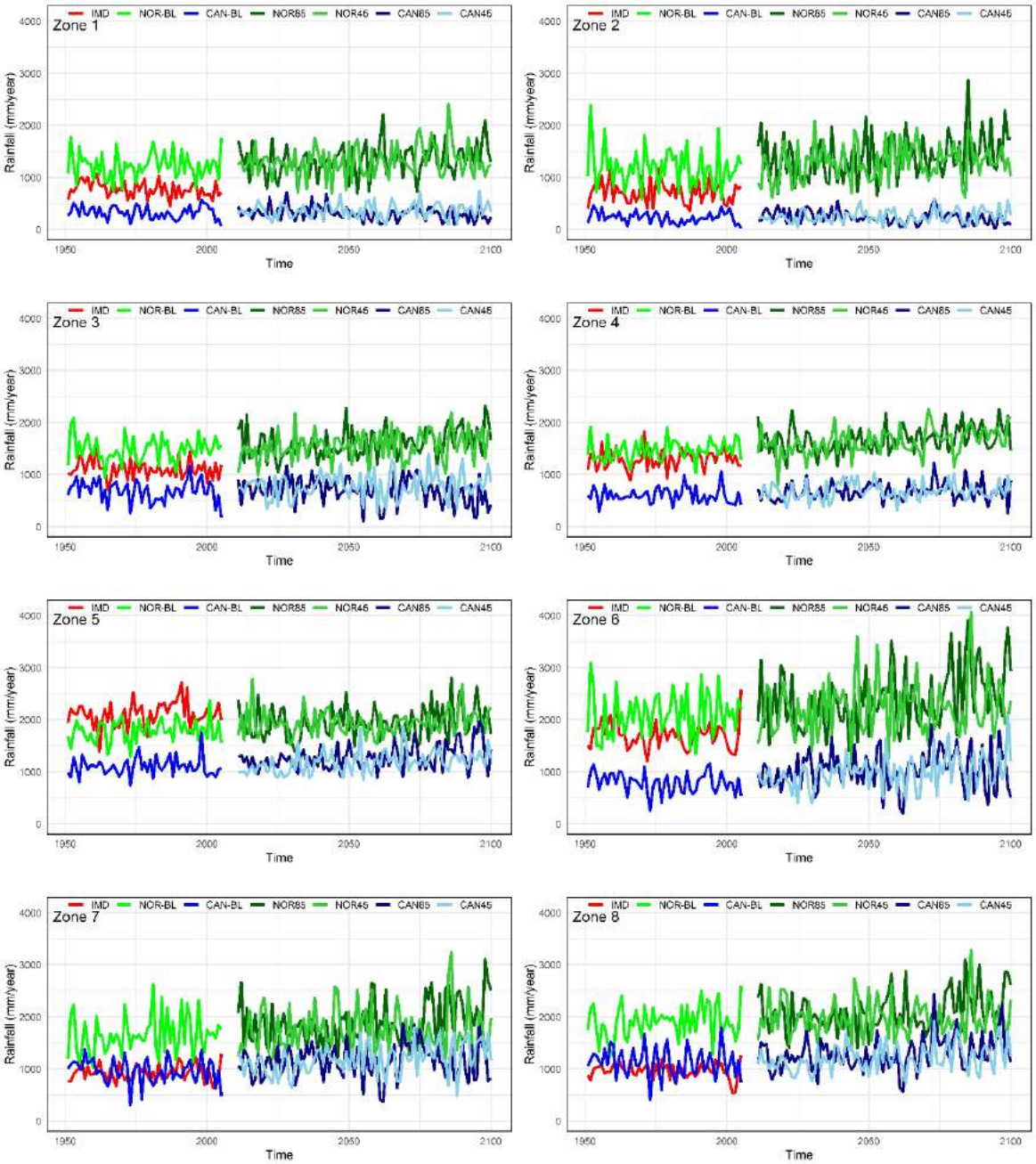

Fig. 29 Zone-wise annual precipitation (mm/year) across 1950-2100. The gap in the 2006-2010 in the graphs was due to the design of 30-year time slices as described in section 2.c.

Kitoh, 2017 reported that many climate models showed a considerable rise in the mean, extremes and interannual variability of monsoon precipitation by the end of the century due to the increase in temperature and atmospheric moisture. 2017). Similar pattern was observed with the raw WRF simulations. However, meaningful conclusions and quantification of the

patterns can happen only after bias correction. This section is just to elucidate briefly about the quality of raw WRF simulations across the 150 years even with the systematic biases from the model and the driving input data.

4.5 Bias correction

The bias correction through the QM method was achieved by using a transfer function and we used gamma distribution to fit the rainfall data in this study. For the bias correction of each RCM grid, the nearest IMD grid was obtained. The daily rainfall values were corrected based on the data pooled for a 31-day sliding window for each day from the climatological period. The shape and scale parameters of gamma distributions were obtained for all the 365 days for observed and RCM rainfall data. The correction for rainfall and temperature was multiplicative and additive respectively. In case of dry pixel in the 31-day window, the effect of neighborhood was also considered to apply the procedure.

The NSE values (Fig. 30) after applying bias correction procedure for precipitation across years 1951-2005. The low NSE values were distributed across the coasts, particularly the east coastal regions.

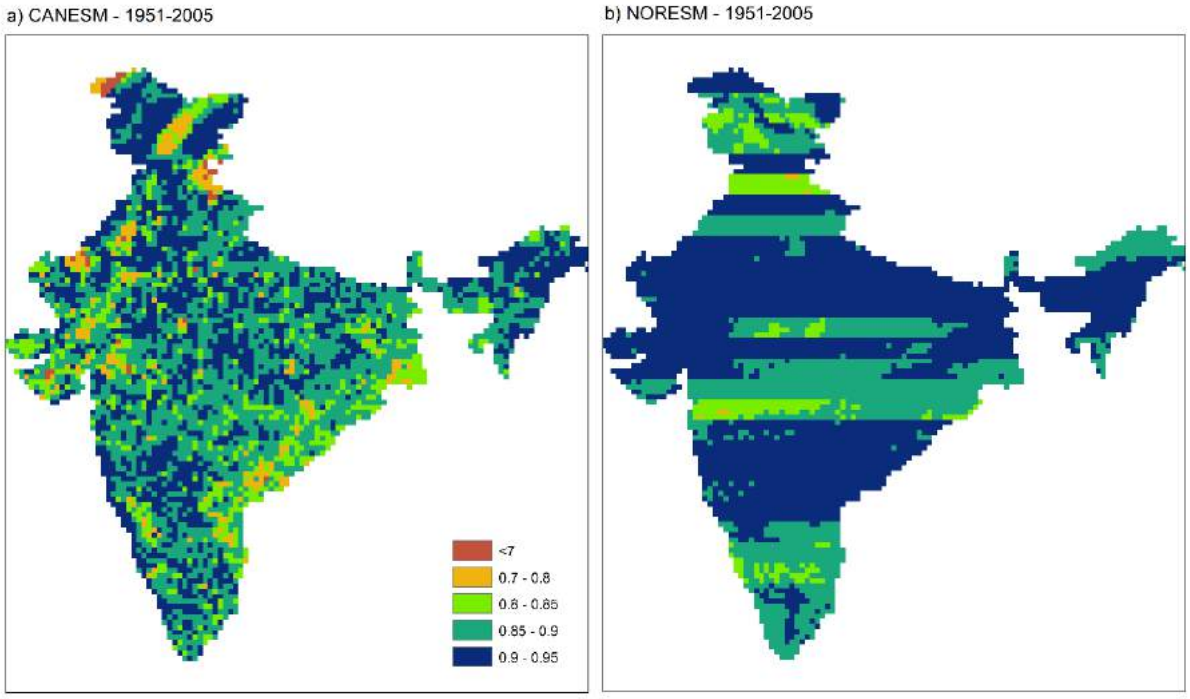

Fig. 30 NSE values for precipitation (a) CANESM 1951-2005 (b) NORESM 1951-2005

4.5.1 Bias corrected maximum and minimum temperature

The underprediction bias in the NORESM maximum temperature (Fig. 31) simulations were reduced after the bias correction procedure. Future projections also showed good agreement between CANESM and NORESM simulations across all the zones.

Similar pattern was also observed in minimum temperature plots after bias corrections (Fig. 32).

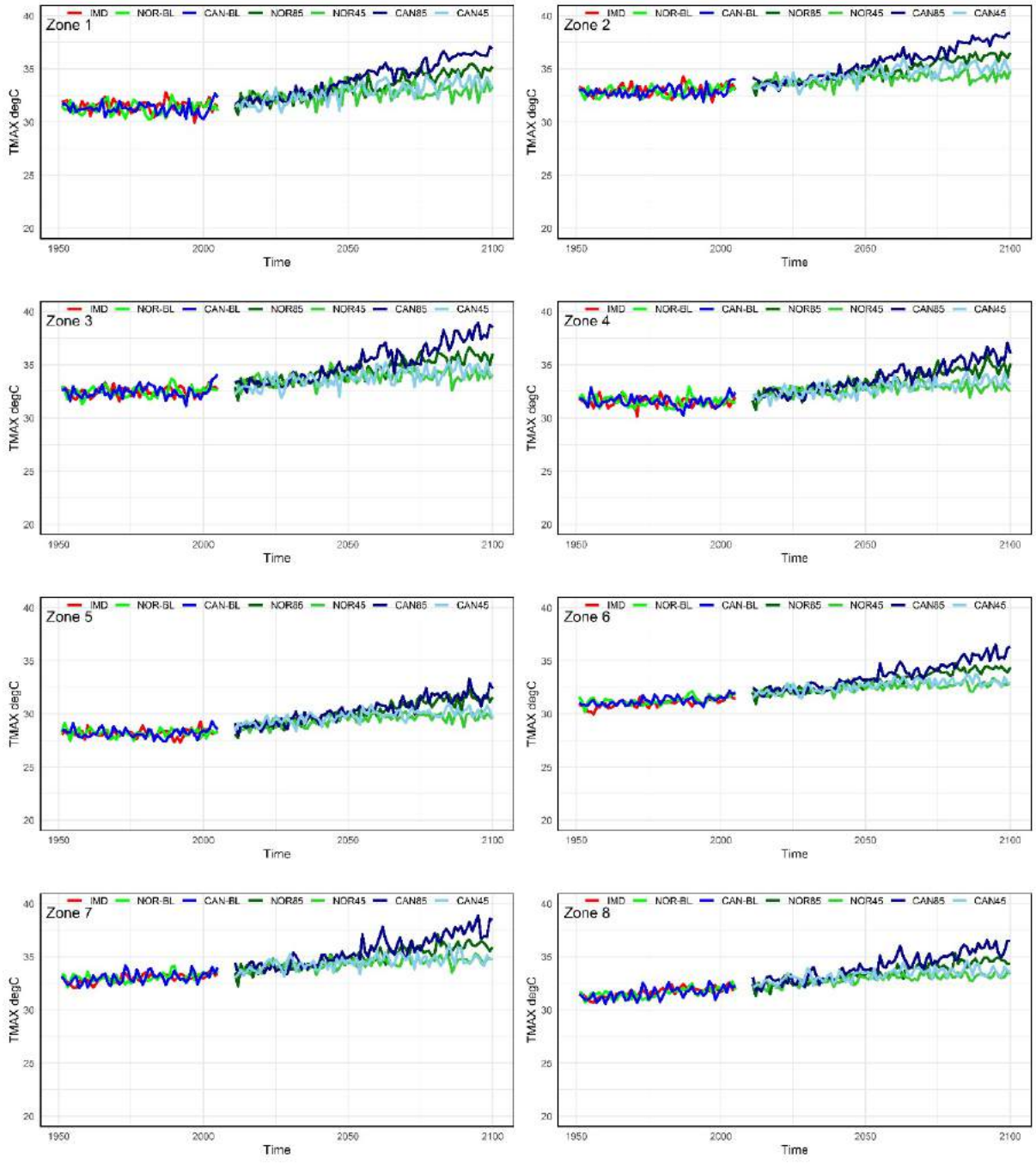

Fig.31 Zone-wise yearly bias corrected maximum temperatures (°C) across 1950-2100. The gap in the 2006-2010 in the graphs was due to the design of 30-year time slices as described in section 2.c.

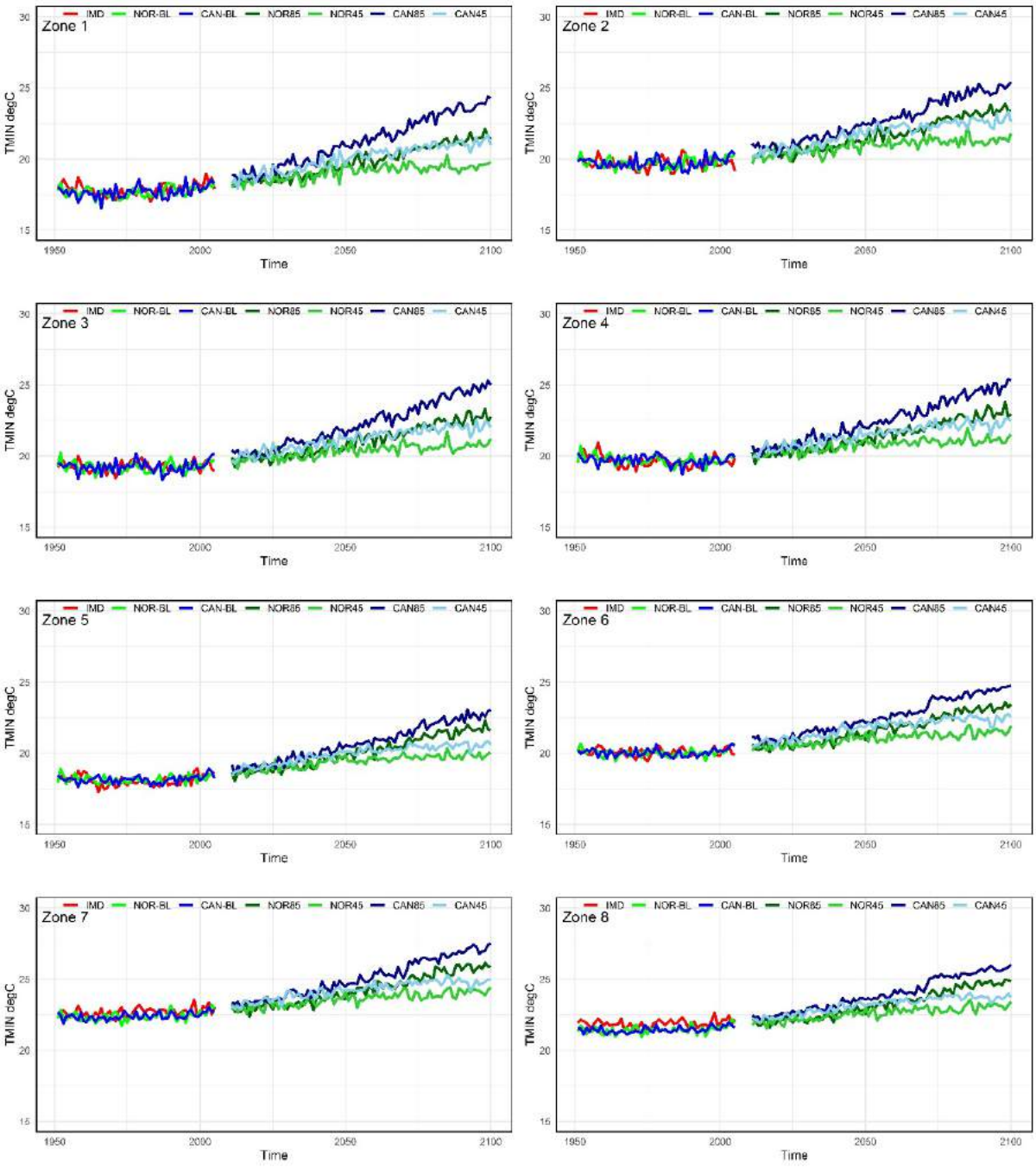

Fig.32 Zone-wise yearly bias corrected minimum temperatures (°C) across 1950-2100. The gap in the 2006-2010 in the graphs was due to the design of 30-year time slices as described in section 2.c.

4.5.2 Bias corrected precipitation

The daily bias correction procedure helped in reducing precipitation bias in most zones (Fig. 33). The future projections match well between the models. However, the CANESM simulations show higher amplitude variability in the future projections.

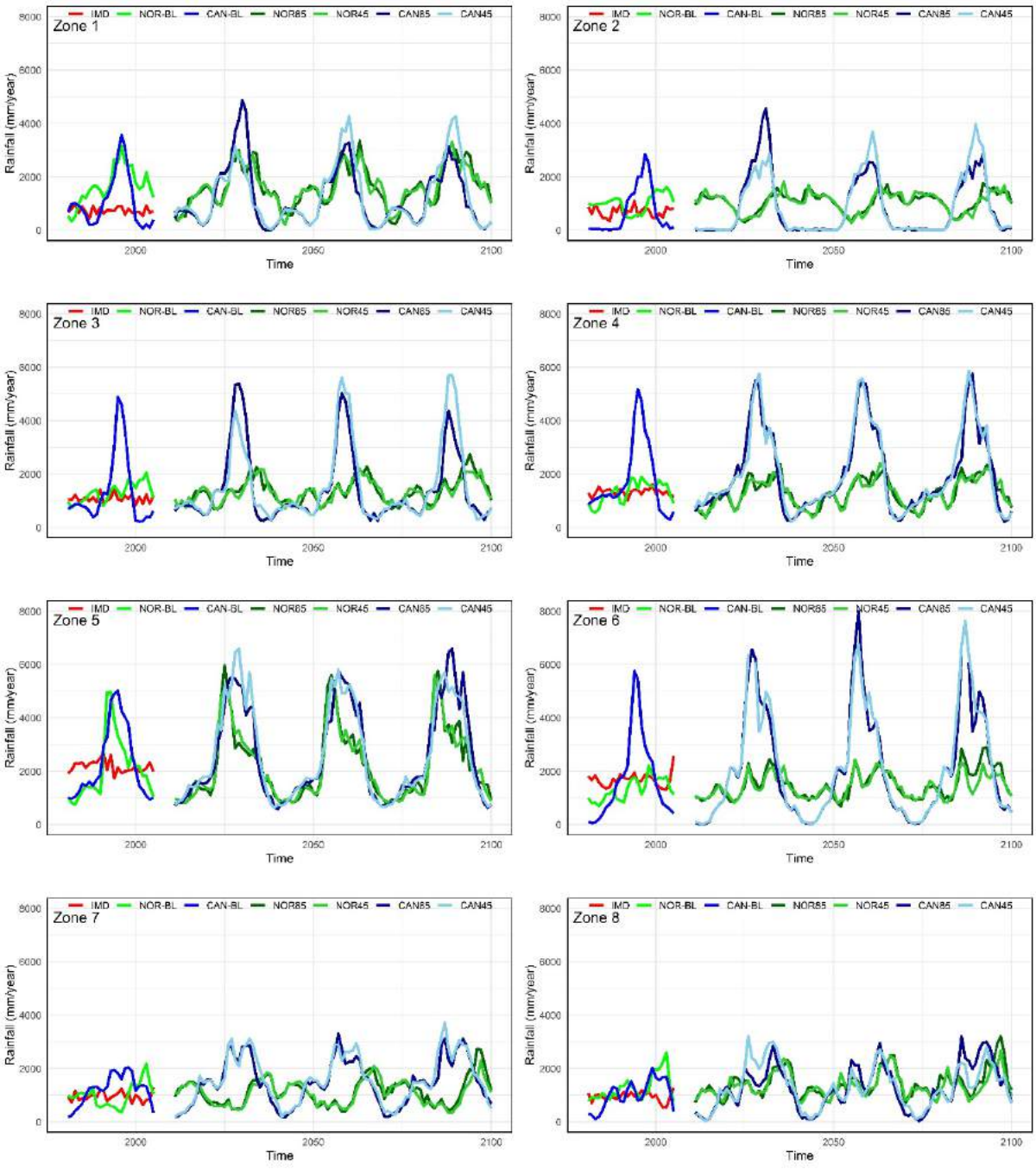

Fig. 33 Zone-wise bias corrected annual precipitation (mm/year) across 1981-2100. The gap in the 2006-2010 in the graphs was due to the design of 30-year time slices as described in section 2.c.

5. Conclusions and Future Scope

The WRF simulations captured the spatio-temporal patterns of the major climatic variables Precipitation, Minimum and Maximum Temperature. Zone-wise and season-wise evaluation of the performance clearly emphasized the problem zones due to model and input errors. In general, the NorESM2 based simulation highlighted that the model has severe cold bias and has over-predicted rainfall, under-predicted the diurnal temperature variability

showing colder days. The bias was observed to be more prominent in the Central and North India and during the winter, pre-monsoon and NEM. CanESM2 based simulations showed dry bias in the simulated precipitation for other zones, while for zone 7-8 the simulations were captured well. The temperature simulations from CanESM showed better spatial agreement with the IMD temperature distributions. The NEM variability was better represented in the CanESM precipitation simulations while SWM variability showed good agreement with IMD in NorESM precipitation simulations. The temperature biases in both the models were high in the winter and pre-monsoon months. The north-eastern region pre-monsoon thunderstorms and resultant extreme rainfall was not well represented in the simulations. The daily bias correction procedure has improved the temperature and precipitation simulations by reducing the biases across various zones.

6. Deliverables

Precipitation, Minimum Temperature, Maximum Temperature, Relative Humidity, Windspeed at 10 m and Solar radiation at daily time-step and at 25 km resolution. 96 NetCDF files (8 time slices x 2 GCMs input x 6 climate variables) were generated with a size of ~ 800 MB each (total size of the final output– 80 GB).

References

1. *Collins W.D., et al., 2004, Description of the NCAR Community Atmosphere Model (CAM 3.0). NCAR Tech. Note NCAR/TN–464+STR. 214 pp.*
2. *Dash S.K., Shekhar M.S., Singh G.P., 2006, Simulation of Indian summer monsoon circulation and rainfall using RegCM3. Theor. Appl. Climatol. 86, 161–172.*
3. *Dasari H.P., Challa V.S., Dodla V.B.R., Yerramilli A., 2011, Simulation of Indian monsoon extreme rainfall events during the decadal period 2000–2009 using a high-resolution mesoscale model. Adv. Geosci. A6, 31–48 (2011)*
4. *Ghodichore N., Vinnarasi R., Dhanya C.T., Roy S.B., 2008, Reliability of reanalyzes products in simulating precipitation and temperature characteristics over India. Journal of Earth System Science 127(8), 115 (2018).*
5. *Giorgi F., Mearns L.O., 1999, Introduction to special section: Regional climate modeling revisited. J. Geophys. Res., 104, 6335-6352.*
6. *Hong, S.–Y., and J.–O. J. Lim, 2006, The WRF single–moment 6–class microphysics scheme (WSM6). J. Korean Meteor. Soc., 42, 129–151.*
7. *Hong, Song–You, Yign Noh, Jimy Dudhia., 2006, A new vertical diffusion package with an explicit treatment of entrainment processes. Mon. Wea. Rev., 134, 2318–2341. doi:10.1175/MWR3199.1*
8. *IPCC, 2014: Climate Change 2014, Synthesis Report. Contribution of Working Groups I, II and III to the Fifth Assessment Report of the Intergovernmental Panel on Climate Change [Core Writing Team, R.K. Pachauri and L.A. Meyer (eds.)]. IPCC, Geneva, Switzerland, 151 pp.*
9. *Kirthiga, S.M., Narasimhan, B. & Balaji, C., 2021, A multi-physics ensemble approach for short-term precipitation forecasts at convective permitting scales based on sensitivity experiments over southern parts of peninsular India. J Earth Syst Sci 130, 68 (2021). https://doi.org/10.1007/s12040-021-01556-8*
10. *Kitoh A., 2017, The Asian monsoon and its future change in climate models: a review. J Meteorol Soc Jpn. Ser. II 95(1):7–33. https://doi.org/10.2151/jmsj.2017-002*
11. *Krishnan R., Sanjay J., Gnanaseelan C., Mujumdar M., Kulkarni A., Chakraborty S., 2020, Introduction to Climate Change Over the Indian Region, Assessment of Climate Change over the Indian Region. Springer, Singapore. https://doi.org/10.1007/978-981-15-4327-2_1*
12. *Li Z., Sun Y., Li T., Ding Y., Hu T., 2019, Future changes in East Asian summer monsoon circulation and precipitation under 1.5 to 5 °C of warming. Earth's Future, 7, 1391– 1406. https://doi.org/10.1029/2019EF001276*

13. *Mishra V., Kumar D., Ganguly A.R., Sanjay J., Mujumdar M.R., Krishnan, and Shah R.D., 2014, Reliability of regional and global climate models to simulate precipitation extremes over India. J. Geophys. Res. Atmos., 119. doi:10.1002/2014JD021636.*
14. *Murray F. W., 1967, On the Computation of Saturation Vapor Pressure. Journal of Applied Meteorology and Climatology, 6(1), 203-204. https://journals.ametsoc.org/view/journals/apme/6/1/1520-0450_1967_006_0203_otcosv_2_0_co_2.xml*
15. *Raju P.V.S., Bhatla R., Almazroui M., Assiri M., 2015. Performance of convection schemes on the simulation of summer monsoon features over the South Asia CORDEX domain using RegCM4.3. Int. J. Climatol. 35, 4695–4706.*
16. *Ratnam J.V., Kumar K.K., 2005, Sensitivity of the simulated monsoons of 1987 and 1988 to convective parameterization schemes in MM5. J. Clim. 18, 2724–2743.*
17. *Seland Ø., et al., 2020, Overview of the Norwegian Earth System Model (NorESM2) and key climate response of CMIP6 DECK, historical, and scenario simulations. Geosci. Model Dev., 13, 6165–6200. https://doi.org/10.5194/gmd-13-6165-2020*
18. *Shen Y., Sun Y., Zhong Z., Li T., 2021, A Quantitative Method to Evaluate the Performance of Climate Models in Simulating Global Tropical Cyclones. Front. Earth Sci. 9:693934. doi: 10.3389/feart.2021.693934*
19. *Skamarock W.C., Klemp J.B., Dudhia J., Gill D.O., et al., 2008 A description of the advanced researchWRF version 3, NCAR Technical Note, NCAR/TN-475+STR (Mesoscale and Micro scale Meteorology Division, National Center for Atmospheric Research, Boulder, Colorado, USA, 2008).*
20. *Smitha P.S., Narasimhan B., Sudheer K.P., Annamalai H., 2018, An Improved Bias Correction Method of Daily Rainfall Data Using a Sliding Window Technique for Climate Change Impact Assessment. Journal of Hydrology, 556, 100-118. https://doi.org/10.1016/j.jhydrol.2017.11.010*
21. *Srinivas C.V., Hariprasad D., Bhaskar Rao D.V., Anjaneyulu Y., Baskaran R., Venkatraman B., 2013, Simulation of the Indian summer monsoon regional climate using advanced research WRF model. Int. J. Climatol, 33: 1195–1210*
22. *Tewari M., Chen F., Wang W., Dudhia J., LeMone M.A., Mitchell K., G. Gayno, et al., 2004, Implementation and verification of the unified NOAH land surface model in the WRF model. 20th conference on weather analysis and forecasting/16th conference on numerical weather prediction. pp. 11–15.*
23. *Varikoden H., Mujumdar M., Revadekar J. V., Sooraj K. P., Ramarao M.V.S., Sanjay J., Krishnan R., 2018, Assessment of regional downscaling simulations for long term mean, excess and deficit Indian Summer Monsoons. Global and Planetary Change, 162, 28–38. doi: 10.1016/j.gloplacha.2017.12.002.*
24. *Yang D., and Saenko O.A., 2012, Ocean Heat Transport and Its Projected Change in CanESM2. J. Climate, 25, 8148–8163. https://doi.org/10.1175/JCLI-D-11-00715.1*
25. *Zhang C., Wang Y., Hamilton K, 2011, Improved representation of boundary layer clouds over the southeast pacific in ARW–WRF using a modified Tiedtke cumulus parameterization scheme. Mon. Wea. Rev., 139, 3489–3513.*
26. *Zhang X., Alexander L., Hegerl G.C., Jones P., Tank A.K., Peterson T.C., et al., 2011, Indices for Monitoring Changes in Extremes Based on Daily Temperature and Precipitation. Wiley Interdisciplinary Reviews: Climate Change, 2(6), 851–870. doi:10.1002/wcc.147.*

Report on

Dynamic Downscaling to Study Climate Change Impacts on Water Resources in India

under

National Water Mission

Submitted to

सत्यमेव जयते
Ministry of Water Resources
Government of India

Ministry of Water Resources, New Delhi

By

Centre for Climate Change & Disaster Management
Anna University, Chennai

JANUARY 2022

Background

Climate change has emerged as one of the major challenges in the twenty-first century. Changes in the global climate are altering the average characteristics of climate systems, intensity, frequency, spatial extent, duration and timing of climate extremes (IPCC 2013 and Herring et al. 2014). The expected impacts of climate change and the global warming range from changing rainfall pattern to increased salinity of the soil, lack of availability of potable water, inundation of coastal areas by sea water, etc. The major factor which causes concern is the steady increase in temperature and variability in rainfall pattern owing to climate change. Globally, in many regions, both temperature and precipitation extremes have already shown amplified responses to changes in means (Lisa 2007 and Folland et al. 2001). Hence, understanding implications of future climate change and its impact on different sectors especially related to water resources is essential to devise better strategies for management and conservation of vulnerable water resources.

Global Climate Models (GCMs) provide a reasonable basis for assessing future climate extremities. GCMs have so far been too coarse to resolve this geographically well-defined region. The GCMs are designed to simulate large-scale phenomena and processes and are not capable of providing local details on a country level. Therefore, downscaling techniques continue to be used as unavoidable alternatives to provide local climate information more accurately. There are two commonly used strategies in downscaling to resolve the geographically induced features: regional climate

downscaling, also referred to as dynamical downscaling (DD), and statistical downscaling (SD) (Cubasch et al. 1996). Statistical downscaling methods apply climate variables from GCMs to statistical transfer functions to evaluate point-scale meteorological series (Diaz-Nieto et al. 2005). These methods try to establish a direct statistical link between the simulated GCMs climate variables and targeted local climate variables. Statistical downscaling methods are easier and less costly to implement as compared to dynamical downscaling but their central premise is uncertain: that observed statistical relationships would remain unchanged in the future climate. Dynamical downscaling uses a limited-area, high-resolution model (a regional climate model, or RCM) driven by boundary conditions from a GCM or Atmosphere-Ocean General Circulation Models (AOGCMs) to derive smaller-scale information. These high-resolution dynamic RCMs nested in GCM are becoming an increasingly important tool in climate research.

Understanding the importance of providing the future climate at high resolution using Dynamical downscaling methods for the impact assessments, the project entitled "**Dynamic Downscaling to Study Climate Change Impacts on Water Resources in India**" has been initiated collaboratively with IITM Delhi, IIT Madras, IIT Varanasi and Anna University, Chennai vide. the proceeding .No.28/09/2017-R&D/378-40 dated Feb . .27th, 2018 of Director (R&D) Ministry of Water Resources RD & GR, Government of lndia, RD & PP Wing, R&D Division, New Delhi-66.

On the side of Anna University, the dynamical downscaling model, PRECIS (Providing Regional Climate for Impact Studies) developed by Met Office Hadley Centre, UK has been utilized to provide the future climate projections at 25 km horizontal resolution under RCP 4.5 and RCP 8.5 scenarios.

PRECIS is an atmospheric and land surface regional climate model used to downscale over a region of interest to the resolutions of 25 x 25 sq.km. It allows for a realistic representation of the climate over the region of interest, accounting for complex surface features such as coastlines, mountains, and islands, which are not resolved in the global climate models (Jones et al. 2004). Many studies used PRECIS to simulate the high-resolution climate change scenarios over different regions of the globe and the PRECIS simulation results show a good performance while calibrating temperature and rainfall for those regions. Nazrul Islam(Islam et al. 2009) and Rajib and Rahman (2012) used PRECIS to evaluate the seasonal forecasting for Bangladesh. Bhaskaran et al. (1996, 1998) and Bhaskaran et al., 2012 have analyzed the seasonal simulations of Indian summer monsoon using PRECIS. Rupa Kumar et al. (2006), Kumar et al. (2010, 2011), Revadekar et al. (2011), Kulkarni et al. (2013) and Bal et al (2016) have simulated the climate variability over the Indian region.

Objectives:

The primary objective of the project is to develop the high resolution (at 25 x 25 sq.km resolution) regional climate model data using **PRECIS** under RCP 4.5 and 8.5 scenarios thereby utilising it for assessing the river basin impact studies.

Data and Methodology:

The overall methodology of the study is shown in Figure 1.

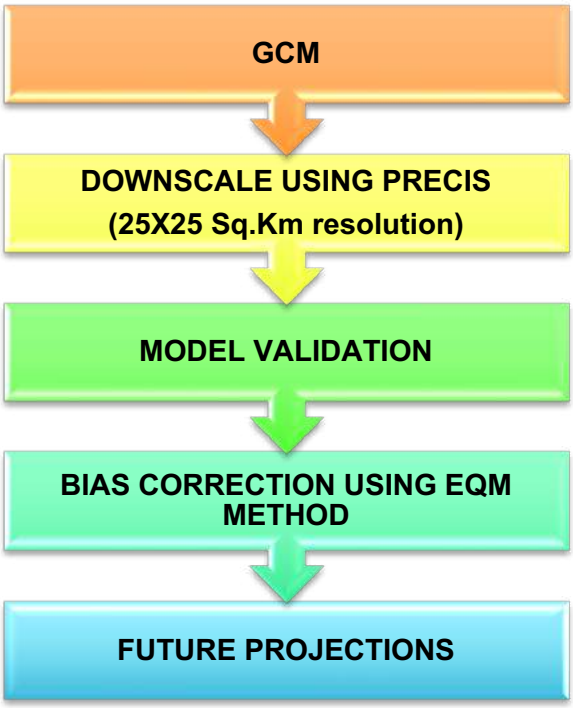

Fig 1. Overall Methodology

The GCM, HadGEM2ES developed by Met office Hadley Centre at 100 x 100 sq.km are downscaled to high resolution Regional Climate model of 25 x25 Sq.km. The model simulated data are validated with the observation data for finding the accuracy of the model. The simulated variables with insignificant bias are corrected with the EQM statistical bias correction method and the resulted simulation are projected for the future climate of India.

Model Downscale

PRECIS has been run at 25 km horizontal grid resolution in a large domain that covers India (3.5° N to 38.5° N, 62.5° E to 101.6° E) to generate a daily time series (1971-2094) using the boundary data from the GCM, HadGEM2-ES under AR5 simulations (Fig.2 and Fig 3). The study uses both RCP (Representative Concentration Pathways)

4.5 and 8.5 Scenarios to assess from moderate to high concentration of aerosol and greenhouse gases. The model dynamics use a split-explicit finite difference scheme on an Arakawa 'B' grid (Arakawa and Lamb 1977) in the horizontal and hybrid vertical coordinates (sigma or pressure normalised by surface pressure in the lower layer changing smoothly to pressure above about 50 hPa). The prognostic input variables in the dynamical layer, cloud and boundary layer schemes are surface pressure (p*), zonal and meridional wind components (u and v), potential temperature adjusted to allow for the latent heat of cloud water and ice (ΘL), and water vapour plus liquid and frozen cloud water (qT).

In the horizontal layout, the momentum variables (u and υ) are offset by half a grid box in both directions from the thermodynamic variables (p*, ΘL , qT).

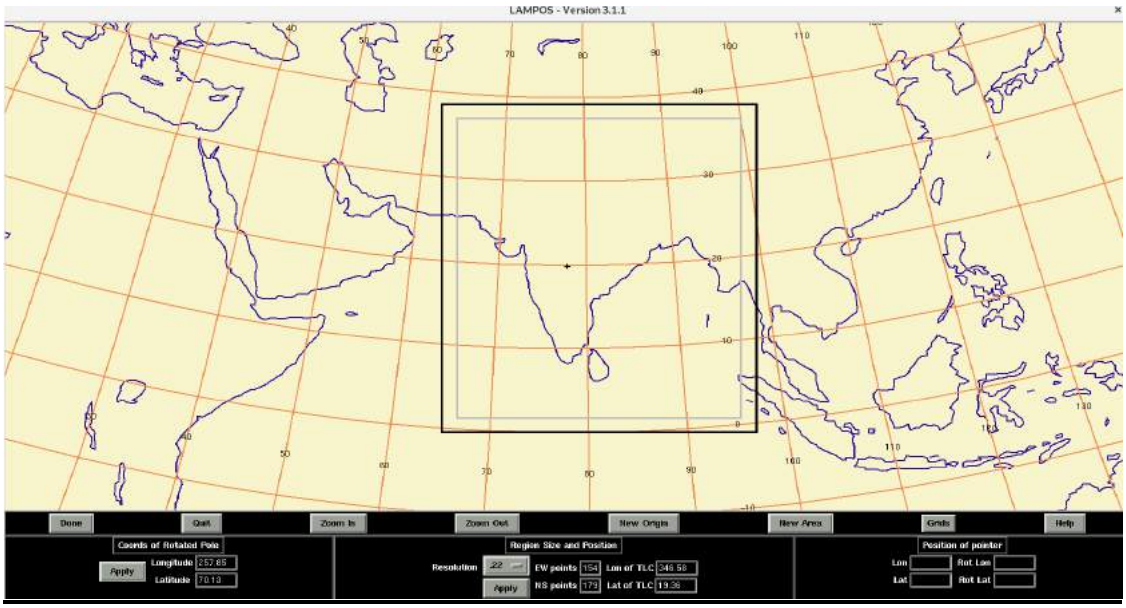

Fig. 2. Domain Selection

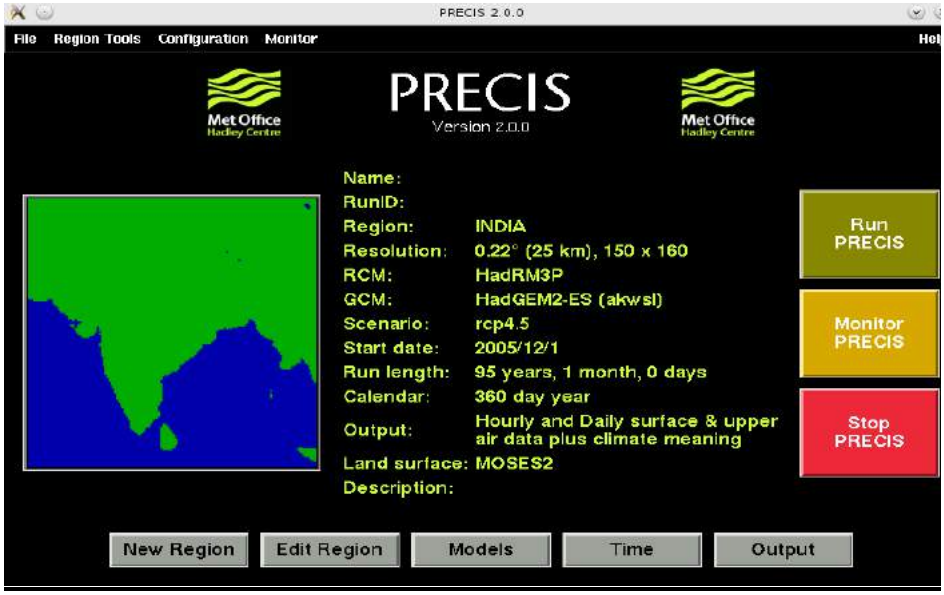

Fig.3. Model Selection in PRECIS Regional Climate Model

BIAS CORRECTION

Even though climate models are considered to be the most suitable tools to provide information on future climate projections, these models have inherent systematic errors or biases. Bias is simply defined as the difference between climate model outputs and observed data. Imperfect conceptualization and parameterization, insufficient length of data records, quality of reference data sets and insufficient spatial resolution are identified as the main sources of bias in climate modelling. To reduce these biases, the application of bias correction approaches is required. This study uses Empirical quantile mapping as bias correction method to remove the biases from the model simulation. The EQM is found to produce the best results in terms of bias correction of model output especially for the water impacts studies (Gutjahr and Heinemann, 2013). Empirical quantile mapping (EQM) is a form of extended bias removal method which aims to calibrate the model simulated cumulative distribution function (CDF) by adding to the quantiles of observed precipitation distribution both the mean and individual delta

changes (Cannon et al., 2015) in the corresponding quantiles. Such quantile-to-quantile matching aligns all moments of probability distribution function (PDF) of model (Piani et al., 2010; Hagemann et al., 2011) by using the PDF of observations, incorporating both the PDFs to CDFs and build a transfer function. This function transforms the raw model precipitation into corrected model precipitation. Theoretically, post-transformation, the CDF of the model should be same as that of observation.

The EQM is based on empirical CDF (ECDF) (Panofsky and Brier, 1968; Wood et al., 2004; Boé et al., 2007; Déqué, 2007; Themeßl et al., 2011; 2012; Gudmundsson et al., 2012; Wetterhall et al., 2012) and is therefore known as empirical quantile mapping (EQM). In this method, the probability integral transform as defined by Angus (1994) is applied and if the distribution of precipitation is known, the transformation is,

$$P_{\mathrm{cor},m,d} = \mathrm{ECDF}^{-1}_{\mathrm{obs},m}(\mathrm{ECDF}_{\mathrm{raw},m}(P_{\mathrm{raw},m,d})),$$

where Pcor,m,d and Praw,m,d are daily values of corrected model precipitation and uncorrected model precipitation respectively. ECDF raw,m is the direct function of Praw,m,d and ECDF−1 obs,m is the inverse (or quantile) function corresponding to observed precipitation distribution.

Results:

The downscaled RCM has the output of 175 parameters inclusive of five major variables such as Maximum Temperature (Unit - °C), Minimum Temperature (Unit - °C), Rainfall (Unit - mm), Relative humidity (Unit - %), Solar Radiation (Unit - Wm−2) and Wind speed (Unit - ms−1) for the period of 1971-2000 as baseline period and 2006-2094 as projection period. This project uses these five parameters to be used for impact studies.

Model Validation:

Temperature

The model simulated temperature data are validated with CRU data for the period (1971-2000). The spatial representation of Maximum and Minimum Temperature indicates the correlation of 0.56 and 0.66 respectively at 95% confidence interval (Figures 4 and 5). The RMSE of daily maximum and minimum temperature with observation shows 1.5°C and 1.1°C respectively. Though, the model has significantly less bias, the simulated data are not bias corrected due to the unavailability of high resolution (25 x 25) observation data. Rogas et al., 2011 stated that with the low-resolution dataset, the accuracy and credibility of the model simulation will be reduced (Rogas et al., 2011). Hence, the resulted simulation used for future projections.

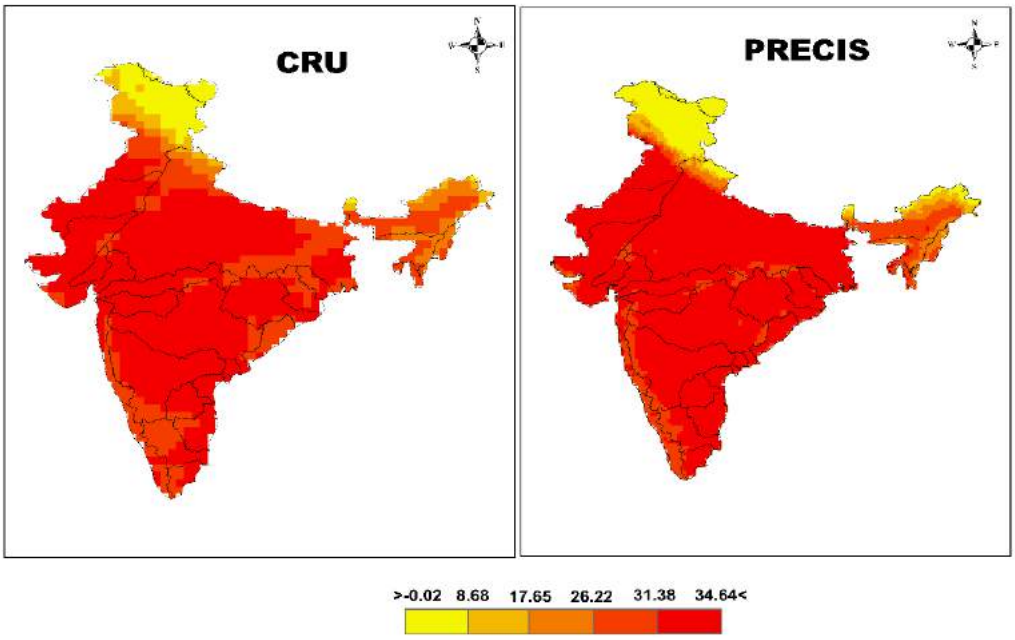

Fig. 4. Validation of Maximum Temperature of CRU with PRECIS for the period of 1971-2000

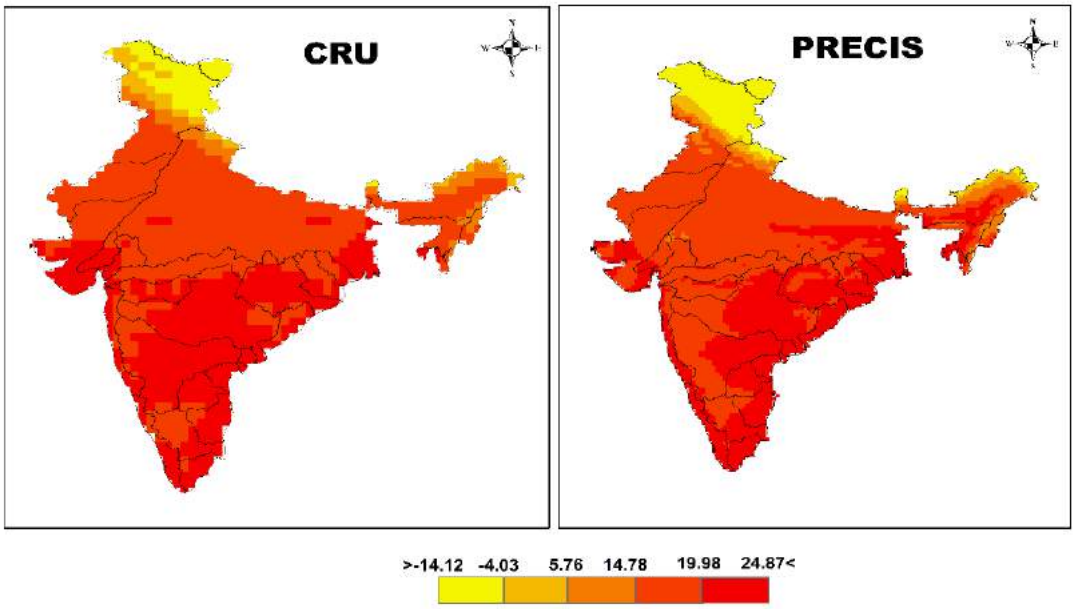

Fig. 5. Validation of Minimum Temperature of CRU with PRECIS for the period of 1971-2000

Maximum temperature projections:

Projections of change in annual mean maximum temperature over India as a whole for 2030s (2005-2035), 2050s and 2080s with reference to the baseline period (1971-2000) at the (Fig. 8). indicate an average increase of 0.3 to 2.2°C, 1.0 to 3.7°C and 1.8 to 5.2 °C respectively under RCP 4.5 simulation (Fig. 5) and -1 to 4.5 °C, -2 to 6.8°C and -3 to 7.2°C under RCP 8.5 simulation (Fig. 6). It has been noted that Northern and North western part of India indicated the maximum increase of temperature for both the scenarios.

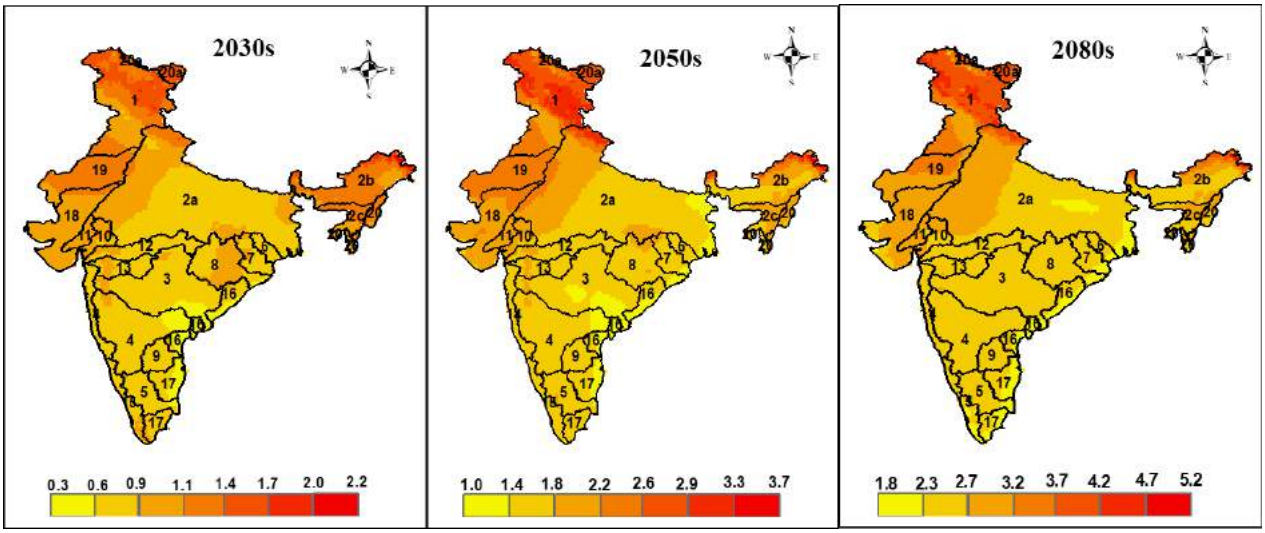

Fig.5 Maximum temperature projections for India under RCP 4.5 Scenario

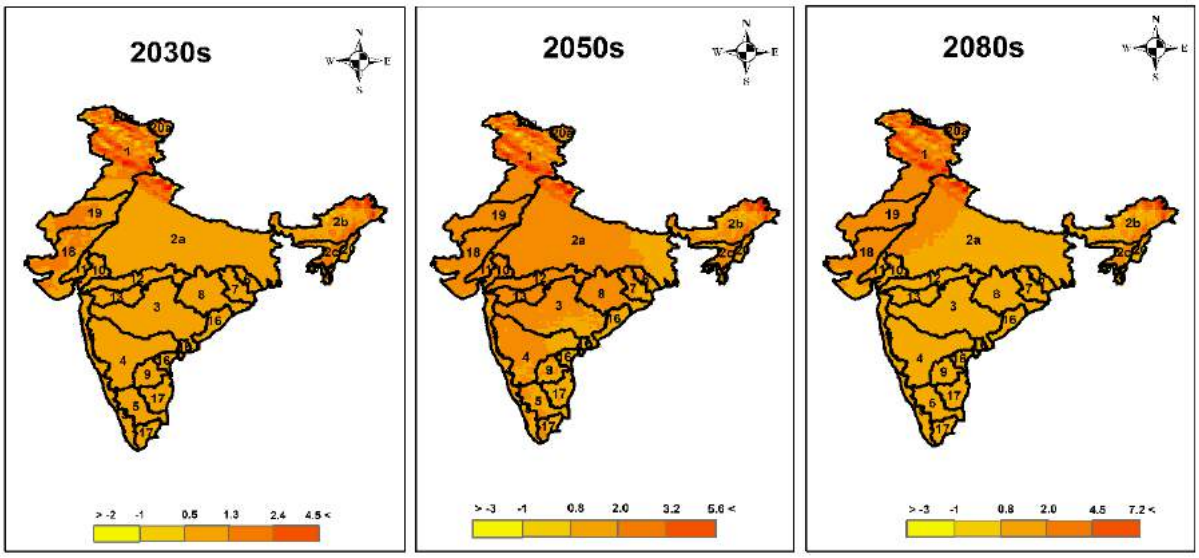

Fig.6 Maximum temperature projections for India under RCP 8.5 Scenario

Minimum Temperature

The projections of change in annual mean minimum temperature over India as a whole for 2030s, 2050s and 2080s with reference to the baseline period indicate an average increase of 0.6 to 2.2 °C, 1.2 to 3.7 °C and 1.5 to 5.0 °C respectively at the emission

scenario of RCP 4.5 (Fig.7). and -2 to 4.2°C, 1.2 to 6.2 °C and 0.8 to 9.3°C under RCP 8.5 Scenario (Fig.8). It has been noted that the entire country indicated the maximum increase in the minimum temperature. Further the change in minimum temperature is found to be higher than the change in maximum temperature.

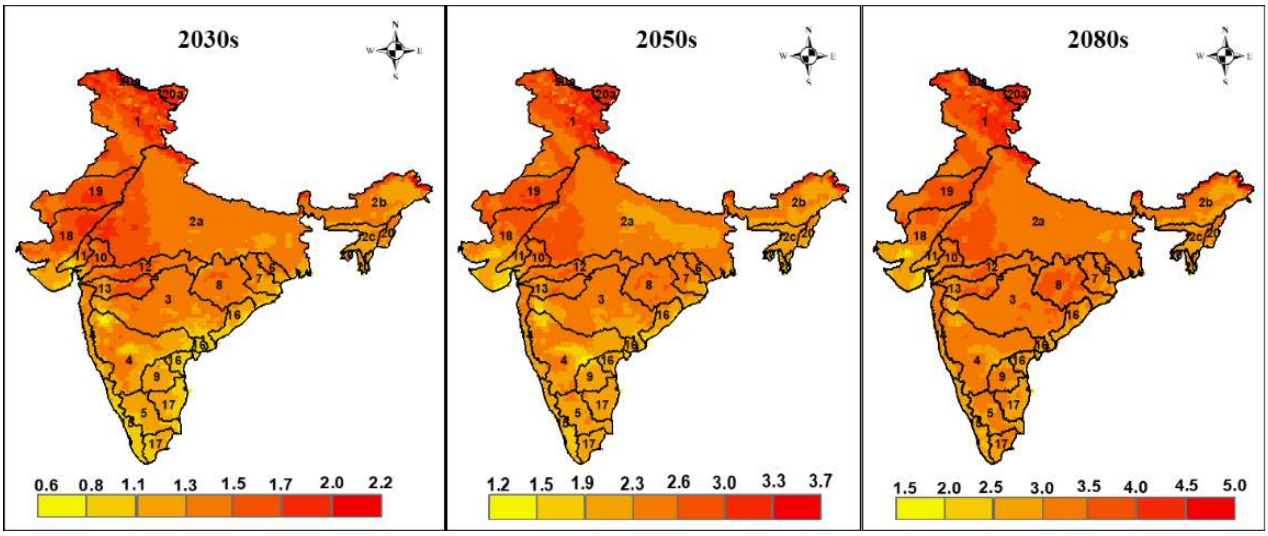

Fig.7 Minimum temperature projections under RCP 4.5 scenario

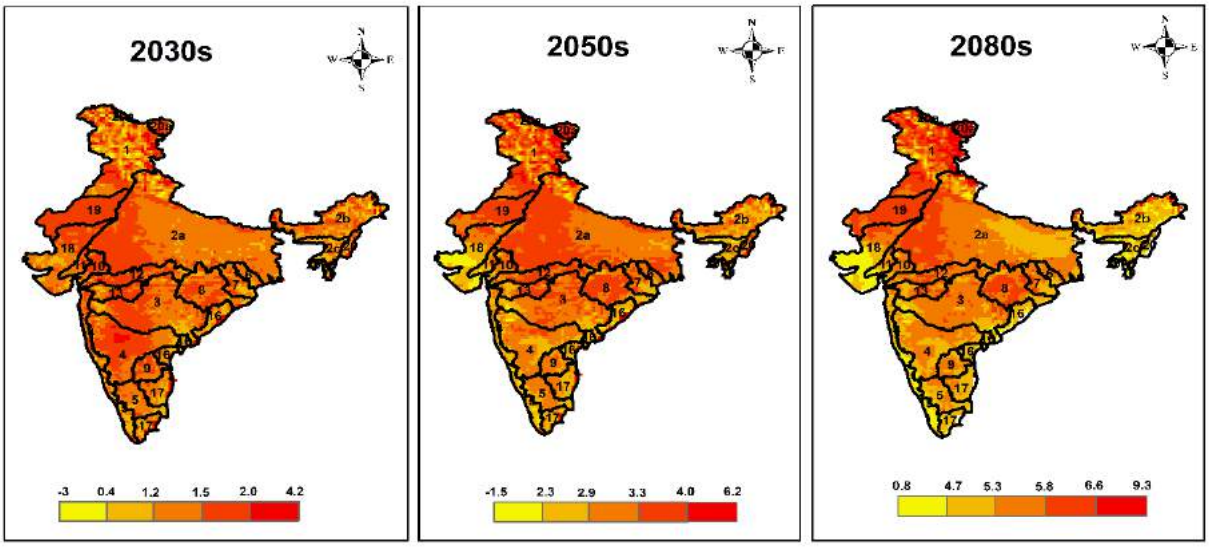

Fig.8 Minimum temperature projections under RCP 8.5 scenario

Rainfall

The annual rainfall from the model output when validated with the IMD rainfall gridded data of 25x 25 km resolution indicated an under estimated value in some areas especially the south eastern part of the country. Hence, the uncertainty of the data is bias corrected using the Empirical quantile mapping method.

Figure 7 depict the bias corrected average annual rainfall of PRECIS data for the period of 1971-2000 and the Root Mean Square Error (RMSE) was evaluated as 11.6 mm. Hence, this bias corrected model data is used for projecting future climate scenarios.

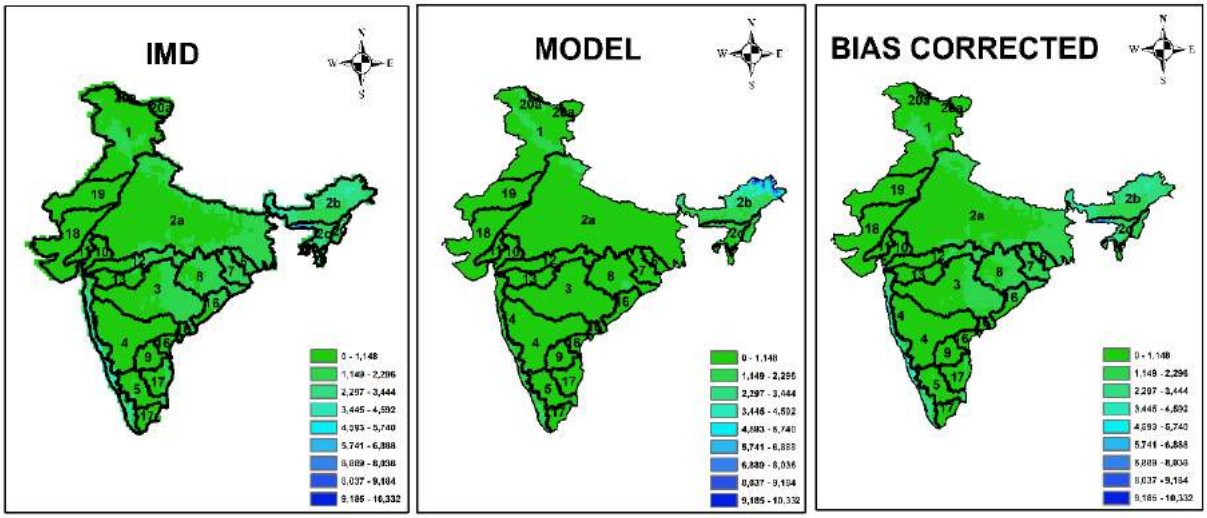

Fig. 9 IMD vs Bias Corrected PRECIS average annual rainfall for the period 1970-2000

Annual Rainfall Projections:

The projections of annual rainfall for India generally indicate no significant changes in 2030s, 2050s and 2080s. The spatial representation of average annual rainfall indicated the maximum increase in the western and south western part of the country under RCP

4.5 scenarios (Fig. 10 and Fig 11). The percentage change of annual rainfall under RCP 4.5 indicates an increase of 16 %, 26 % and 28% respectively for 2030s, 2050s and 2080s. Similarly for the RCP 8.5 scenario, the increase of rainfall is about 25%, 28% and 60% respectively for 2030s, 2050s and 2080s.

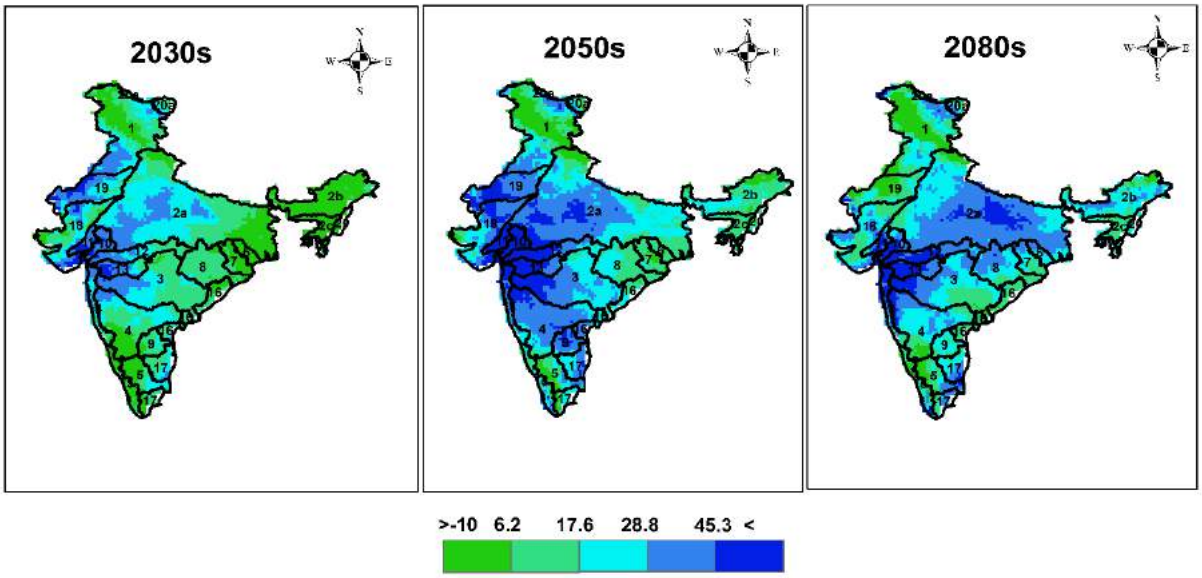

Fig.10 Annual Rainfall projections for India under RCP 4.5 Scenario

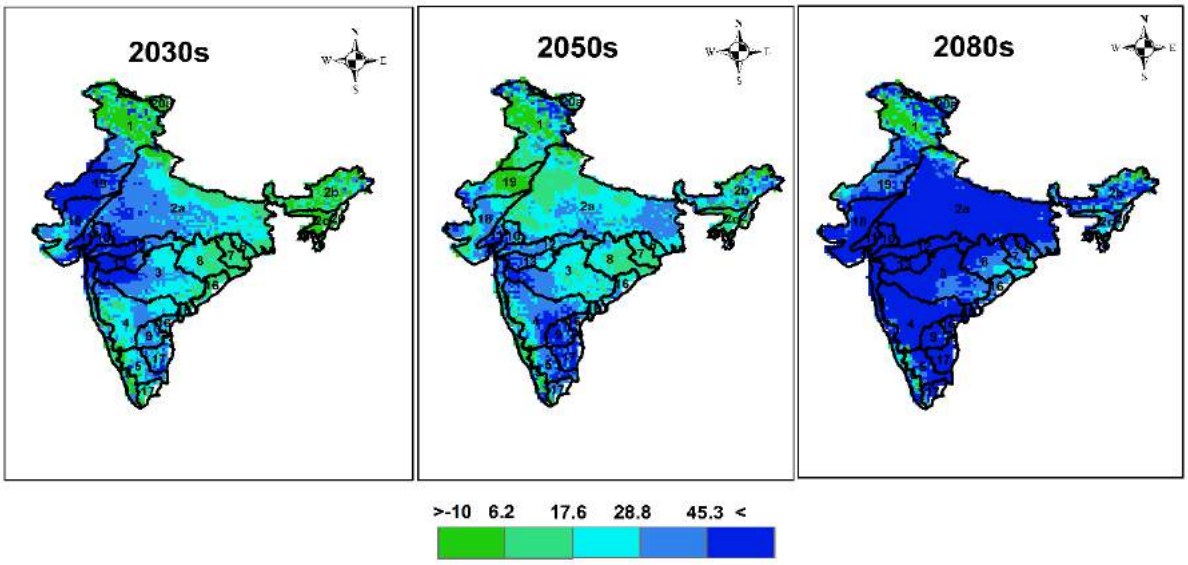

Fig.11 Annual Rainfall projections for India under RCP 8.5 Scenario

Conclusion:

The project aims to provide future climate data for India at higher resolution of (25x 25km) using regional climate model, PRECIS under AR5 scenarios for both RCP 4.5 and 8.5 simulations. The projection of change in maximum temperature indicated an increase of 1.8 to 5.2 °C by the end of the century under RCP 4.5 scenario and -3.0 to 7.2 °C by the end of the century under RCP 8.5 scenario. The change in minimum temperature indicated an increase of 1.5 to 5.0 °C by the end of the century and 0.8 to 9.3°C under RCP 8.5 Scenario. It has been noted that the increase of minimum temperature is identified to be more than maximum temperature.

The annual rainfall for the model were validated with the IMD and the model simulation underestimated in some of the regions especially in the eastern part of India. Hence, the bias correction of annual rainfall using empirical quantile mapping method was executed. The RMSE of the bias corrected simulation has indicated the less bias than the raw simulation. The projection annual rainfall for India from the bias corrected result indicate an increase of 28% by the end of the century under RCP 4.5 scenario. and increase of 60% under RCP 8.5 scenario. Generally, more rainfall is projected in the western and south western part of the country.

OUTCOME:

The five major climate parameters such as Relative Humidity, Solar Radiation, Wind Speed, Temperature and Rainfall from the model simulation for the period of 1971-

2000 as baseline and 2006-2094 as projections data under RCP 4.5 and 8.5 scenarios are provided in Netcdf format in the below link.

The link to access file is :
https://get.massive.app/01FTZTZSP49FYJ2Y9ZFXKG0Y7D?secret=qShWiyfEAlrGraHr

Password for the link is : climate

Password for unzipping file is : Cccdm

References:

1. Bal PK, Ramachandran A, Palanivelu K, Thirumurugan P, Geetha R, Bhaskaran B (2016) Climate change projections over India by a downscaling approach using PRECIS. Asia-Pac J Atmos Sci 52(4):353–369
2. Cannon, A.J., Sobie, S.R. and Murdock, T.Q. (2015) Bias correction of GCM precipitation by quantile mapping: how well do methods preserve changes in quantiles and extremes? Journal of Climate, 28(17), 6938–6959.
3. Cubasch U, Von Storch H, Waszkewitz J and Zorita E (1996) Estimates of climate change in Southern Europe derived from dynamical climate model output, *Climate Research,* Vol. 7: 129-149, 19
4. Déqué, M. (2007) Frequency of precipitation and temperature extremes over France in an anthropogenic scenario: model results and statistical correction according to observed values. Global and Planetary Change, 57(1–2), 16–26.
5. Diaz-Nieto J and Wilby RL (2005) A comparison of statistical downscaling and Climate Change factor methods: impacts on low flows in the river Thames, United Kingdom, Climatic Change, Vol. 69: 245–268
6. Folland CK, Karl TR, Christy JR, Clarke RA, Gruza GV, Jouzel J, Mann ME, Oerlemans J, Salinger MJ and Wang SW (2001) Observed climate variability and change. In: Climate Change 2001: The Scientific Basis. Contribution of Working Group I to the Third Assessment Report of the Intergovernmental Panel on Climate

Change. Cambridge University Press, Cambridge, UK, and New York, USA, 881 pp

7. Gudmundsson, L., Bremnes, J.B., Haugen, J.E. and Skaugen, T.E. (2012) Downscaling RCM precipitation to the station scale using quantile mapping—a comparison of methods. Hydrology and Earth System Sciences Discussions, 9(5), 6185–6201.
8. Gutjahr, O. and Heinemann, G. (2013) Comparing precipitation bias correction methods for high-resolution regional climate simulations using COSMOCLM. Theoretical and Applied Climatology, 114(3–4), 511–529.
9. Hagemann, S., Chen, C., Haerter, J.O., Heinke, J., Gerten, D. and Piani, C.(2011) Impact of a statistical bias correction on the projected hydrological changes obtained from three GCMs and two hydrology models. Journal of Hydrometeorology, 12(4), 556–578.
10. Herring SC, Hoerling MP, Peterson TC and Stott PA (2014) Explaining extreme events of 2013 from a climate perspective. B. Am. Meteorol. Soc. 95, S1–S96
11. IPCC (2013) Summary for Policymakers. In: Climate change 2013: the physical science basis. Contribution of working group I to the Fifth Assessment Report of the Intergovernmental Panel on Climate Change [Stocker TF, Qin D, Plattner GK, Tignor M, Allen SK, Boschung J, Nauels A, Xia Y, Bex V and Midgley PM (eds.)].Cambridge University Press, Cambridge, United Kingdom and New York, NY, USA
12. Jones RG, Noguer M, Hassell DC, Hudson D, Wilson SS, Jenkins GJ and Mitchell JFB (2004) Generating high resolution climate change scenarios using PRECIS, Met Office Hadley Centre, Exeter, UK, 40 pp
13. Krishna Kumar K, Patwardhan SK, Kulkarni A, Kamala K, Koteswara RK, Jones R (2011) Simulated projections for summer monsoon climate over India by a high-resolution regional climate model (PRECIS). Curr Sci 101:3–10
14. Kulkarni A, Patwardhan S, Krishna Kumar K, Ashok K, Krishnan R (2013) Projected climate change in the Hindu Kush-Himalayan region by using the high-resolution regional climate model PRECIS. Mt Res Dev 33:142–151. doi:10.1659/MRD-JOURNAL-D-11-00131.1

15. Lisa VA (2007) Trends in Australia's climate means and extremes: a global context. Australian Meteorological Magazine, 56:1
16. Panofsky, H.W. and Brier, G.W. (1968) Some Application of Statistics to Meteorology.University Park, PA: Pennsylvania State University, p. 6186.
17. Piani, C., Haerter, J.O. and Coppola, E. (2010) Statistical bias correction for daily precipitation in regional climate models over Europe. Theoretical and Applied Climatology, 99(1–2), 187–192.
18. Revadekar JV, Patwardhan SK, and Kumar KR (2011) Characteristic Features of Precipitation Extremes over India in the Warming Scenarios. Hindawi Publishing Corporation, Advances in Meteorology, Volume 2011, Article ID 138425, p 11, doi:10.1155/2011/138425
19. Rupa Kumar K, Sahai AK, Krishna Kumar K, Patwardhan SK, Mishra PK, Revadekar JV, Kamala K and Pant GB (2006) High-resolution climate change scenarios for India for the 21st century, Current Science, vol. 90, no. 3, 334-345.

Final Report

On

Dynamical Downscaling to study Climate Change Impact on Water Resources in India

Submitted by

Prof. R. K. Mall
Prof R. Bhatla
Dr. T. Banerjee
Dr. P. K. Srivastava

काशी हिन्दू विश्वविद्यालय
BANARAS HINDU UNIVERSITY
ESTABLISHED BY PARLIAMENT BY NOTIFICATION NO. 225 OF 1916

Mahamana Centre of Excellence in Climate Change Research • MCECCR •

DST-Mahamana Centre of Excellence in Climate Change Research
Institute of Environment & Sustainable Development,
Banaras Hindu University
Varanasi-221005, India

Objectives of the proposal:

- Baseline data, information, and past studies considered for downscaling.
- Sensitivity analysis, calibration, and validation of RegCM4, a high-resolution regional climate model.
- Projection of future climate scenarios (near future 2015-2040, and distant future 2040-2070) using the high-resolution regional climate model (RCM), i.e., RegCM 4.6 using dynamic downscaling techniques.

1. Project Overview

The impact of Climate Change on Water Resources in India will be assessed using dynamically downscaled regional climate model simulations. The Regional Climate Model (RegCM) developed at International Centre for Theoretical Physics (ICTP) has been utilized to dynamically downscale the coarser-resolution data obtained from various Global Climate Model (GCMs). The latest version, i.e., the RegCM4.6 model, has been employed over the South Asia Coordinated Regional Downscaling Experiment (SA-CORDEX) domain (22°S–50°N;10°E–130°E) to generate the regional climate date of climate variables such as temperature (daily maximum; Tmax & minimum; Tmin), daily total precipitation (PrecT), daily net radiation (Rnet), atmospheric relative humidity (RH) at 25 km high spatial resolution during the following time periods:

a) Time period:

(i) Historical or reference period - 1951-2005.

(ii) Future projections - 2006-2100 (for RCP4.5 & RCP8.5 scenarios).

b) GCM forcing:

(i) MPI-ESM-MR (**ii)** GFDL-ESM2M

The MPI- ESM-MR and GFDL-ESM2M are comprehensive Earth system models, and consist of component models for the ocean, ice, atmosphere, and land surface. These components are coupled through the exchange of energy, momentum, water, and important trace gases such as carbon dioxide. MPI- ESM-MR and GFDL-ESM2M are global climate models that run at a coarse resolution of 1.8653° latitude x 1.875° longitude. These models have been widely employed in various inter-comparison projects, including the most recent CMIP6.

2. Regional Climate Model (RegCM):

The RegCM is the first limited area model developed for long-term regional climate simulation and has been used widely for climate studies. The RegCM system is a community model, open source and specially designed for use by scientists in industrialized countries and developed nations (Pal et al 2007). It is supported through the Regional Climate research NETwork, or RegCNET, a widespread network of scientists coordinated by the Earth System Physics section of the Abdus Salam International Centre for Theoretical Physics (ICTP), Italy.

The RegCM modeling system has four components: Terrain, ICBC, RegCM, and Postprocessor. Terrain and ICBC constitute two components of RegCM pre-processor. Terrestrial variables (including elevation, landuse, and sea surface temperature) and three-dimensional isobaric meteorological data are horizontally interpolated from a latitude-longitude mesh to a high-resolution domain on either one of the Rotated (and Normal) Mercator, Lambert Conformal, and Polar Stereographic projections. Vertical interpolation from pressure levels to the σ coordinate system of RegCM is also performed.

Initially, first version of the model was developed in the eighties (RegCM1, Dickinson et al. [1989]), Giorgi [1990]), to later versions in the early nineties (RegCM2, Giorgi et al. [1993b], Giorgi et al. [1993c]), late nineties (RegCM2.5) followed by more evolved version RegCM 3 in 2000s (Giorgi and Mearns [1999]) (RegCM3, Pal et al. [2007]). The ICTP RegCM 4 is the most improved and state-of-the-art version of the model (Giorgi *et al*. 1993a,b). It is a hydrostatic limited area model, compressible, sigma-p vertical co-ordinate model with

Arakawa B-grid system in which wind and thermodynamic variables are horizontally staggered using a time splitting explicit integration scheme.

Table 1. Model configuration of RegCM 4.6

Model Dynamics	Hydrostatics
Map projection	Normal Mercator
Model domain	South Asia CORDEX domain (22°S–50°N;10°E–130°E)
Resolution	25 km horizontal and 18 sigma vertical levels
Initial and boundary conditions	MPI-ESM-MR , GFDL-ESM2M, EIN15
Sea Surface Temperature	MPI-ESM-MR, GFDL-ESM2M, OI_WK
Radiation scheme	NCAR CCM3 (Community Climate Model 3; Kiehl et al., 1996)
Land surface model	Biosphere-Atmosphere Scheme (BATS) (Dickinson et al., 1989)
Planetary boundary layer scheme	Holtslag (Holtslag et al., 1990)
Convective precipitation Scheme	Grell scheme (Grell 1993) with closure assumption of the Arakawa and Schubert closure (AS74) (Grell et al 1994)
Large-Scale Precipitation Scheme	Subgrid explicit moisture scheme (SUBEX) Sundqvist etal.,1989
Convective parameterization scheme	1. Emanuel 2. Grell 3. Tiedtke 4. KF 5. Different combinations of core convection schemes (over land and ocean)

Since the RegCM4.5 release, the model can also use a non-hydrostatical dynamical core, and allows for small horizontal resolutions of the order of a few kilometres. Also compared to previous versions, RegCM4 includes new land surface, planetary boundary layer and air-sea flux schemes, mixed convection and tropical band configuration, modifications to the pre-existing radiative transfer and boundary layer schemes and a full upgrade of the model code toward improved flexibility, portability and user-friendliness. The ICTP regional climate model (RegCM) has a wide range of applications for climate change simulation and prediction.

3. **Methodology:**

3.1 Dynamical downscaling:

The dynamical downscaling approach is employed to provide adequate spatial and temporal resolution to represent the regional and local scale climatic parameter. Dynamical downscaling of 6 hourly meteorological data from MPI-ESM-MR and GFDL-ESM2M at 1.86° x 1.8° grids resolution is used to generate six-hourly model outputs at 25 x 25 km grids for the Indian domain using latest version of RegCM 4.6. The selection of domain, buffer zone in terms of spatial extent and resolution is one of the important phenomena of dynamical downscaling.

RegCM 4.6 has been used for simulating Indian summer monsoon rainfall over different homogeneous regions of India. The South Asia CORDEX domain (22°S–50°N;10°E–130°E) has been selected as the model domain with 25 km horizontal resolution and 18 sigma vertical level (Giorgi *et al.* 2008). In this study, high resolution (0.5^{o}x0.5^{o}) RegCM 4.6 model (Giorgi *et al*. 2012) has been used, which is an improved version of ICTP RegCM 4 (Giorgi *et al*. 1993a,b). It is a hydrostatic limited area model, compressible, sigma-p vertical co-ordinate model with Arakawa B-grid system in which wind and thermodynamic variables are horizontally staggered using a time splitting explicit integration scheme as described in Table 1.

The Initial and boundary condition is derived six hourly at 1.86° x 1.8° grids to generate six-hourly model outputs at 25 x 25 km grids for the Indian domain using the latest version of RegCM 4.6. The sea surface temperature datasets have been obtained from ERSST – ERA-Interim at every 6 hours at a resolution of 1.5^{o}x1.5^{o}. NCAR's community climate model version

3 (CCM3) radiation parameterization scheme is used in this model (Kiehl *et al.* 1996). The land surface parameterization is given by Biosphere-Atmosphere Scheme (BATS) (Dickinson *et al.* 1989) and planetary boundary layer parameterization given by the scheme of Holtslag (Holtslag et al., 1990) are used. For convective precipitation scheme, modified Kuo scheme, Grell scheme (Grell 1993) with closure assumption of The Arakawa and Schuber closure given by Grell *et al.* (1994), and MIT Emanuel scheme have been used. The Subgrid explicit moisture scheme (SUBEX) given by Sundqvist *et.al*. (1989) is used for the large-scale precipitation scheme. The time period for the historical run is taken as 1950 – 2005.

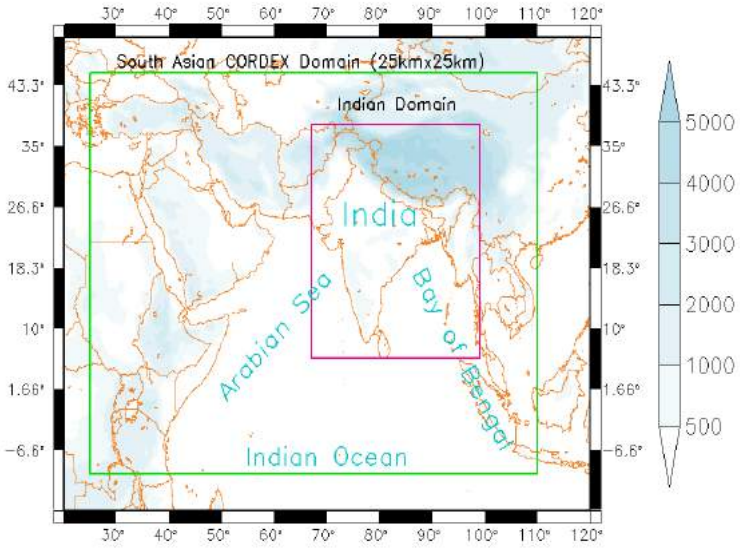

Fig.1 *Model Domain for the proposed simulation*

The model parent domain used for the study is the south Asian CORDEX domain (22°S–50°N;10°E–130°E) mentioned in Figure 1. The performance of RegCM 4.6 CPS scheme is calibrated and validated using observed gridded rainfall data of the India Meteorological Department (IMD) and Climate Research Unit (CRU) precipitation and temperature dataset with the resolution of 0.25° x 0.25° and 0.50° x 0.50° respectively. The validation of model output data has been done using Mean Bias, Root Mean Square Error (RMSE), Standard Deviation (SD), and correlation. For this study, RegCM 4.6 has been simulated for a period of 30 years (1982-2012), forced by various initial and boundary conditions (ICBCs) and sea surface temperature (SSTs) (Table 1). A detailed description of the convective parameterization scheme describes below:

3.2 Convective Scheme:

For the simulation and validation of variability of Indian summer monsoon rainfall over different homogeneous regions of India, four core convective parameterization schemes (CPS) i.e. Emanuel, Grell, and Tiedtke have been used for the study. Also, two mixed convection schemes of RegCM 4.6 i.e., Emanuel over the ocean; Grell over land (Mix99) Emanuel over land; Grell over the ocean (Mix98) have been used. Detailed description of all six scheme of RegCM 4.6 has been listed below:

a) **Kuo Scheme:** It is the first scheme incorporated in RegCM 4.6 known as kuo- type scheme of Anthes *et al.* (1977). Convective activity in the Kuo scheme is based on moisture convergence.

b) **Grell Scheme:** Grell scheme implemented using two closure assumptions i.e, the Arakawa and Schubert closure and the Fritsch and Chappell closure hereafter referred to as AS74 and FC80, respectively. In this scheme clouds are considered as two steady state circulations: an updraft and downdraft (Grell, 1993). No direct mixing occurs between the cloudy air and the environment air except at the top and bottom of the circulations. The mass flux is constant with the height and no entrainment or detrainment occurs along the cloud edges. This scheme is activated when a lifted parcel attains moist convection.

c) **Emanuel:** the processes involved in this scheme is quite complex and provide additional physical representation of convection. It assumes that the mixing in cloud is highly episodic and inhomogeneous and consider convective fluxes based on an idealized model of sub-cloud-scale updraft and downdrafts (Emanuel, 1991). Convection started when neutral buoyancy level is higher than the cloud base.

d) **Tiedtke:** It is the fourth available convection scheme in RegCM4.6 which is based on mass flux and moisture convergence closure. It has shallow and deep convection, detrainment of the cloud base mass flux from the PBL equilibrium, and mass flux closure from CAPE, respectively (Ali *et al.* 2015). It is a mass-flux type scheme that was originally designed for use in the global climate model, with a particular focus on the correct representation of deep tropical convection. (Bao *et al*. 2013)

e) **Mixed convection scheme**: Model has the capability of running different schemes over land and ocean. Hence, new mixed convection schemes are added as different schemes have different performances over different regions. This includes Grell, Emanuel, and Tiedtke scheme over land and ocean vice versa.

4. Sensitivity analysis, calibration and validation of RegCM4, a high resolution regional climate model:

The Regional climate model (RegCM) developed by the Earth system physics group of ICTP, Italy. All over the world, it has been used in simulating world climate and weather phenomena. This regional model is flexible, portable, and widely applicable over the different parts of the Earth. Numerous sensitivity analyses have been done regarding the selection of domain, adequate horizontal resolution, and applied Convective parameterized Scheme (Davis et al 2009, Giorgi et al 2012). A descriptive study by Pal et al (2007) proves that selecting appropriate convective parameterization schemes in RCMs is a major source of error and has a significant impact on regional climate model prediction.

4.1 Sensitivity of Regional climate model in the selection of appropriate Convective Parameterization Scheme (CPS):

Firstly, the sensitivity study using two CPS, namely Emanuel, Grell, and a mixed scheme (Emanuel over land and Grell over the ocean) as well as the Tiedtke convection scheme are used to simulate summer monsoon features using RegCM version 4.6. In each experiment, the model is initialized on 1st May 1950 and integrated continuously up to 1st October 2005 with a horizontal resolution of 25-km and 18 sigma levels in the vertical. The first months of simulation are excluded as spin-up time, and only the summer monsoon season (JJAS) from 1950 to 2005 is considered for the analysis. The results show that the mixed scheme simulates the summer monsoon precipitation over the Indian subcontinent and is in close agreement with the CRU observations compared with the three other schemes (Fig. 2). The circulation features are better represented with the mixed convection scheme. Further, the northward propagation of monsoon is also reasonably better simulated in the mixed convection scheme as compared with three other schemes.

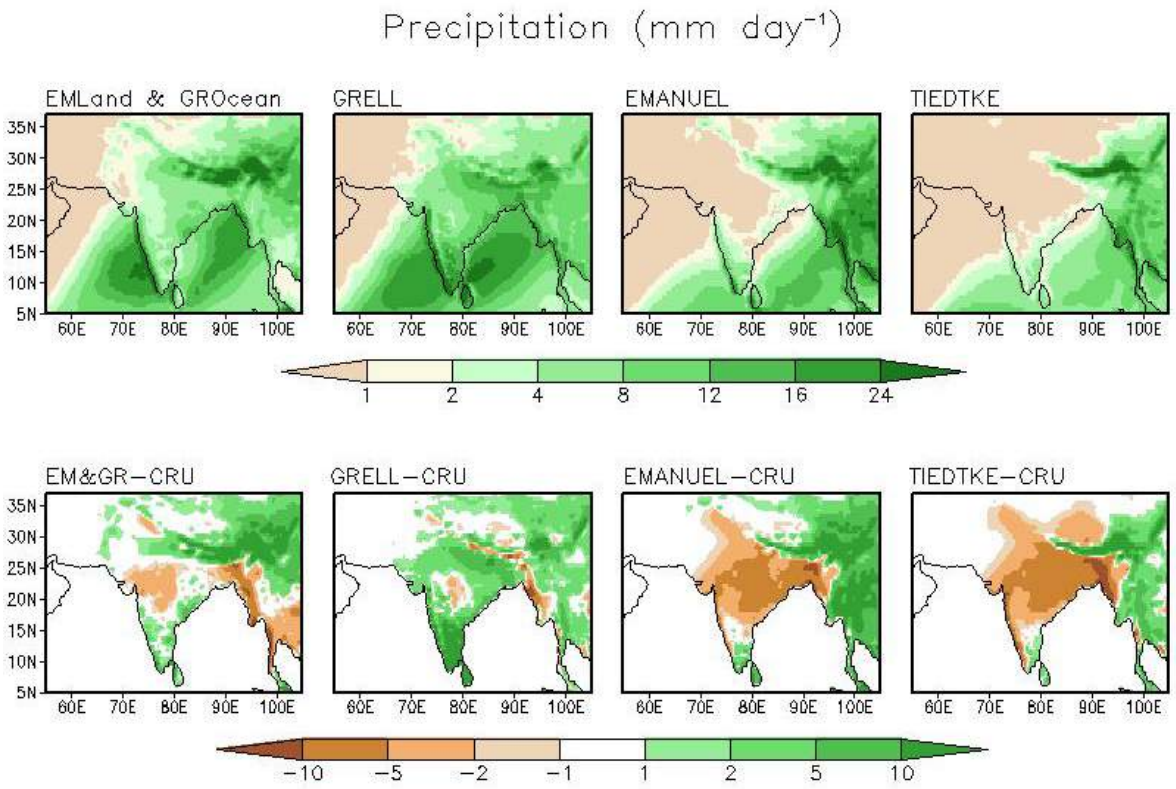

Fig. 2 *Indian summer monsoon (JJAS) precipitation (top panels) of four convection schemes -Mixed Emanuel & Grell, Grell, Emanuel and Tiedtke and the corresponding bias with respect to CRU precipitation (bottom panel)*

In the second experiment, for the sensitivity analysis of MPI-ESM-MR driven RegCM 4.6 simulation (at 25Km horizontal resolution) by using various CPSs has been done in order to reproduce the flood (1988) and drought (1987) conditions over India. The spatial distribution of rainfall differences (mm) during the Indian summer monsoon (ISM) season for the years 1988 and 1987 has been shown in Fig. 3. The Fig. 3a represents the IMD observed rainfall difference over India, while Figure 3b-k shows the RegCM4.6 simulated rainfall with the 10 available CPSs combinations. Observations show a positive difference in the range 0 – 600 mm over most of the country, while over some of the regions of central India, eastern and north-eastern India, a negative difference (up to -600mm) has been reported. These observations inferred that 1987 was a rainfall deficit year and 1988 was an excess rainfall year as far as the ISM season is concerned. This situation is satisfactorily simulated by Grell, Tiedtke, GL_EO, EL_GO, and GL_TO CPSs.

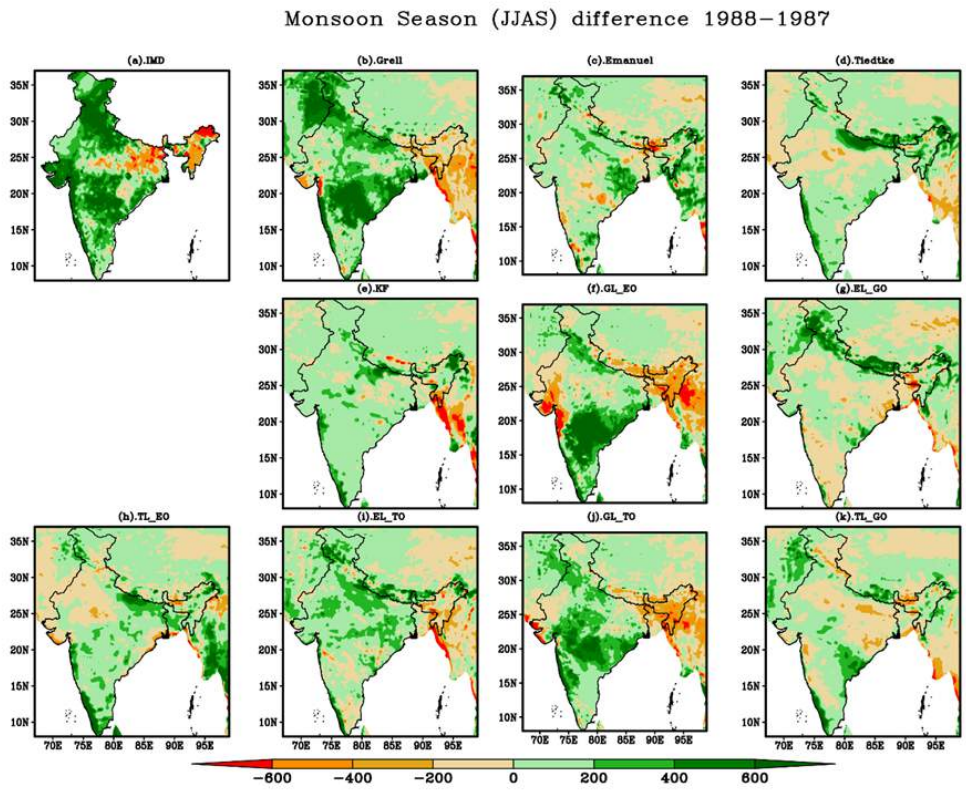

Fig.3 *Spatial distribution of (a). IMD (observed) and RegCM4.6 simulated (by using different CPSs) ISM rainfall difference (b to k) during 1988 and 1987.*

In the third experiment, the ability of RegCM4.6 to simulate extreme rainfall events over Mumbai has been analyzed. The Regional climate model (RegCM4.6) was developed by the Earth system physics group of the International Centre for Theoretical Physics (ICTP), Italy driven by the ERA-interim data dynamically downscaled over the South Asian CORDEX domain at 25km resolution. Various sensitivity experiments have been performed to simulate extreme rainfall events with three core Cumulus Parameterization Schemes (CPSs) namely Grell, Emanuel, and Tiedtke along with their six different combinations (1. Grell over land & Tiedtke over the ocean (GL_TO), 2. Tiedtke over land & Grell over the ocean (TL_GO), 3. Grell over land & Emanuel over the ocean (GL_EO), 4. Emanuel over land & Grell over the ocean (EL_GO), 5. Emanuel over land & Tiedtke over the ocean (EL_TO) and 6. Tiedtke over land & Emanuel over the ocean (TL_EO). Analysis showed that among 9 considered CPSs, EL_GO performed well in simulating extreme rainfall events. The spatiotemporal distribution of rainfall and associated thermodynamical and dynamical aspects are captured satisfactorily (Fig. 4).

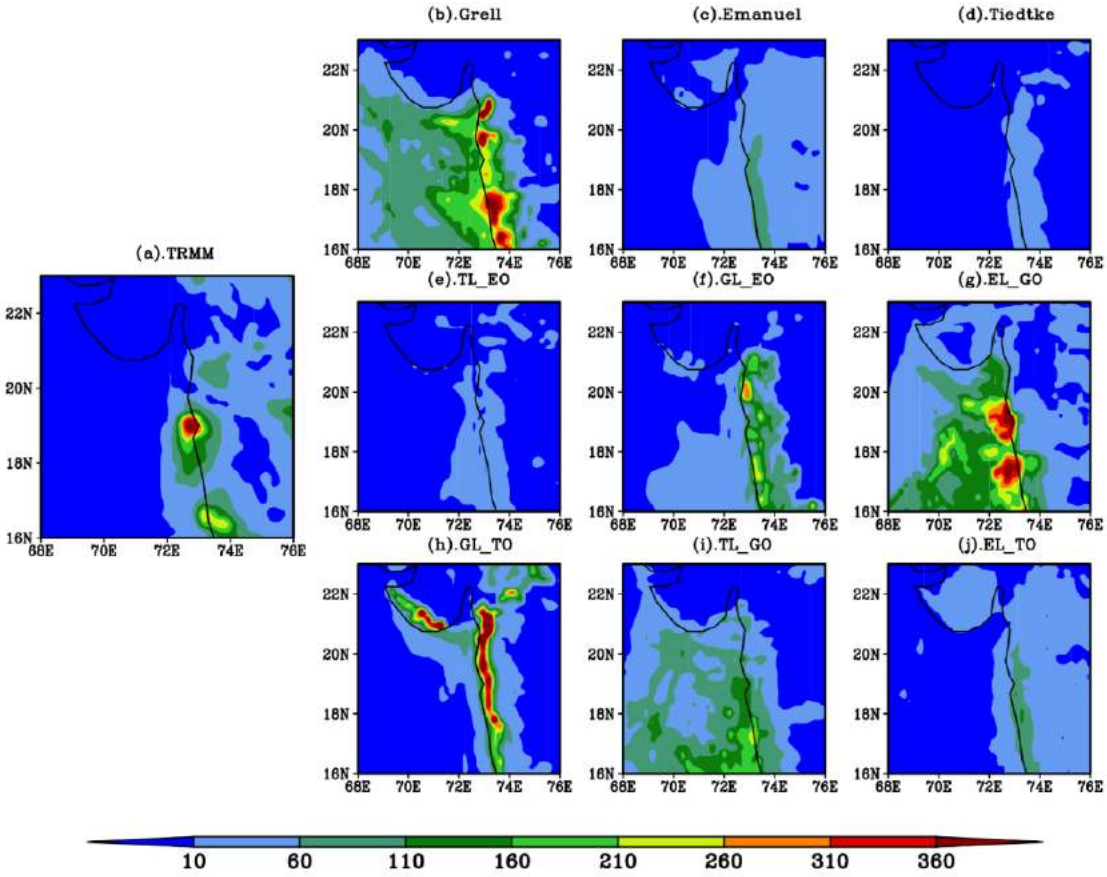

Fig.4 *. Spatio-temporal distribution of accumulated rainfall (mm) within 24 hrs on 26th July 2005 (16^0N-23^0N & 68^0E-76^0E).*

In the fourth experiment, the simulation of surface temperature and analysis of synoptic characteristics of extreme weather events like Heatwaves is simulated with RegCM 4.6 model with 25 km horizontal resolution over the Indian subcontinent during the year 2005. It is observed maximum temperature variation during the heatwave events is well simulated by the model in comparison with observed India Meteorological Department (IMD) maximum temperature data as shown in Figure 5 & 6.

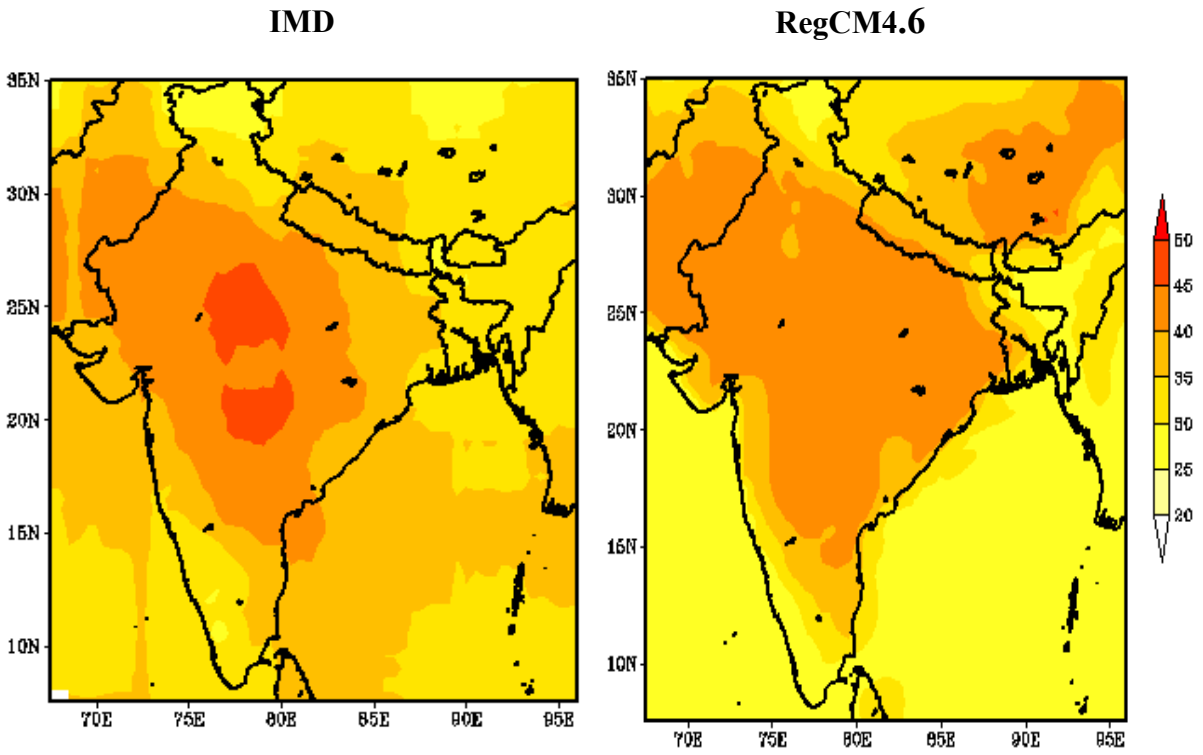

Fig. 5 *Spatial distribution of maximum temperature during heatwave events over India from (a) IMD observation and (b) RegCM model simulation.*

The study of extreme weather events (Heat Wave) shows that maximum temperature simulated by RegCM4.6 is good over north and north-west region compared to the east and south-east region. It is noticed that heatwave conditions developed over the northwest region and then gradually spread over the central, south and south-east region of India. A temperature bias of range 1.5- 2° C is also found in some regions.

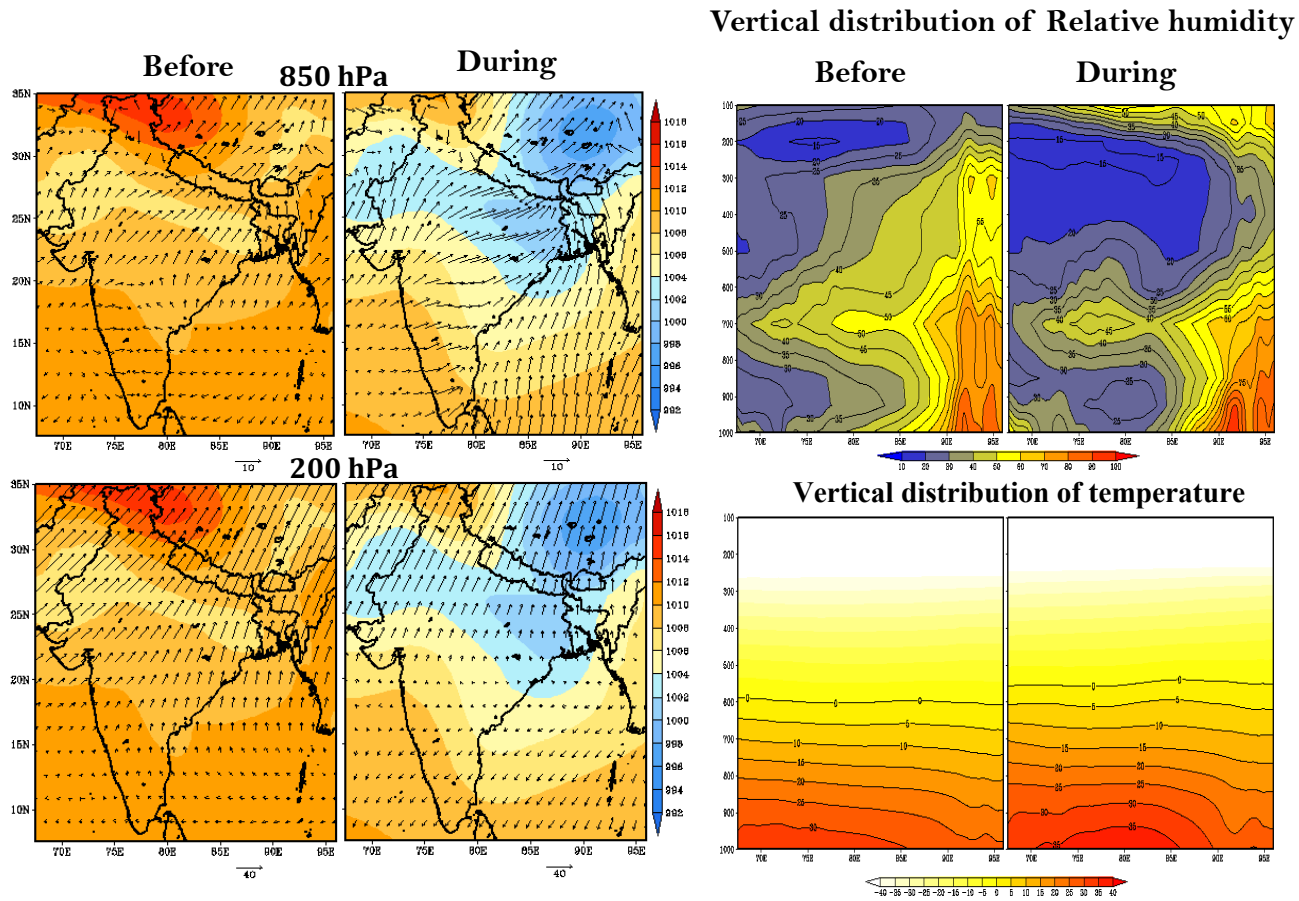

Fig. 6 *Synoptic features of maximum temperature (heat wave) events in the year of 2005.*

In the fifth experiment, interannual variability and regional modulating behaviour of rainfall have been examined in the framework of the spatial and temporal dimensions of drought and flood over eight homogenous rainfall zones or subregions of the Indian subcontinent. The brief description of rainfall subregion/zones described in Table1 viz *North west India (NWI), Northcentral India (NCI), Western peninsular India (WPI), Eastern peninsular India (EPI) and Southern peninsular India (SoPI)* (Bhatla et al., 2019; Verma et al., 2021), based on the changing behaviors of extreme rainfall three important regions i.e. *North east India (NEI), Central India (CI) and Western ghat (WG)* have been updated in this study shown in Figure 7. CORDEX South Asia RCMs of three high resolution (at 0.22° resolution or 25 km) RCMs (RegCM4.7, COSMO & REMO2015) ERA-Interim-driven simulations of over SA CORDEX-SA domain has been selected to investigate the spatial and temporal dimensions of extreme climate indices along with meteorological droughts and flood over India and its subregions.

The RCM evolution CORDEX-SA data are regridded to the observational grid (0.25° × 0.25°). to compare the spatial rainfall pattern and its variability, the climatological mean, interannual variability or standard deviation (SD), mean bias (MB), root mean square error

(RMSE) of SWM rainfall at each grid level were calculated for RCM output (RegCM4.7, COSMO, REMO) as well as IMD observational data set (IMD) during 1981-2015.

The spatial behavior of the observed climatological mean of the Indian summer monsoon rainfall (ISMR) is shown in Figure 7(a). The accumulated rainfall pattern shows the lowest rainfall over NWI and SoPI except WG i.e., in the range of 2-4 mm/day. On the other hand, the maximum rainfall is observed in the range of 24-32 mm/day over the mountainous region of WG and NEI. The Indo-Gangetic Plain (IGP) along with the CI experienced moderate rainfall. The observed spatial ISMR distribution compared with the ERA-Interim driven three RCMs simulations (RegCM4.7, COSMO and REMO2015) (Figs. 7b-g). The performance of RegCM4.7 is relatively good in simulating mean ISMR distribution over India and its sub-regions and is capable of simulating areas of minimum and maximum rainfall rates (Fig.7b) except over the NEI where the simulation shows higher average rainfall (18 mm/day) than the IMD (CI: 12.8 mm/day). Also, the spatial distribution of the mean bias is illustrated in the Fig.7c, which depicts that the RegCM4.7 clearly overestimated (~4-6 mm/day) the mean rainfall along the mountainous topography of WG, WPI, NEI and foothills of the Himalaya (Fig. 7c).

The COSMO simulated rainfall was not distributed as observed in IMD over the Indian subcontinent. According to the IMD rainfall distribution highest rainfall occurs in the west coast, WG, sub-Himalayan areas in the NE, west Bengal and southern slope of eastern Himalayas which is not correctly portrayed in the COSMO simulation, it has been showing high dry bias (~6 mm/day) over highest rainfall regions (Fig.7 d-e). On the other hand, the north and central regions of India including NEI showing normal rainfall in the range of 8-12 mm/day in COSMO RCM. Next, the precipitation simulation of REMO2015 RCM displayed a satisfactory amount of ISMR over WG, CI and NEI except excess precipitation over the WPI, EPI region (Fig. 7 f-g). The excessive wet bias (~6-8 mm/day) over the EPI region might affect the performance of REMO2015 in simulating the ISMR and its modulated properties over a particular region. The distribution of ISMR over the WG, CI and NCI are sensitive for qualitative and quantitative evaluation of RCMs to portray the progression of monsoon.

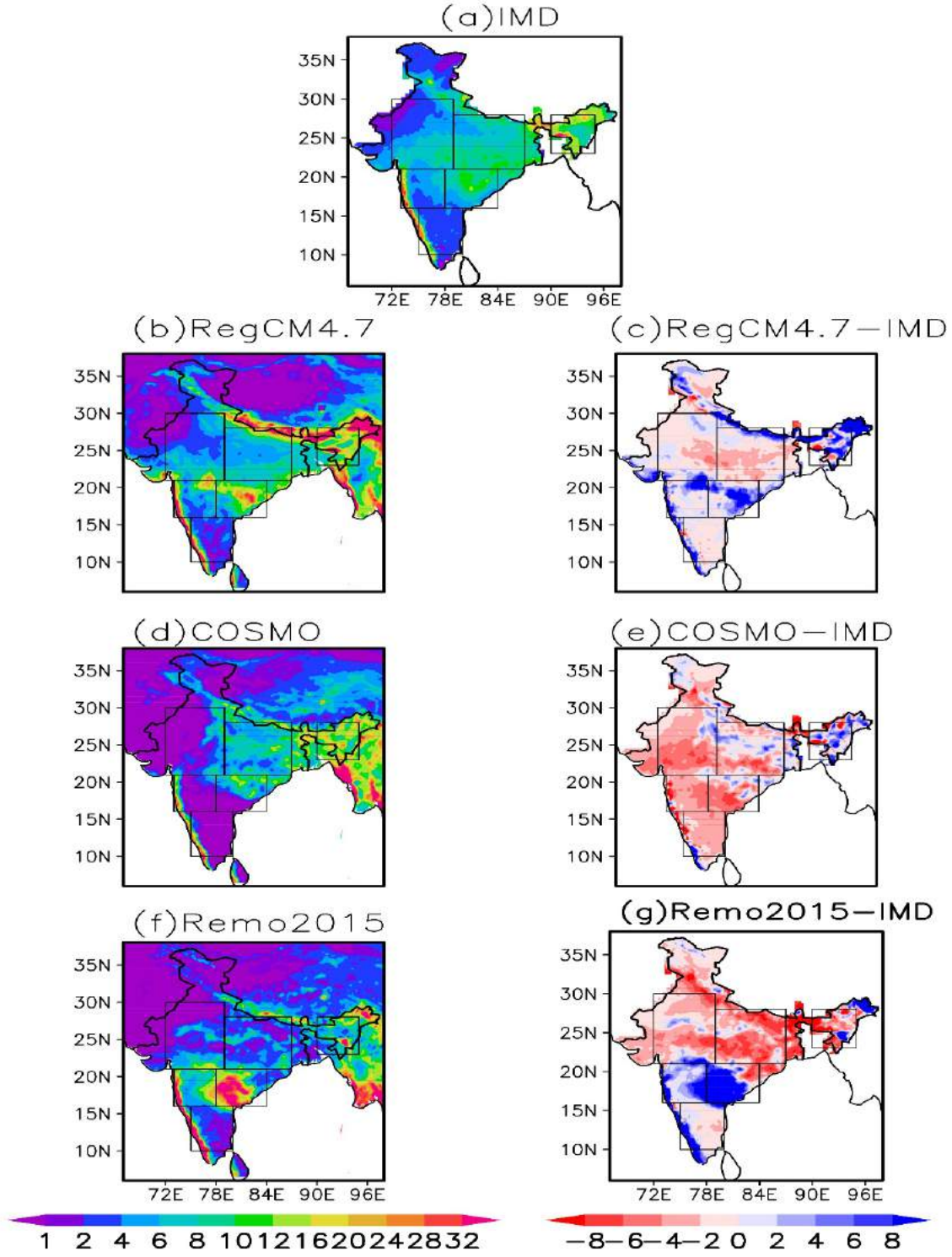

Fig. 7 *Climatological spatial Indian summer monsoon rainfall (mm/day) distribution (first column) and mean bias (Second column) over India and its region during 1981-2015, (a). observation (IMD); (b&c). RegCM4.7; (d&e). COSMO; (f&g). REMO.*

The study of dynamically downscaled AOGCM (MPI-ESM_MR and GFDL-ESM2M) for baseline climate has been done using RegCM4.6. The model sensitivity experiment in the selection of appropriate convection parametrized scheme has been performed in the simulation of summer monsoon rainfall. The results show that the mixed convection scheme performs better in simulating the summer monsoon precipitation over the Indian subcontinent due to the land- Ocean coupling effect. Also, RegCM4.6 performed satisfactorily in simulating the deficit and excess monsoon features using RegCM4.6. The latest version of RegCM4.6 shows good performance in the simulation of extreme weather events such as heatwaves in agreement with the observations. The model clearly simulates the heatwave condition developed over the north-west region and then gradually spread over the central, south and south-east region of India. Therefore, based on the validated RegCM4.6 simulations, the climate projections for the various microclimatic variables (Maximum and Minimum Temperature (Tmax & Tmin), Total Precipitation (PrecT), Net Radiation (Rnet) , atmospheric Relative humidity (RH)) have been done under RCP 4.5 & 8.5 climate scenarios over India during 2006-2100. Further, the bias-corrected data sets have been generated using advanced statistical bias correction techniques such as variance scaling and linear scaling for above mentioned variables.

Work Done:

- Installation of the latest version of the Regional climate model (RegCM 4.6).
- Customization of RegCM 4.6 over SA-CORDEX and Indian domain.
- Downloading of the AOGCMs data (MPI-ESM-MR & GFDL-ESM-2M).
- Pre-processing of the global climate data for RegCM 4.6.

- Dynamical downscaling of AOGCM (MPI-ESM-MR, GFDL-ESM-2M) data using RegCM4.6 to generate high-resolution data at 25 x 25 km grids over the Indian domain has been done for the historical time period (1950-2005).
- Post-processing of dynamically downscaled climate data of historical run (1950-2005).
- Sensitivity experiments have been carried out, such as selection of buffer zone and selection of domain.
- Conducted various sensitivity experiments in order to identify the best performing convective parameterized scheme (CPS) for simulating the climate parameter on the interannual scale.
- The interannual variability of Indian summer monsoon rainfall of four convection schemes Grell, Emanuel Tiedtke, and Mixed Emanuel & Grell has been carried out to analyze the model validation with observed data (CRU) from 1950 to 2005.
- Model performance in simulating rainfall patterns over the Indian subcontinent has been assessed during flood and drought years by different convective parameterization schemes of RegCM4.6 for the period 1950-2005.
- The simulation and validation of extreme weather events during 2005 (Heat Wave) were simulated by RegCM 4.6.
- Validated RegCM4.6 has been used for dynamical downscaling for future projection (2006-2100) using AOGCM (GFDL-ESM-2M, MPI-ESM-MR) at 25x25 km resolution under RCP4.5 and 8.5 scenarios..
- Qulality checks of MPI-ESM-MR and GFDL-ESM2M data and metadata consistency (Technical Quality Assurance - TQA) have been completed (Projected data 2006-2100 period).
- Bias-corrected datasets have been prepared for the India region in the NetCDF format.
- The dynamically downscaled output for RCP scenarios 4.5 and 8.5 scenrio contains the daily microclimatic variables (Maximum and Minimum Temperature (Tmax & Tmin), Total Precipitation (PrecT), Net Radiation (Rnet) , atmospheric Relative humidity (RH)) at 25 km spatial resolution for years 1951-2100 across India.

<u>Final output:</u>

- Dynamical downscaled bias-corrected 25x25 Km resolution data (GCMs - MPI-ESM-MR and GFDL-ESM2M, both RCP4.5 & 8.5 scenarios, 1950-2005 & 2006-2100) using RegCM4.6 has been generated and would be delivered at any time.

Publications:

1) Ghosh, S., Sinha, P., Bhatla, R., Mall, R.K. and Sarkar, A., 2022. Assessment of Lead-Lag and Spatial Changes in simulating different epochs of the Indian summer monsoon using RegCM4. *Atmospheric Research*, 265, p.105892.
2) Verma, S., Bhatla, R., Shahi, N.K. and Mall, R.K., 2022. Regional modulating behavior of Indian summer monsoon rainfall in context of spatio-temporal variation of drought and flood events. *Atmospheric Research*, p.106201.
3) Pant, M., Ghosh, S., Verma, S., Sinha, P., Mall, R. K., & Bhatla, R. (2022). Simulation of an extreme rainfall event over Mumbai using a regional climate model: a case study. Meteorology and *Atmospheric Physics*, 134(1), 1-17.